# PHY 564
# Advanced Accelerator Physics
# Lecture 25

# Nonlinear elements and nonlinear dynamics. Part I


Vladimir N. Litvinenko
Yichao Jing
Gang Wang

CENTER for ACCELERATOR SCIENCE AND EDUCATION
Department of Physics & Astronomy, Stony Brook University
Collider-Accelerator Department, Brookhaven National Laboratory

# Chromaticity and correction

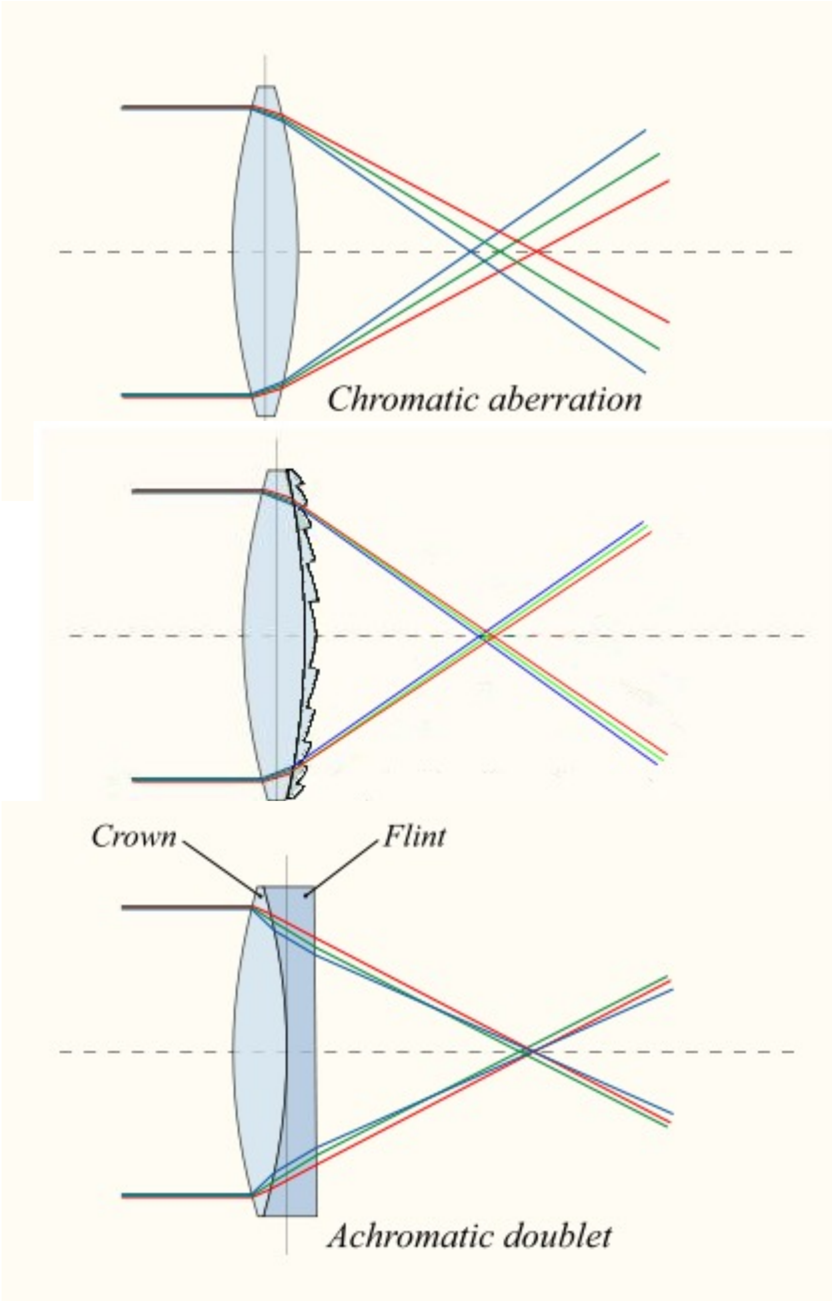

Nonlinear effects in particle's motion arise from various sources: high order kinematic terms in Hamiltonian expansion, spatial and temporal inhomogeneity of EM fields, edge effects, bending (e.g. bending plus gradient generates third order term), collective fields (space charge, wake-fields, beam-beam collisions). Typical methods include Hamiltonian perturbation methods or numerical tracking of many types (from particles tracking to particle-in-cell codes). A novel approach, exploiting symmetries of Hamiltonian systems and power of Lie algebraic tools, is the most comprehensive approach to the non-linear beam dynamics. Hence, a short introduction to this method.

But first, let us start by discussing a typical – and very important – nonlinear effect called chromaticity. It is nothing else than dependence of the betatron tune on particle's energy. While you can do this for fully coupled motion using our well-developed parameterization and perturbation methods, here –for compactness - we will consider just an uncoupled betatron motion with Hamiltonian in transverse magnetic field:

$$\tilde{h} = -P_s = -(1+Kx)\sqrt{p^2 - p_x{}^2 - p_y{}^2} + \frac{e}{c}A_s; \quad p = p_o(1+\delta);$$

$$\frac{d(x,y)}{ds} = \frac{\partial \tilde{h}}{\partial p_{x,y}} = -(1+Kx)\frac{p_{x,y}}{\sqrt{p^2 - p_x{}^2 - p_y{}^2}} \cong -(1+Kx)\frac{p_{x,y}}{p_o(1+\delta)} + O\left(p_{x,y}{}^3\right); \quad (25\text{-}1)$$

$$\frac{dp_x}{ds} = -\frac{\partial \tilde{h}}{\partial x} = K\sqrt{p^2 - p_x{}^2 - p_y{}^2} - \frac{e}{c}\frac{\partial A_s}{\partial x}; \frac{dp_y}{ds} = -\frac{\partial \tilde{h}}{\partial y} = -\frac{e}{c}\frac{\partial A_s}{\partial y};$$

with

$$A_2 = \sum_{n=1}^{\infty}\left\{\partial_x^{n-1}\left((1+Kx)B_y\right)_{ro}\frac{x^n}{n!} - \partial_y^{n-1}\left((1+Kx)B_x\right)_{ro}\frac{y^n}{n!}\right\} \quad (25\text{-}2)$$

If we consider easiest scenario for a storage ring using pure dipole and quadrupole field we get:

$$\frac{eA_2}{c} = \frac{eB_y}{c}x + \frac{eG}{c}\frac{x^2 - y^2}{2} + p_o K^2 \frac{x^2}{2}; \quad K = \frac{eB_{yro}}{p_o c}. \tag{25-3}$$

expression which does not contain any nonlinear terms (cubic or higher). Remember that linear term in (25-3) disappears because of the condition on the reference orbit. We can see that angle is $x', y'$ inverse proportional to the particle's momentum $p = p_o(1+\delta)$ while the force $p'_{x,y}$ does not depend on the particle's momentum. Hence, the lowest order (cubic) term in the Hamiltonian expansion are $\delta \cdot p_{x,y}{}^2$.

Since here we are considering constant energy of our particles ($p$=const) and betatron oscillations, we also can rewrite (25-1) in more traditional form

$$h = -(1+Kx)\sqrt{1-\pi_x{}^2-\pi_y{}^2} + \frac{e}{pc}A_s(x,y,s); \quad \pi_{x,y} = \frac{p_{x,y}}{p} = \frac{p_{x,y}}{p_o(1+\delta)};$$

$$\frac{d(x,y)}{ds} = \frac{\partial h}{\partial \pi_{x,y}} = -(1+Kx)\frac{\pi_{x,y}}{\sqrt{1-\pi_x{}^2-\pi_y{}^2}} \cong -(1+Kx)\pi_{x,y} + O\left(\pi_{x,y}{}^3\right) \tag{25-4}$$

$$\frac{d\pi_{x,y}}{ds} = -\frac{\partial h}{\partial(x,y)} = -\frac{e}{pc}\frac{\partial A_s}{\partial(x,y)} = -\frac{e}{p_o c(1+\delta)}\frac{\partial A_s}{\partial(x,y)}.$$

which clearly indicates that with fixed magnetic field, its affect on the particle is inverse proportional to particle's momentum $p_o$. This is traditional way of consider chromatic effect. Naturally, both descriptions are identical and gave exactly the same result! But this is always lost in description of chromatic effects that its origin is purely geometrical – for the same "so-called normalized" transverse emittance, angle of trajectory is inverse proportional to the particle's longitudinal momentum. In the Hamiltonian (25-4), the lowest (cubic) terms are $\delta \cdot x^2, \delta \cdot y^2$.

From our Hamiltonians it is obvious that there are nonlinear kinematic terms $\sim \pi_{x,y}^{\ 4}$, $\pi_x^{\ 2}\pi_y^{\ 2}$ and higher in the Hamiltonian expansion. Furthermore, there are always third order $Kx\pi_{x,y}^{\ 2}$ terms. While this term can cause third order resonance (we will look at them later) its role is not as important as that of the chromaticity of betatron oscillations. Hence, let's leave in the Hamiltonian (25-4) only linear (up to quadratic term) for transverse motion while keeping particle momentum arbitrary:

$$H = \frac{\pi_x^{\ 2} + \pi_y^{\ 2}}{2} + \frac{1}{1+\delta}\left(\left(K_1 + K^2\right)\frac{x^2}{2} - K_1\frac{y^2}{2}\right);$$
$$H = H_o + \Delta H; \quad \Delta H = -\frac{\delta}{1+\delta}\left(\left(K_1 + K^2\right)\frac{x^2}{2} - K_1\frac{y^2}{2}\right). \tag{25-5}$$

Note, that similar (but much-much longer) expression can be derived for arbitrary magnetic and electric fields. While possible, it does not bring any new physics into what we considering here.

We already found what (in first order of perturbation) the tune shift will result from variation of the Hamiltonian (using our perturbation method):

$$\Delta Q_x \cong -\frac{1}{4\pi}\frac{\delta}{1+\delta}\oint \beta_x\left(K_1 + K^2\right)ds; \ \Delta Q_y \cong \frac{1}{4\pi}\frac{\delta}{1+\delta}\oint \beta_y K_1 ds; \tag{25-6}$$

e.g. the betatron tunes in such storage ring depend on the particle momentum (energy). Note that keeping $1+\delta$ in the denominator is overestimation of accuracy in (25-6) – there are other terms of order $\delta^2$ and higher. The linear term in (25-6) is called chromaticity

$$C_x = \frac{\Delta Q_x}{\delta} \cong -\frac{1}{4\pi}\oint \beta_x\left(K_1 + K^2\right)ds; \ C_y = \frac{\Delta Q_y}{\delta} \cong \frac{1}{4\pi}\oint \beta_y K_1 ds; \tag{25-7}$$

Note that the linear chromatic term is strictly speaking is result of non-linear (third order) term in the Hamiltonian. Still, there is tradition to call it linear chromaticity and call the higher orders - higher order chromaticity. One important observation is that natural chromaticity (25-7) usually has negative values ("focusing of higher energy particles is weaker") for practically all storage rings. While statement in brackets is not strictly rigorous, it is true that for very high energy particles tunes will go to zero. A better explanation is coming from observation that in strong-focusing storage rings beta-functions are reaching maxima in focusing elements (e.g. $\beta_x$ reaches maxima in focusing quadrupoles, while $\beta_y$ reaches maxima in horizontally de-focusing quadrupoles where $K_1$<0) and therefore this tendency is correct. Furthermore, expectation for their values is that of the storage ring tune: $C_{x,y} \sim -(1 \div 2) \cdot Q_{x,y}$. Still, it is impossible to prove this rule explicitly in general case.

Chromaticity has multiplicity of effects on particle's dynamics in storage rings. In modern storage rings with Q ~ 10-100, chromatic effects are very important. Chromaticity can generates spread of betatron tunes (for a typical energy spread ~$10^{-3}$-$10^{-4}$), which can move particles onto linear and non-linear resonances. It also can impede injection into the storage rings as dynamics aperture (e.g. limit amplitudes of stable oscillations). Hence, chromaticity is usually corrected (by sextupoles, as we discuss it later in the lecture) to few units.

But the most important problem that natural (e.g. negative) chromaticity creates is so called head-tail instability, which occurs at energies above the critical, e.g. when the slip factor is negative. Head-tail instability is one of few major menaces in storage rings, which can simply kill the beam if not taken care off.

Incomplete list of major instabilities in a storage ring:

1. Wrong lattice, where motion is unstable;
2. Robertson instability (operating RF cavities with wrong sign of frequency detuning - we are not discussing it in this course);
3. Integer and parametric resonances (and frequently 3rg and $4^{th}$ order resonances);
4. Head-tail instability.

While a nasty microwave instability would fortunately saturate by inducing growth of energy spread, but not head-tail instability. It could be major killer of the beams.

Let's consider this menace using a simple two-macro-particle model, which was originally used to describe this experimentally observed phenomena. In Fig. 1 we depict this simple model when two macro-particles execute slow synchrotron oscillations 180-degrees out of phase – hence the name, head and tail: when one particle is in front of the bunch, the other is at the tail, and vice-versa.

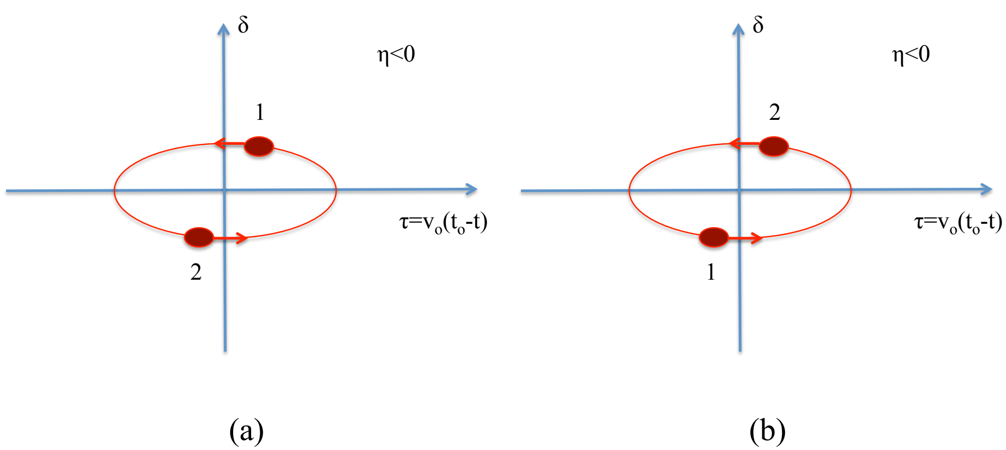


Fig. 1 Two macro-particles executing synchrotron oscillations. (a) particle 1 is in front of particles 2, (b) 180-degrees later – particles exchange the positions.

Since instability is sensitive to the chromaticity, details (such as strength of the wake-field and value of the amplitude of the oscillations) are not important. It is also an indication of universality of this problem – it just occurs if chromaticity is on a wrong sign! (e.g. negative for negative slippage). We will simply use some arbitrary values assuming that synchrotron oscillations are much slower that betatron ones. Finally, one more important fact you learned from the class on wake-fields and instabilities: particles in front of the bunch generate wake sensed by those in the tail, not vice-versa! Hence: for the Fig. 1 (a) we can write equations of motions as (we use y as generic transverse coordinate):

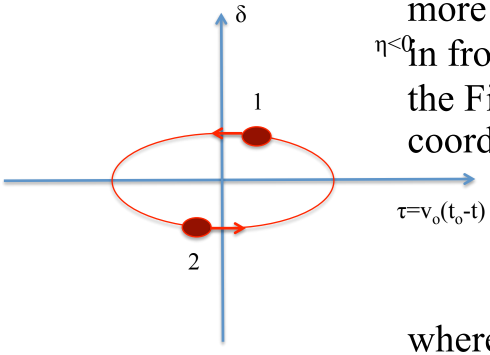


$$\begin{aligned} y_1'' + K_1(s)\left(1-\delta_1\right)y_1 &= 0; \\ y_2'' + K_1(s)\left(1-\delta_2\right)y_2 &= W\cdot y_1; \end{aligned} \tag{25-7}$$

where $W$ is a transverse focusing (or defocusing) induced by macro-particle ahead. 180-degrees later, it changes to

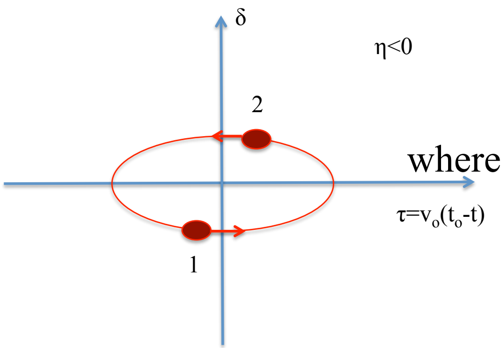


$$\begin{aligned} y_1'' + K_1(s)\left(1-\delta_1\right)y_1 &= W\cdot y_2; \\ y_2'' + K_1(s)\left(1-\delta_2\right)y_2 &= 0; \end{aligned} \tag{25-7}$$

where we just need to add

$$\delta_1 = \delta\cos\varphi_s; \delta_2 = -\delta\cos\varphi_s;\ \ \varphi_s = \Omega_s s;\ \ S = \frac{\pi}{\Omega_s};$$

$$\tau_1 = \tau\sin\varphi_s; \tau_2 = -\tau\sin\varphi_s;$$

$$\begin{aligned} y_1'' + K_1(s)\left(1-\delta_1\right)y_1 &= W\frac{1-sign(\tau_2-\tau_1)}{2}\cdot y_2; \\ y_2'' + K_1(s)\left(1-\delta_2\right)y_2 &= W\frac{1+sign(\tau_2-\tau_1)}{2}\cdot y_1; \end{aligned} \tag{25-8}$$

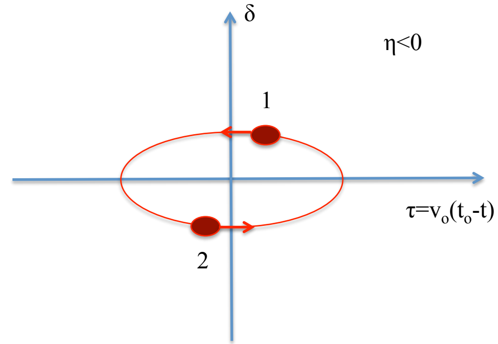


Let's consider particle (1) and (2) having complex amplitudes of oscillations $a_1$ and $a_2$ starting at zero s. For the first $\varphi_s=\{0,180\}$ degrees in picture (a).

$$y_1 = w_y \operatorname{Re} a_{10} e^{i(\psi+\Delta\psi)};\ y_2 = w_y \operatorname{Re} a_{20}\, e^{i(\psi-\Delta\psi)};$$

$$\Delta\psi(s) = 2\pi C_y \delta \int_0^s \cos\Omega_s s\, ds = \frac{2\pi C_y \delta}{\Omega_s}\sin\Omega_s s; \qquad S = \frac{\pi}{\Omega};$$

$$a_2(s) = a_{20} + \frac{a_{10}}{2i}\int_o^s W w_y{}^2 e^{2i\Delta\psi} ds;\ a_{21} = a_2(S) = a_{20} + a_{10}\left\langle W w_y{}^2 \right\rangle \frac{1}{2i}\int_o^S e^{2i\Delta\psi}\, ds; \qquad (25\text{-}9)$$

$$\begin{pmatrix} a_1(S) \\ a_2(S) \end{pmatrix} = \begin{bmatrix} 1 & 0 \\ u & 1 \end{bmatrix} \begin{pmatrix} a_{10} \\ a_{20} \end{pmatrix};\ u = \left\langle W w_y{}^2 \right\rangle \frac{1}{2i}\int_o^S e^{2i\Delta\psi}\, ds.$$

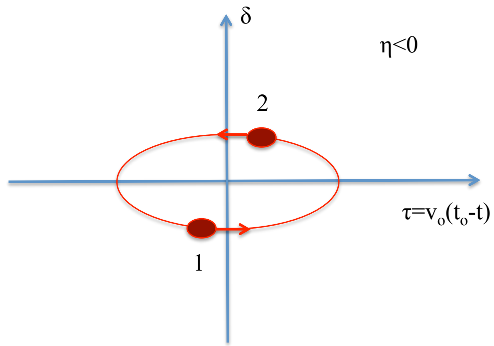


Now, let’s look how the amplitude of oscillation of first particles changes during next half of the synchrotron oscillation:

$$y_1 = w_y \operatorname{Re} a_1(s) e^{i(\psi - \Delta\psi)}; y_2 = w_y \operatorname{Re} a_{21} \mathrm{e}^{i(\psi + \Delta\psi)};$$

$$a_1(s) = a_{10} + a_{21}\frac{1}{2i}\int_S^s W w_y{}^2 e^{2i\Delta\psi} ds;\ a_{11} = a_1(2S) = a_{10} + a_{21}\left\langle W w_y{}^2\right\rangle \frac{1}{2i}\int_S^{2S} e^{2i\Delta\psi}\, ds; \text{(25-10)}$$

$$\begin{pmatrix} a_1(2S) \\ a_2(2S) \end{pmatrix} = \begin{bmatrix} 1 & u \\ 0 & 1 \end{bmatrix} \begin{pmatrix} a_{10} \\ a_{21} \end{pmatrix};\ u = \left\langle W w_y{}^2\right\rangle \frac{1}{2i}\int_o^S e^{2i\Delta\psi}\, ds.$$

The overall matrix for a single synchrotron oscillation period is

$$\begin{pmatrix} a_{11} \\ a_{21} \end{pmatrix} = \begin{bmatrix} 1 & u \\ 0 & 1 \end{bmatrix} \begin{bmatrix} 1 & 0 \\ u & 1 \end{bmatrix} \begin{pmatrix} a_{10} \\ a_{20} \end{pmatrix} = \begin{bmatrix} 1+u^2 & u \\ u & 1 \end{bmatrix} \begin{pmatrix} a_{10} \\ a_{20} \end{pmatrix};$$

$$\det \begin{bmatrix} 1+u^2-\lambda & u \\ u & 1-\lambda \end{bmatrix} = (1-\lambda)(1+u^2-\lambda) - u^2 = (1-\lambda)^2 - \lambda u^2; \quad (25\text{-}11)$$

$$\lambda_{1,2} = 1 + \frac{u^2}{2} \pm u\sqrt{1+\frac{u^2}{4}}; u = \langle W w_y{}^2 \rangle \frac{1}{2i} \int_o^S e^{2i\Delta\psi}\, ds.$$

Note that determinant of matrix is 1, hence is one solution is growing, the other is damped. Since we are considering weak wake-field, we can write the eigen values as

$$u \approx \langle W w_y^2 \rangle \left( \frac{S}{2i} + \frac{2\pi C_y \delta}{\Omega_s} \right); \;\; \lambda_{1,2} \cong e^{\pm \langle W w_y^2 \rangle \left( \frac{S}{2i} + \frac{2\pi C_y \delta}{\Omega_s} \right)} \qquad (25\text{-}12)$$

and the growth rate is proportional to the chromaticity and its value should be limited. The detailed studies (which we have to skip) show that + (sign instability corresponding to positive chromaticity) is much weaker and that having a small positive chromaticity for storage ring above transition (negative slip factor) is required for stability of the beam – this is the mode in which most of electron storage ring and high energy hadron colliders do operate.

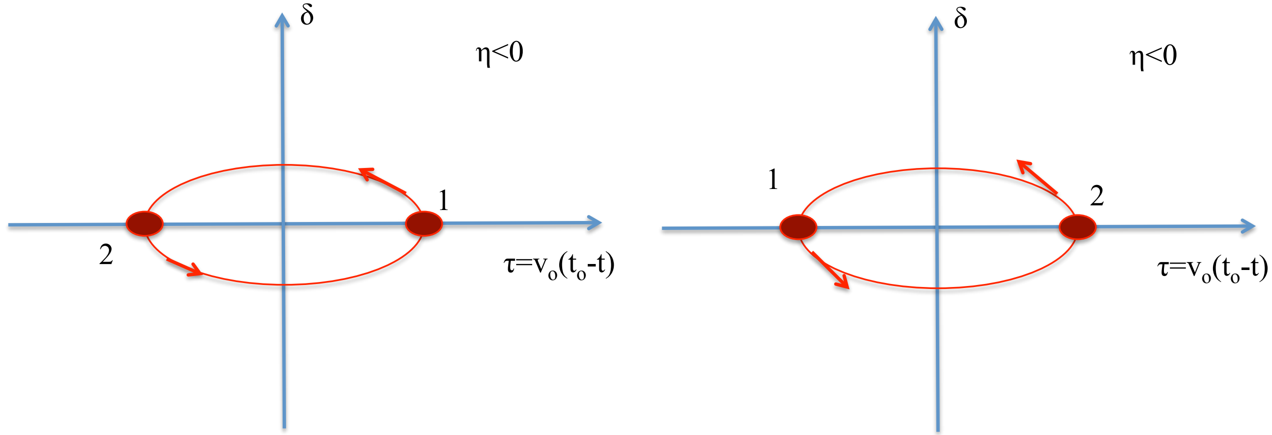


Fig.2. Two extreme positions.

Intuitively this can be described as follows. Let's consider negative chromaticity and the fact that the strength of the transverse wakefield is increasing with the distance between particles, e.g. most of the impact will come from the head particle (1) when it is in extreme forward position. (1) excites the tail particle (2) resonantly it oscillates in phase.

$$\tilde{y}_2 = \tilde{y}_{20} + T\varepsilon\tilde{y}_{10}$$

When they exchange position, the exited the tail particle (2) oscillates with higher betatron frequency (it passes through lower energy) than the (1) having higher energies. It means that particle (2) comes to head position with positive phase advance – it corresponds to an effective response from the future

$$\Delta\tilde{y}_1(t) = T\varepsilon\tilde{y}_{20}(t+\tau) + T\varepsilon^2\tilde{y}_{10}(t+\tau)$$

We can equivalently write

$$y_1''(t) + \omega^2 y_1(t) = T\varepsilon^2\tilde{y}_1(t+\tau) \approx T\varepsilon^2\left(\tilde{y}_1(t) + \tau\tilde{y}_1'(t)\right); \qquad (25\text{-}13)$$

generating growth rate of $\tau\ T\varepsilon^2$. We should note that $\tau = -\dfrac{4\pi C_y\delta}{\Omega_s c}$ is proportional to the chromaticity and has opposite sign for negative slippage. For positive slippage (below transition), natural sign of chromaticity is favored for head-tail stability.

These exercises were to establish a need for chromaticity compensations. Naturally, linear element cannot do this (they are introducing the chromaticity, not compensating it!). Hence, lest consider sextupole fields with

$$\frac{eA_2}{c} = \frac{eS}{c}\frac{x^3 - 3xy^2}{3!} \tag{25-14}$$

you can easily check that it satisfies 2D Maxwell equation. We are aware that in storage ring closed orbit depends on particle's momentum as

$$x_\delta = \eta_x(s)\delta \tag{25-15}$$

and introduction of sextupoles in (25-5) will result is:

$$H = \frac{\pi_x{}^2 + \pi_y{}^2}{2} + \frac{1}{1+\delta}\left(\left(K_1 + K^2\right)\frac{x_\beta{}^2}{2} - K_1\frac{y^2}{2}\right) + \frac{1}{1+\delta}\frac{K_2}{3!}\left(x^3 - 3xy^2\right)$$

$$x = \eta_x(s)\delta + x_\beta; K_2 = \frac{eS}{p_o c};$$

$$H = H_o + \Delta H_1 + \Delta H_{NL} \tag{25-16}$$

$$\Delta H_1 = -\delta\left(\left(K_1 + K^2\right)\frac{x^2}{2} - K_1\frac{y^2}{2}\right) + \delta\cdot\eta_x\cdot K_2\frac{x_\beta{}^2 - y^2}{2}$$

$$\Delta H_{NL} = \frac{K_2}{3!}\left(x_\beta{}^3 - 3x_\beta y^2\right) + O\left(\delta^2\right);$$

We can calculate the linear chromaticity in the same fashion we deed above:

$$C_x = \frac{\Delta Q_x}{\delta} \cong -\frac{1}{4\pi}\oint \beta_x\left(K_1 + K^2 - \eta_x K_2\right)ds;$$
$$C_y = \frac{\Delta Q_y}{\delta} \cong \frac{1}{4\pi}\oint\left(\beta_y K_1 - \eta_x K_2\right)ds; \tag{25-17}$$

To zero chromaticities we should find distribution of sextupole fields (as function of s) such that that

$$\oint K_2(s)\eta_x(s)\beta_x(s)ds = \oint \beta_x(s)\left(K_1(s)+K(s)^2\right)ds;$$
$$\oint K_2(s)\eta_x(s)\beta_y(s)ds = \oint \beta_y(s)K_1(s)ds; \tag{25-18}$$

Assuming positive dispersion (which is usual) it can be done by placing focusing sextupoles ( $K_2$>0) in areas where $\beta_x$ is large and $\beta_y$ is small, and vice versa for defocusing quadrupoles with $K_2$<0. For most of know strong focusing lattices this can be done. The only exception is weak-focusing lattice where all terms are constants the compensation

$$\langle K_2\rangle\eta_x = \left(K_1 + K^2\right);$$
$$\langle K_2\rangle\eta_x = -K_1; \tag{25-19}$$

could be possible only when $K_1 = -K^2/2$, which is exactly on the top the coupling resonances $Q_x = Q_y$. Hence, in general, in a weak-focusing storage ring chromaticity could be compensated only in one plane.

How the chromaticity compensation works: particle's average orbits shifts as function of energy and displacement is sextupoles generates effective gradient (quadrupole) field, which compensate change of the focusing from regular quadrupoles. This process is called feed-down – displacement of a high (n-th) order multipole generates lower orders multipoles, from dipole up to (n-1).

One important notion – compensating chromaticity requires orbit dependence on energy, which comes only as result of bending magnet. It means, that it is impossible to compensate chromaticity in a perfectly linear accelerator (no bends!) since transverse dispersion is always equal zero.

Thus, we established that in a modern storage rings chromaticity could be compensated using sextupoles. What is not obvious is that this can create significant problems. Indeed, modern light sources in order to generate high brightness beams reducing emittance (22-25)

$$\left\langle a_x^2 \right\rangle = \frac{55}{32\sqrt{3}} \gamma^2 \frac{\hbar}{mc} \frac{\left\langle |K|^3 \left( \left( \mathrm{w}_x \eta'_x - \mathrm{w}'_x \eta_x \right)^2 + \left( \frac{\eta_x}{\mathrm{w}_x} \right)^2 \right) \right\rangle}{\left(1 - \xi_{xy}\right) \left\langle K^2 \right\rangle}$$

strong focusing resulting in very large betatron tunes (~30) and very small beta-functions $\beta \sim R/Q$ and dispersion $\eta \sim R/Q^2$ measured in few cm. As follows from (25-17), we will need sextupole strength

$$\left\langle |K_2| \right\rangle \sim \left\langle |K_1| \right\rangle / \eta_x;$$

e.g. field inside the aperture of accelerator is very nonlinear and particle oscillating with large amplitudes can become unstable.

Since we introduced sextupoles, we should notice that equations of motion become non-linear. Even though the kick is locally proportional to a square of the transverse displacement, we cannot assume that it will generate some kind of expansion to a map of second order. One can simply observe that there is no analytical solution for equation of motion in a sextupole, or that two short sextupoles will already generate forth order terms in the transformations. Needless to say that multiple thick non-linear elements making the map tractable only by computers. But there is a BIG BUT – there is still a lot we can do to describe and to understand this nonlinear map – beyond just staring on them helplessly.

# NSLS II arc lattice

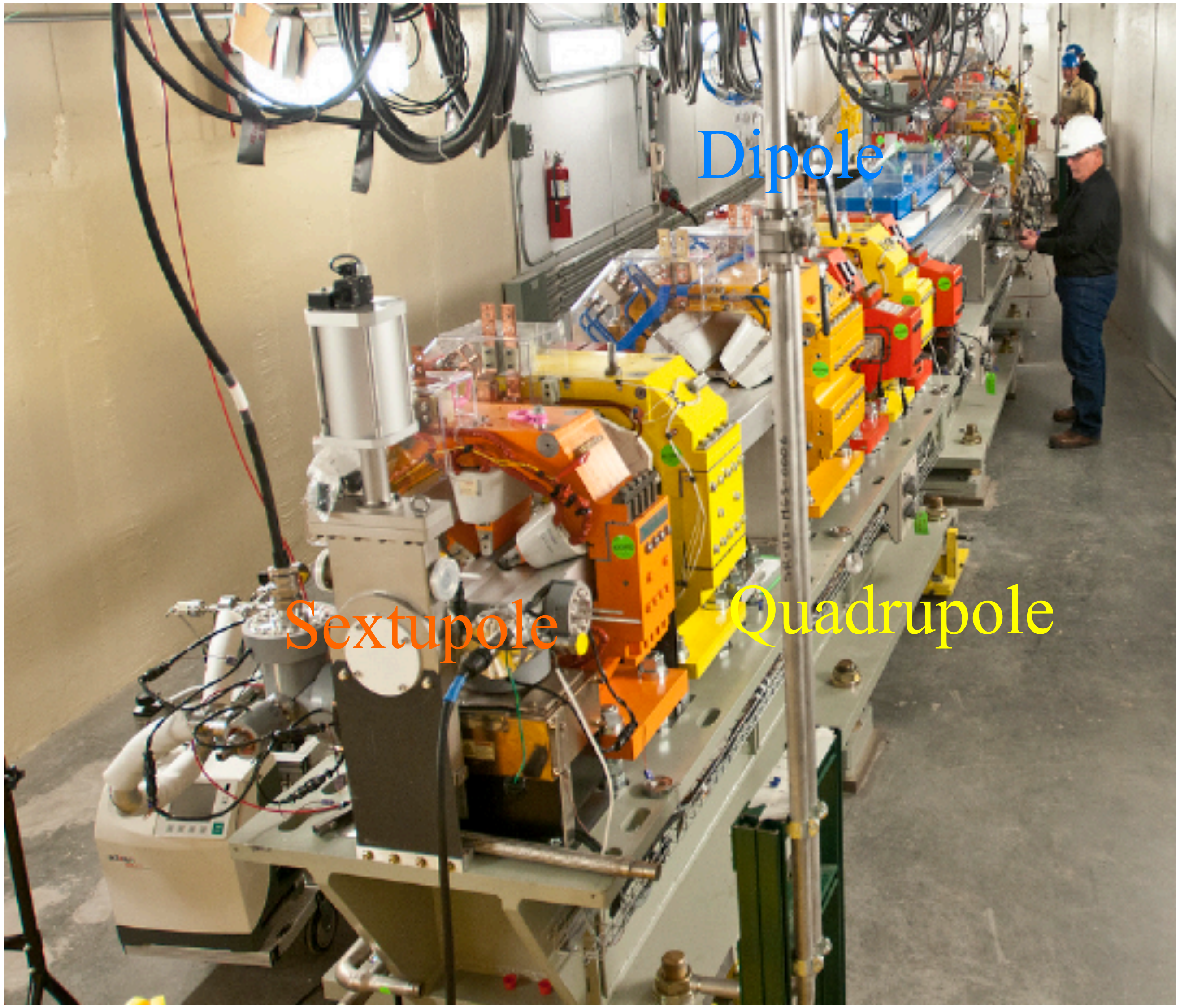

## 1. Tune shift, or tune spread, due to chromatic aberration:

$$\Delta\nu_x = \left[-\frac{1}{4\pi}\oint \beta_x(s)K_x(s)ds\right]\delta \equiv C_x\delta, \quad C_x = d\nu_x/d\delta$$

$$\Delta\nu_z = \left[-\frac{1}{4\pi}\oint \beta_z(s)K_z(s)ds\right]\delta \equiv C_z\delta, \quad C_z = d\nu_z/d\delta$$

The chromaticity induced by quadrupole field error is called natural chromaticity. For a simple FODO cell, we find

$$\Delta\nu_x = \left[-\frac{1}{4\pi}\oint \beta_x(s)K_x(s)ds\right]\delta \approx -\frac{1}{4\pi}\sum \frac{\beta_{xi}}{f_i}\ \delta$$

$$C_{y,\mathrm{nat}}^{\mathrm{FODO}} = -\frac{1}{4\pi}N\left(\frac{\beta_{\max}}{f} - \frac{\beta_{\min}}{f}\right) = -\frac{\tan(\Phi/2)}{\Phi/2}\nu_y \approx -\nu_y$$

We define the specific chromaticity as $\xi_x = C_x/\nu_x, \quad \xi_z = C_z/\nu_z$

The **specific chromaticity is about −1 for FODO cells**, and can be as high as -4 for high luminosity colliders and high brightness electron storage rings.

$$\sin\frac{\Phi}{2} = \frac{L_1}{2f} \qquad \beta_{\max} = \frac{2L_1(1+\sin(\Phi/2))}{\sin\Phi}, \quad \beta_{\min} = \frac{2L_1(1-\sin(\Phi/2))}{\sin\Phi}$$

# Examples:

BNL AGS (E. Blesser 1987):
Chromaticities measured at the AGS.

$$C_{y,\mathrm{nat}}^{\mathrm{FODO}} = -\frac{\tan(\Phi/2)}{\Phi/2}\nu_y \approx -\nu_y$$

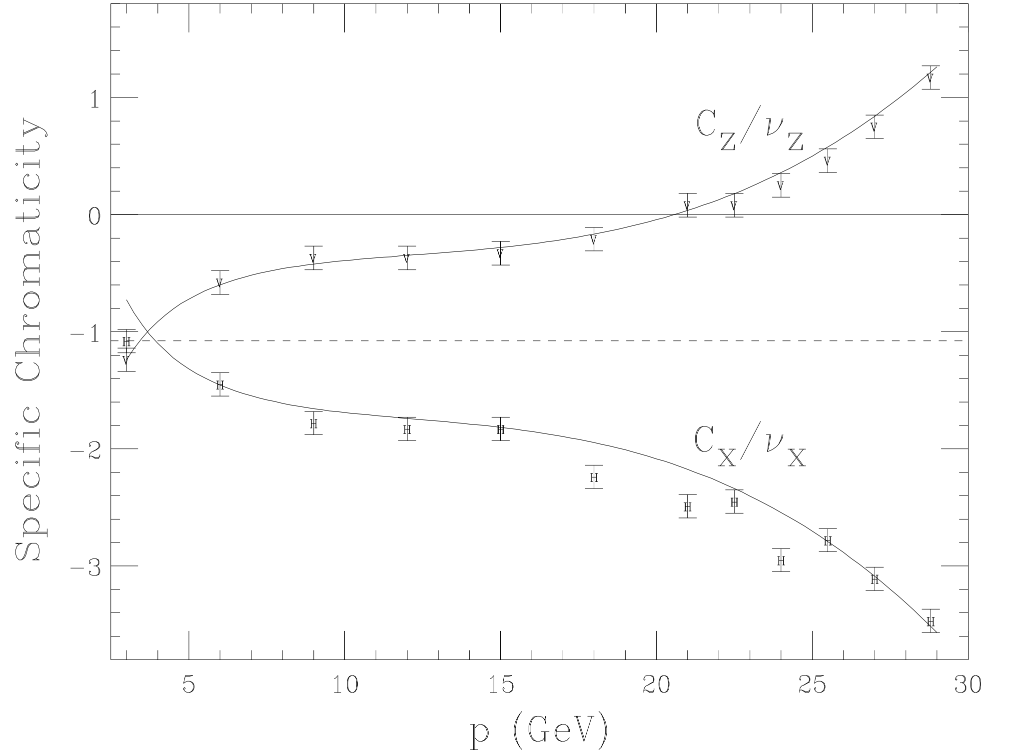


Fermilab Booster (X. Huang, Ph.D. thesis, IU 2005): The measured horizontal chromaticity $C_x$ when SEXTS is on (triangles) or off (stars), and the measured vertical chromaticity $C_z$ when SEXTS is on (dash, circles) or off (squares). The error bar is estimated to be 0.5. The natural chromaticities are $C_{\mathrm{nat},z}=-7.1$ and $C_{\mathrm{nat},x}=-9.2$ for the entire cycle.

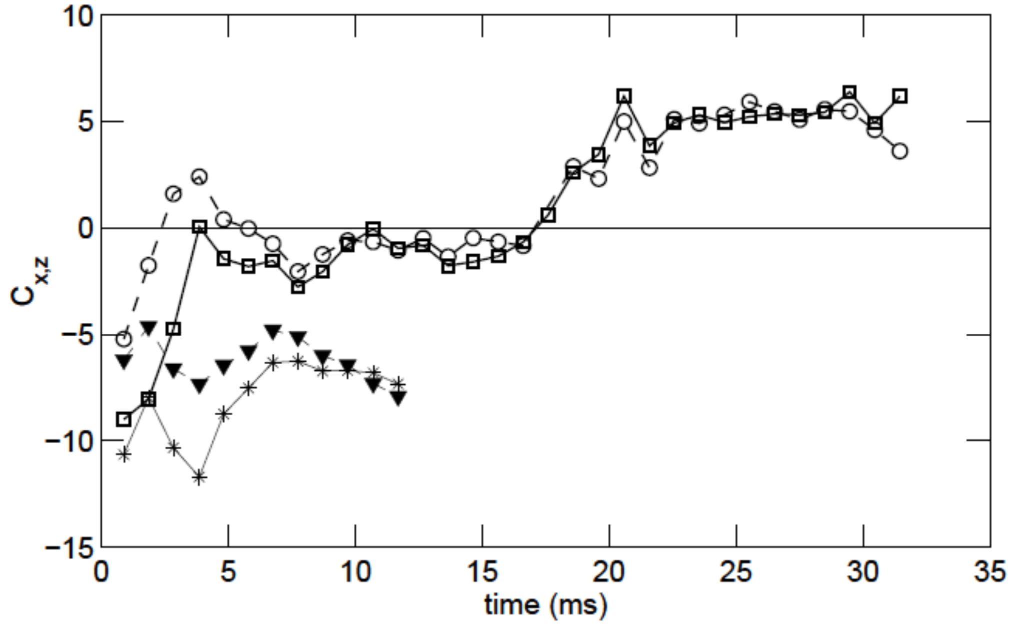

## Chromaticity measurement:

The chromaticity can be measured by measuring the betatron tunes vs the rf frequency f, i.e.

$$\frac{\Delta T}{T_0} = \frac{\Delta C}{C} - \frac{\Delta v}{v} = (\alpha_c - \frac{1}{\gamma^2})\frac{\Delta p}{p_0} = \eta\delta,$$

$$\Delta f / f_0 = -\eta\delta,$$

$$C = \frac{d\nu}{dp/p} = -\eta f_{rf} \frac{d\nu}{df_{rf}}$$

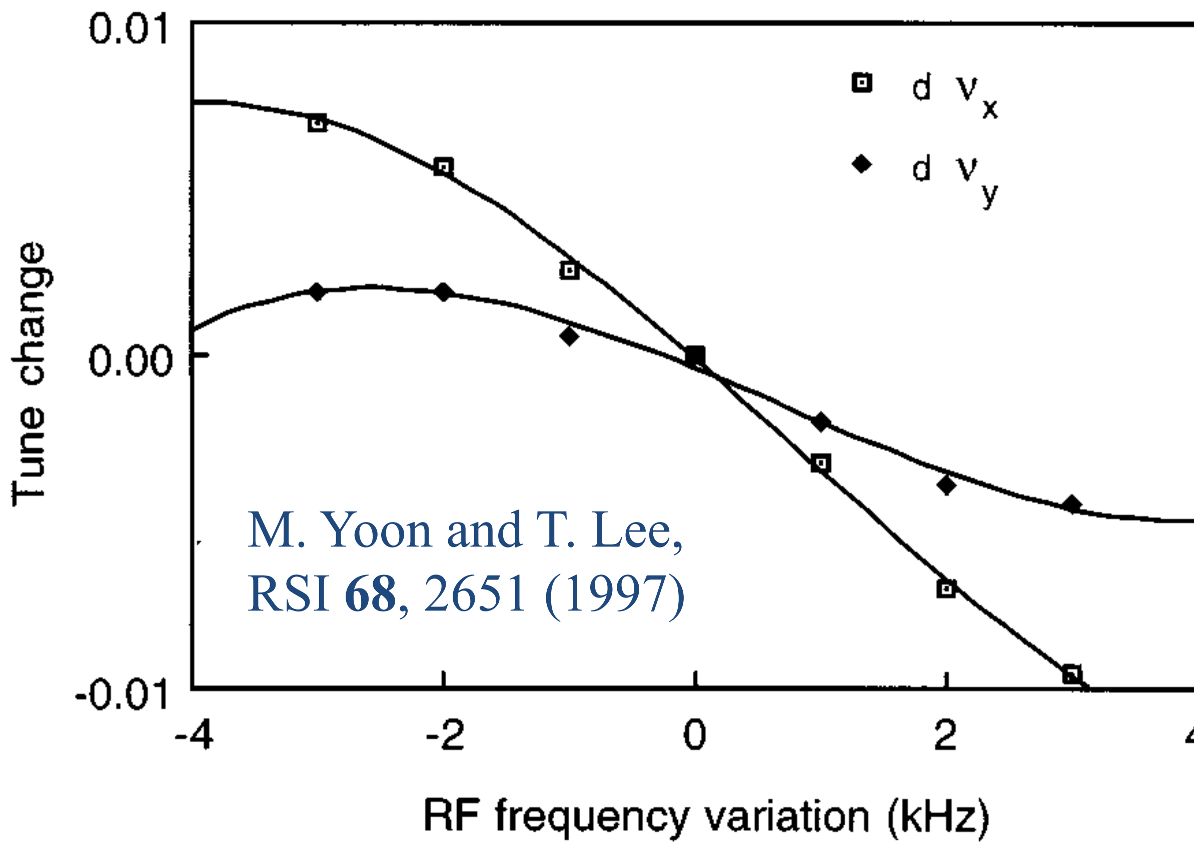


M. Yoon and T. Lee, RSI **68**, 2651 (1997)

The chromaticites are $C_x$=+2.9, $C_y$=+1.4.

The **Natural chromaticity** can be obtained by measuring the tune variation vs the bending-magnet current at a **constant rf frequency**. Change of the bending-magnet current is equivalent to the change of the beam energy. Since the orbit is not changed, the effect of the sextupole magnets on the beam motion can be neglected. The Figure shows the horizontal and vertical tune vs the bending-magnet current in the PLS storage ring.

$$C = \frac{d\nu}{dp/p} = \frac{d\nu}{dB/B} = \frac{d\nu}{dI/I}$$

The data give
$C_x = -18.96$,  $C_z = -13.42$;
vs theory:
$C_x = -23.36$, $C_z = -16.19$.

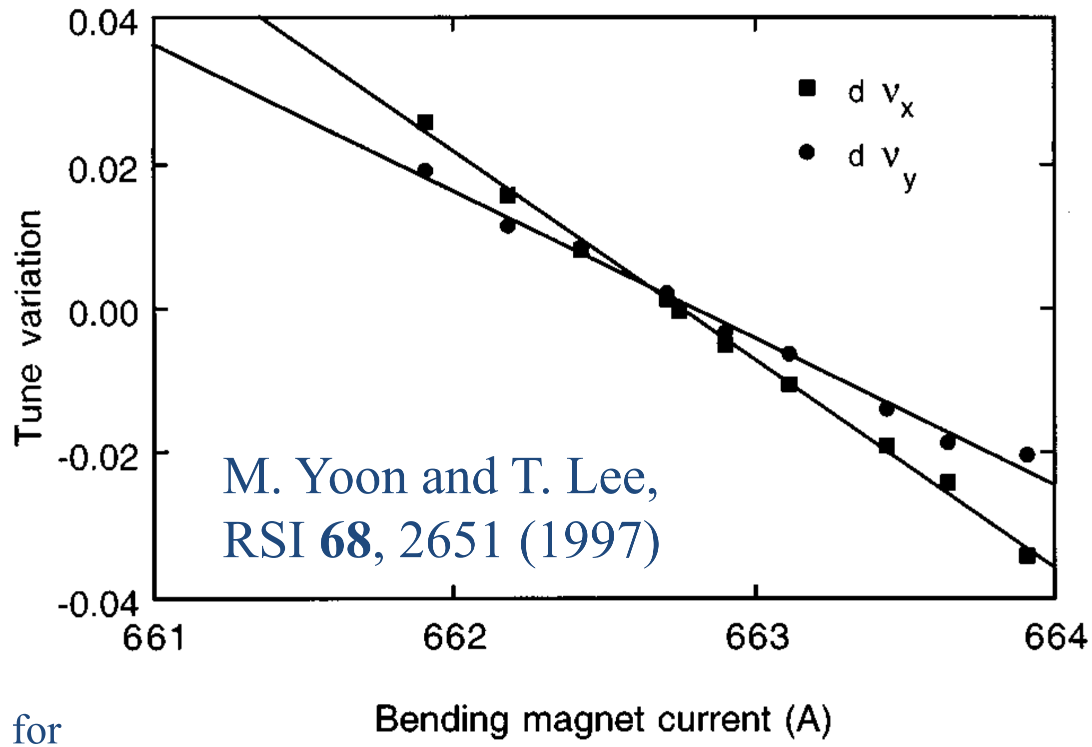


M. Yoon and T. Lee, RSI **68**, 2651 (1997)

Note that this method may not applicable for combined function dipoles.

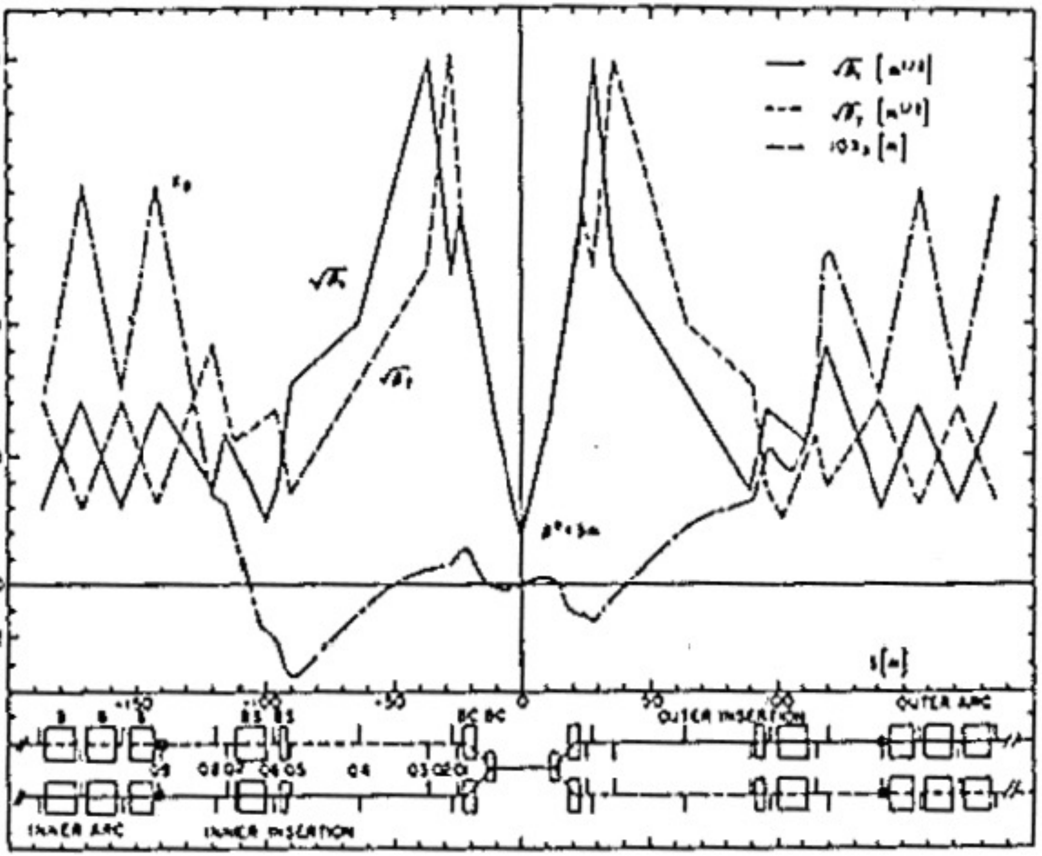

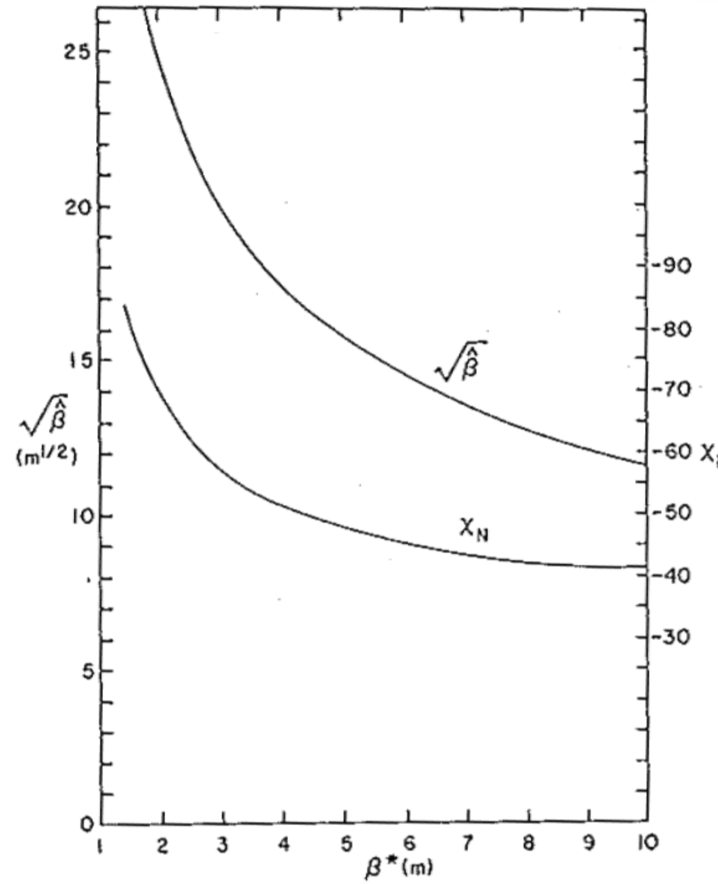


Contribution of low β triplets in an IR to the natural chromaticity is

$$C_{IR} = -\frac{2\Delta s}{4\pi\beta^*} \approx -\frac{1}{2\pi}\sqrt{\frac{\beta_{max}}{\beta^*}}$$

$$C_{total} = N_{IR}C_{IR} + C_{bare\ machine}$$

The total chromaticity is composed of contributions from the low β-quads and the rest of accelerators that is made of FODO cells. The decomposition to fit the data is **Δs≈35** m in RHIC.

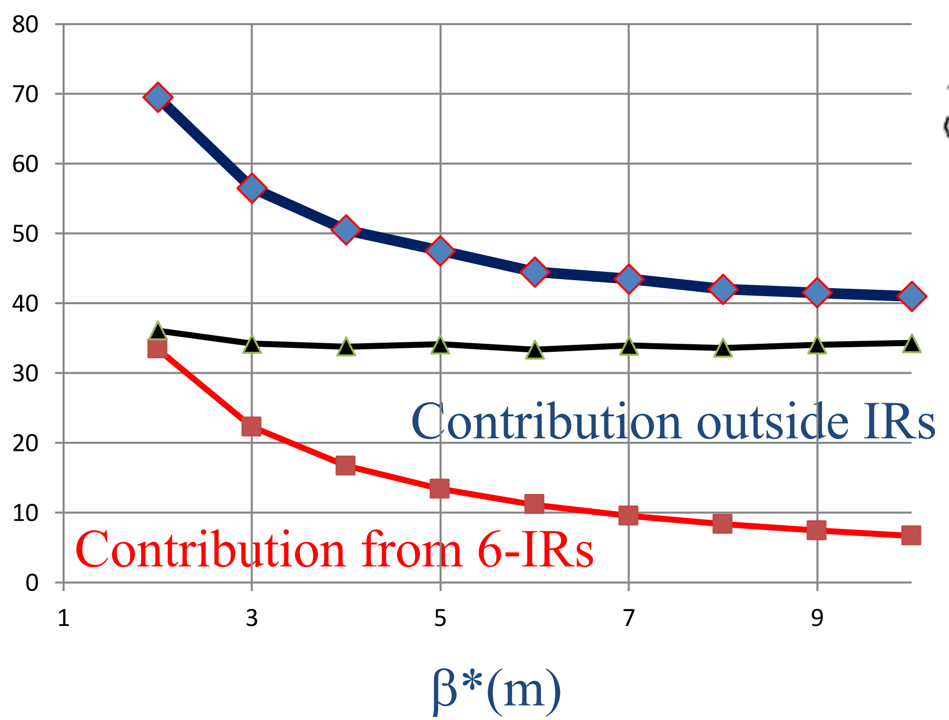


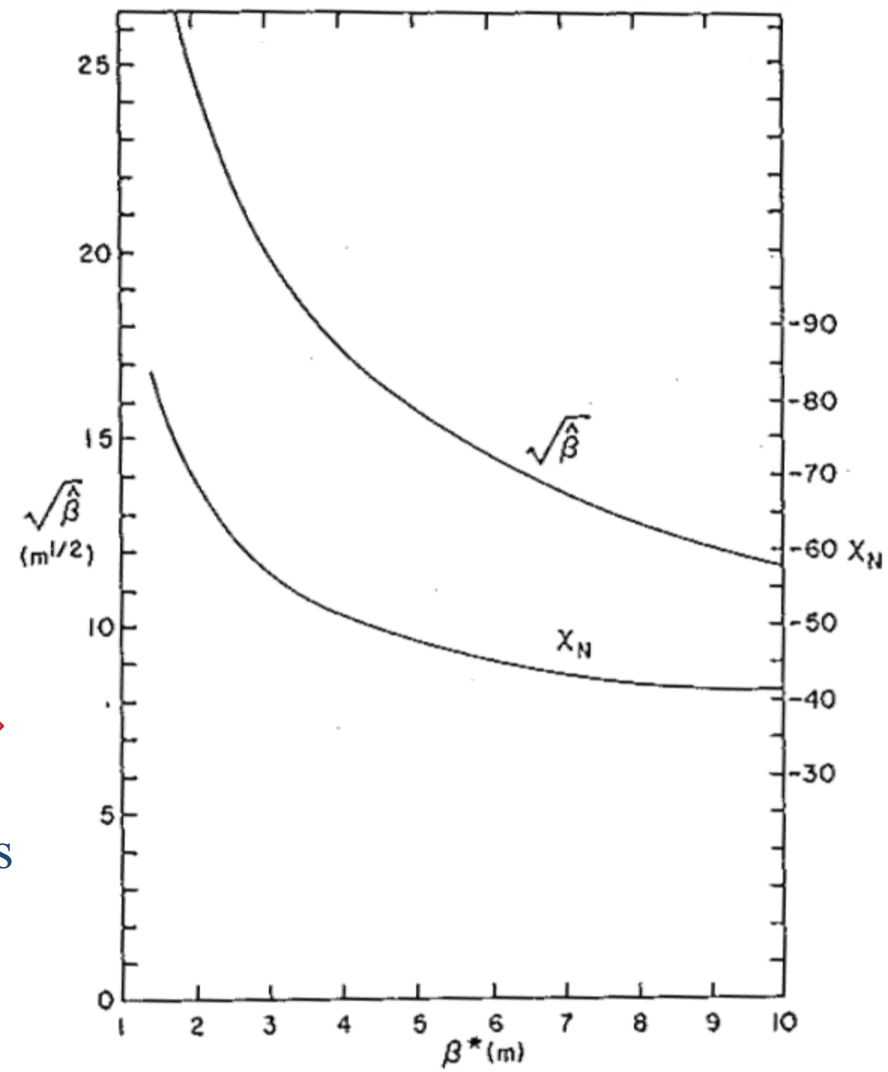

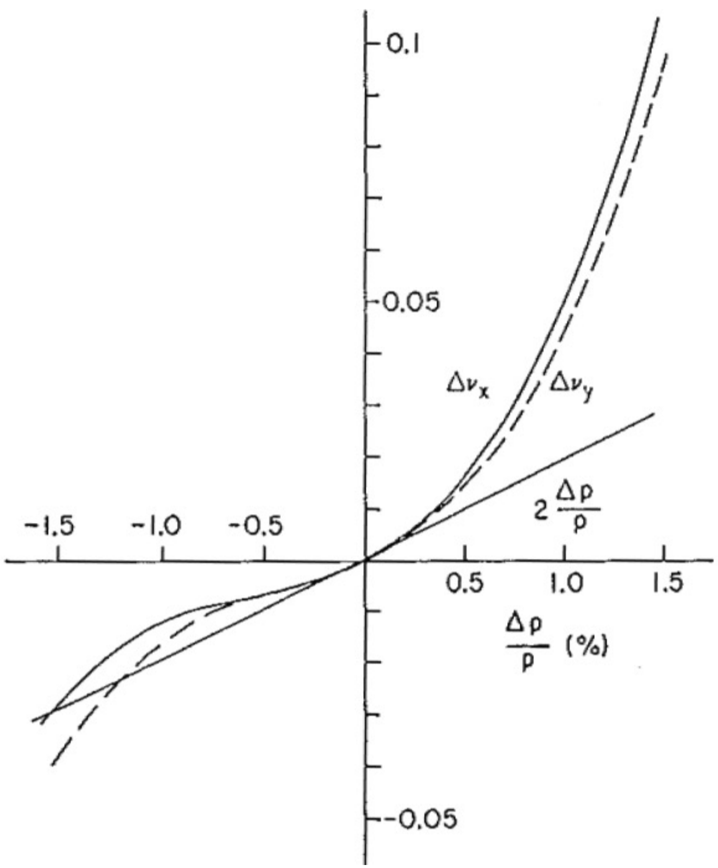


ν vs Δp/p

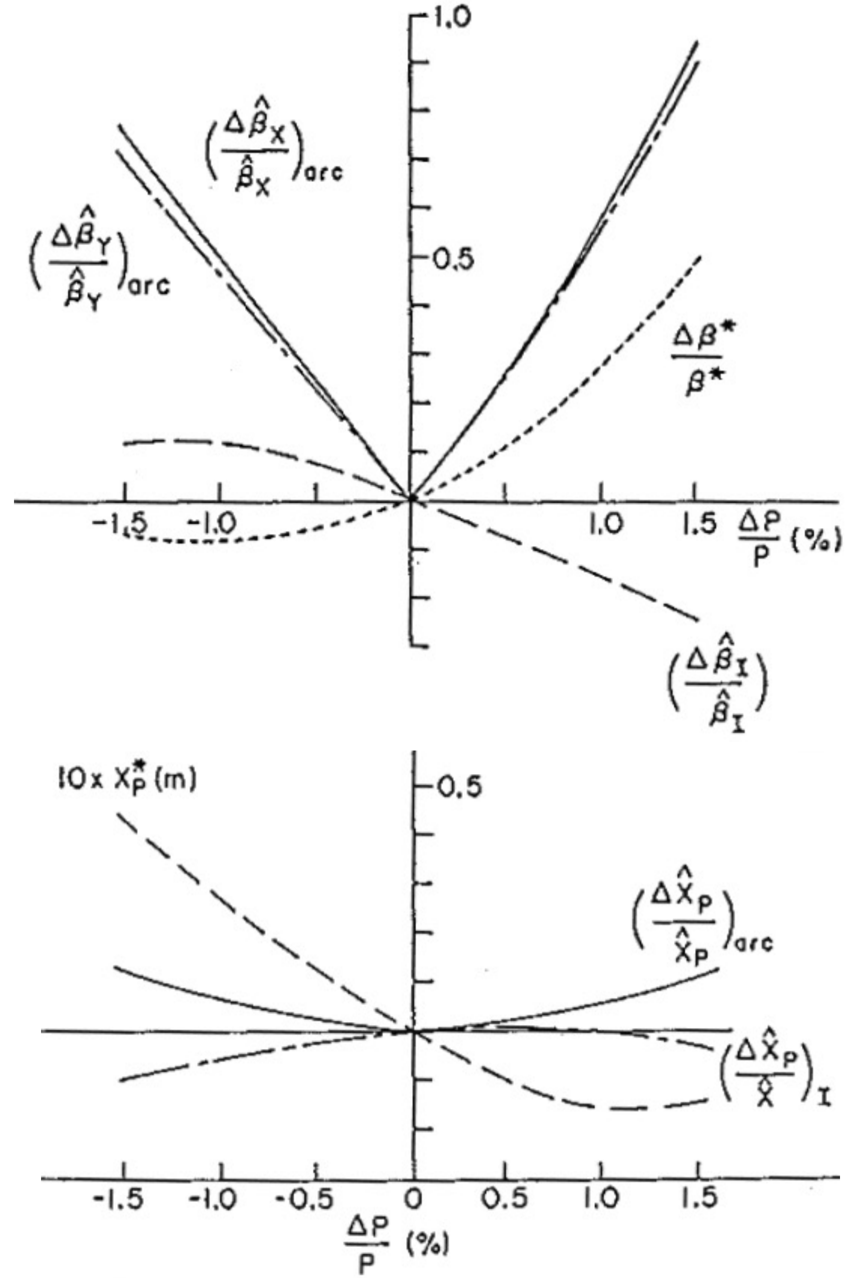


β and D vs Δp/p

## 2. Chromaticity correction:

The chromaticity can cause tune spread to a beam with momentum spread $\Delta\nu = C\delta$. For a beam with $C=-100$, $\delta=0.005$, $\Delta\nu=0.5$. The beam is not stable for most of the machine operation. Furthermore, there exists collective (head-tail) instabilities that requires positive chromaticity for stability! To correct chromaticity, we need to find magnetic field that provide stronger focusing for off-(higher)-momentum particles. We first try sextupole with

$$\Delta B_z + j\Delta B_x = B_0 b_2 (x + jz)^2, \qquad A_s = \tfrac{1}{3}\mathrm{Re}\left\{B_0 b_2 (x + jz)^3\right\}$$

$$x'' + K_x(s)x = \frac{\Delta B_z}{B\rho}, \quad z'' + K_z(s)z = -\frac{\Delta B_x}{B\rho} \qquad \begin{aligned} x &= x_\beta + D\delta \\ z &= z_\beta \end{aligned}$$

$$\Delta B_z = B_0 b_2 (x^2 - z^2) = B_0 b_2 (2x_\beta D\delta + D^2\delta^2 + x_\beta^2 - z_\beta^2)$$

$$\Delta B_x = B_0 b_2 2xz = B_0 b_2 2z_\beta D\delta + B_0 b_2 2x_\beta z_\beta$$

Let $K_2 = -2B_0 b_2/B\rho = -B_2/B\rho$, we obtain:

$$x_\beta'' + (K_x(s) + K_2 D\delta)x_\beta = 0, \quad z_\beta'' + (K_z(s) - K_2 D\delta)z_\beta = 0$$

$$\frac{\Delta B_z}{B\rho} = \frac{B_2}{2B\rho}(x^2 - z^2), \quad \frac{\Delta B_x}{B\rho} = \frac{B_2}{B\rho}xz, \qquad x = x_\beta(s) + D(s)\delta$$

$$\begin{cases} \dfrac{\Delta B_z}{B\rho} = -[S(s)D(s)\delta]x_\beta - \dfrac{S(s)}{2}(x_\beta^2 - z_\beta^2) - \dfrac{S(s)}{2}D^2(s)\delta^2, \\ \dfrac{\Delta B_x}{B\rho} = -[S(s)D(s)\delta]z_\beta - S(s)x_\beta z_\beta, \end{cases} \qquad S(s) = -B_2/B\rho$$

$$\Delta K_x = S(s)D(s)\delta, \quad \Delta K_z = -S(s)D(s)\delta$$

$$C_x = \frac{-1}{4\pi}\oint \beta_x[K_x(s) - S(s)D(s)]ds,$$
$$C_z = \frac{-1}{4\pi}\oint \beta_z[K_z(s) + S(s)D(s)]ds.$$

- In order to minimize their strength, the chromatic sextupoles should be located near quadrupoles, where $\beta_x D_x$ and $\beta_z D_x$ are maximum.
- A large ratio of $\beta_x/\beta_z$ for the focusing sextupole and a large ratio of $\beta_z/\beta_x$ for the defocussing sextupole are needed for optimal independent chromaticity control.
- The families of sextupoles should be arranged to minimize the systematic half-integer stopbands and the third-order betatron resonance strengths.

To model the AGS, we assume that the sextupole fields arise from systematic error at the ends of each dipole, the eddy current sextupole due to the vacuum chamber wall, and the iron saturation sextupole at high field.

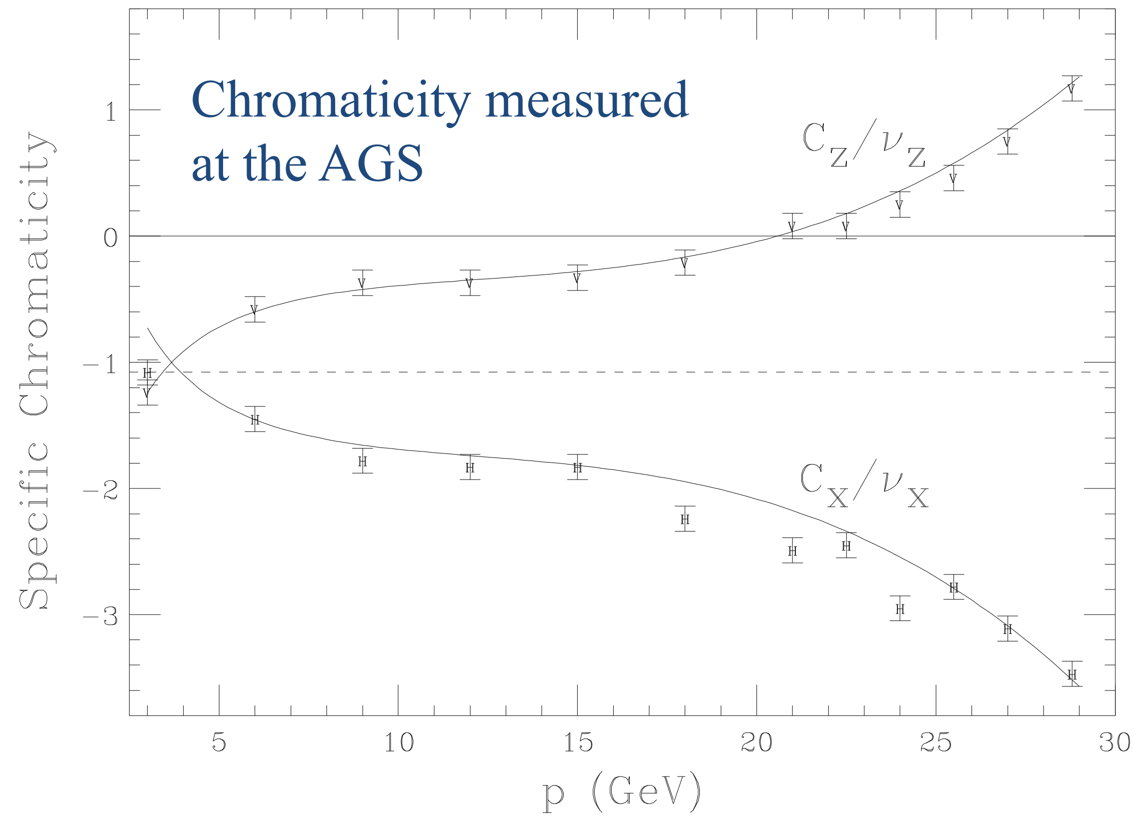


The systematic error is independent of the beam momentum; the eddy current sextupole field depends inversely on the beam momentum; and the saturation sextupole field depends on a higher power of the beam momentum. The solid lines represent theoretical calculations with the integrated body and end sextupole strengths

$$
\begin{aligned}
S_{\rm b} &= -5.2\times 10^{-4} + 5.8\times 10^{-2}/p \\
&\quad -(3.6\times 10^{-4}p - 7.0\times 10^{-5}p^2 + 2.8\times 10^{-6}p^3)\ ({\rm m}^{-2}), \\
S_{\rm e} &= -0.017\ ({\rm m}^{-2}),
\end{aligned}
$$

With sextupoles, the chromaticities becomes

$$C_x = -\tfrac{1}{4\pi}\oint \beta_x(s)[K_x(s) - K_2(s)D(s)]ds$$

$$C_z = -\tfrac{1}{4\pi}\oint \beta_z(s)[K_z(s) + K_2(s)D(s)]ds$$

For FODO cells, the integrated sextupole strength is

$$S_{\mathrm{F}} \equiv K_2\ell_{\mathrm{SF}} = \frac{\sin(\Phi/2)}{2f^2\theta(1+\tfrac{1}{2}\sin(\Phi/2))},\quad S_{\mathrm{D}} \equiv K_{2\mathrm{D}}\ell_{\mathrm{SD}} = -\frac{\sin(\Phi/2)}{2f^2\theta(1-\tfrac{1}{2}\sin(\Phi/2))}$$

For high energy colliders and high brightness synchrotron light sources, the sextupole strength can be much higher. Even more important is the effect of the systematic half-integer stopbands.

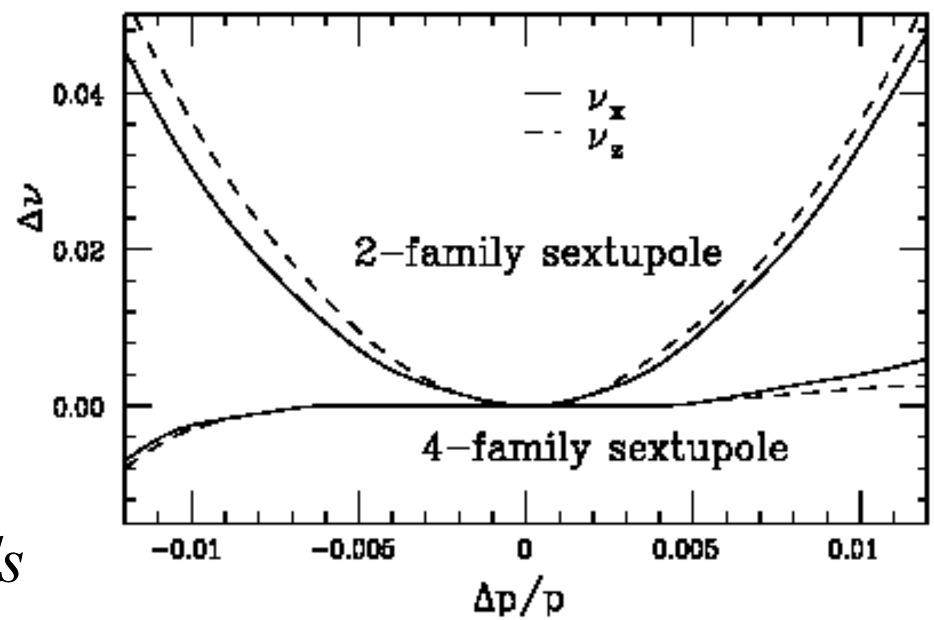


$$J_{y,p} = \frac{1}{2\pi}\oint \left[\beta_y(s)\Delta K_y(s)\right] e^{-jp\phi_y(s)} ds$$

## Chromatic Aberration and Correction

Defining the betatron amplitude difference functions A and B as

$$A = \frac{\alpha_1\beta_0 - \alpha_0\beta_1}{\sqrt{\beta_0\beta_1}}, \quad B = \frac{\beta_1 - \beta_0}{\sqrt{\beta_0\beta_1}}$$

$$\frac{dB}{ds} = -A\left(\frac{1}{\beta_0} + \frac{1}{\beta_1}\right), \quad \frac{dA}{ds} = +B\left(\frac{1}{\beta_0} + \frac{1}{\beta_1}\right) + \sqrt{\beta_0\beta_1}\,\Delta K,$$

where $\Delta K = K_1 - K_0$ is the gradient error; the betatron amplitude functions $\beta_0$ and $\beta_1$ satisfy the Floquet equation

$$\beta_0' = -2\alpha_0, \quad \alpha_0' = K_0\beta_0 - \gamma_0, \quad d\psi_0/ds = 1/\beta_0,$$
$$\beta_1' = -2\alpha_1, \quad \alpha_1' = K_1\beta_1 - \gamma_1, \quad d\psi_1/ds = 1/\beta_1,$$

and $\psi_0$ and $\psi_1$ are the unperturbed and perturbed betatron phase functions.

$A^2 + B^2 =$ constant in regions where $\Delta K = 0$.

The change of A across a quadrupole is

$$\Delta A = \int \sqrt{\beta_0\beta_1}\,\Delta K\, ds \approx -\frac{\beta_0}{f}\frac{\Delta p}{p_0}$$

$$A = \frac{\alpha_1\beta_0 - \alpha_0\beta_1}{\sqrt{\beta_0\beta_1}}, \quad B = \frac{\beta_1 - \beta_0}{\sqrt{\beta_0\beta_1}}$$

$$\frac{dB}{ds} = -A\left(\frac{1}{\beta_0} + \frac{1}{\beta_1}\right), \quad \frac{dA}{ds} = +B\left(\frac{1}{\beta_0} + \frac{1}{\beta_1}\right) + \sqrt{\beta_0\beta_1}\,\Delta K;$$

$$\frac{d^2B}{d\bar{\phi}^2} + 4\bar{\nu}^2 B = -4\bar{\nu}^2\frac{(\beta_0\beta_1)^{3/2}}{\beta_0+\beta_1}\Delta K \qquad \bar{\phi} = \frac{1}{2\bar{\nu}}\int_{s_0}^{s}\left(\frac{1}{\beta_0} + \frac{1}{\beta_1}\right)ds;$$

$$\bar{\nu} = \frac{1}{4\pi}\int_{s_0}^{s_0+C}\left(\frac{1}{\beta_0} + \frac{1}{\beta_1}\right)ds,$$

$$\begin{aligned}\frac{\Delta\beta(s)}{\beta(s)} &= -\frac{1}{2\sin\Phi_0}\int_s^{s+C} k(s_1)\beta(s_1)\cos[2\nu_0(\pi+\phi-\phi_1)]\,ds_1 \\ &= -\frac{\nu_0}{2\sin\Phi_0}\int_\phi^{\phi+2\pi} k(\phi_1)\beta^2(\phi_1)\cos[2\nu_0(\pi+\phi-\phi_1)]\,d\phi_1,\end{aligned}$$

where $\phi = (1/\nu_0)\int_0^s ds/\beta$. It is easy to verify that $\Delta\beta/\beta$ satisfies

$$\frac{d^2}{d\phi^2}\left[\frac{\Delta\beta(s)}{\beta(s)}\right] + 4\nu_0^2\left[\frac{\Delta\beta(s)}{\beta(s)}\right] = -2\nu_0^2\beta^2 k(s).$$

$$\frac{\Delta\beta(s)}{\beta(s)} = -\frac{\nu_0}{2\sin\Phi_0}\int_{\phi}^{\phi+2\pi} d\phi_1 \beta^2(\phi_1) k(\phi_1) \sin 2\nu_0(\pi + \phi - \phi_1)$$

$$\frac{d^2}{d\phi^2}\frac{\Delta\beta(s)}{\beta(s)} + 4\nu_0^2 \frac{\Delta\beta(s)}{\beta(s)} = -2\nu\beta^2 k(s)$$

$$\left[\nu_0 \beta^2 k(s)\right] = \sum_{p=-\infty}^{\infty} J_p e^{jp\varphi},$$

$$J_p = \frac{1}{2\pi}\oint \left[\beta k(s)\right] e^{-jp\varphi} ds$$

Half integer stopband

$$\frac{\Delta\beta(s)}{\beta(s)} = -\frac{\nu_0}{2}\sum_{p=-\infty}^{\infty} \frac{J_p}{\nu_0^2 - (p/2)^2} e^{jp\phi}$$

What symmetry can do to stopbands?

# Systematic chromatic half-integer stopband width

The effect of systematic chromatic gradient error on betatron amplitude modulation can be analyzed by using the chromatic half-integer stopband integrals

$$\begin{cases} J_{p,x} = \dfrac{1}{2\pi}\oint \beta_x \Delta K_x e^{-jp\phi_x} ds, \\ J_{p,z} = \dfrac{1}{2\pi}\oint \beta_z \Delta K_z e^{-jp\phi_z} ds. \end{cases}$$

We consider a lattice made of P superperiods, where L is the length of a superperiod with K(s + L) = K(s), β(s + L) = β(s). Let C = PL be the circumference of the accelerator. The integral becomes

$$\begin{aligned} J_{p,y} &= -\left\{\frac{\delta}{2\pi}\int_0^L \beta_y K_y e^{-jp\phi} ds\right\}\left[1 + e^{-jp\frac{2\pi}{P}} + e^{-j2p\frac{2\pi}{P}} + e^{-j3p\frac{2\pi}{P}} + \cdots\right] \\ &= -\left\{\frac{\delta}{2\pi}\int_0^L \beta_y K_y e^{-jp\phi} ds\right\} \zeta_P\left(\frac{p}{P}\right) e^{-j\pi p\frac{P-1}{P}}, \end{aligned}$$

$$\zeta_P(u) = \frac{\sin(Pu\pi)}{\sin(u\pi)} \qquad\qquad J_{p,y} = 0, \quad \text{unless} \quad p = 0 \ (\text{Mod } P)$$

At $p = 0$ (Mod $P$), the half-integer stopband integral increases by a factor of $P$, i.e. each superperiod contributes additively to the chromatic stopband integral.

Since the perturbation of betatron functions is most sensitive to the chromatic stopbands near $p \approx [2\nu_x]$ and $[2\nu_z]$, a basic design principle of strong-focusing synchrotrons is to avoid important systematic chromatic stopbands. This can be achieved by choosing the betatron tunes such that $[2\nu_x]$ and $[2\nu_z]$ are not divisible by the superperiod $P$. For example, the AGS lattice has $P = 12$, and the betatron tune should avoid a value of 6, 12, 18, etc. The actual betatron tunes at $\nu_{x/z} = 8.8$ are indeed far from systematic half-integer stopbands at $p = 6$ and 12, and the resulting chromatic perturbation is small. In fact, the AGS lattice can be approximated by a lattice made of 60 FODO cells. The important stopbands are located at $p = 30, 60, 90 \cdots$, which are far from the betatron tunes. Similarly, the TEVATRON has a super-periodicity of $P = 6$, and the betatron tune should avoid 18, 24, 30, etc.[90]

Generally, it is beneficial to design an accelerator with high super-periodicity so that the betatron tunes can be located far from the important chromatic stopbands. Some examples of high superperiod machines are $P = 12$ for the ALS, $P = 40$ for the APS, $P = 16$ for the ESRF, and $P = 22$ for the SPRING-8 at JSRF. However, a high energy accelerator or storage ring with large super-periodicity is costly. Thus the goal is to design an accelerator such that the chromatic stopband integral of each module is zero, or the stopband integrals of two modules cancel each other.

# Chromatic stopband integrals of FODO cells

The chromatic stopband integral of the arc, which is composed of N FODO cells, in thin-lens approximation is

$$\begin{aligned} J_p &= -\frac{\delta}{2\pi}\left(\frac{\beta_{\rm max}}{f} - \frac{\beta_{\rm min}}{f}e^{-jp\frac{\Phi}{2\nu}}\right)\left[1 + e^{-jp\frac{\Phi}{\nu}} + e^{-j2p\frac{\Phi}{\nu}} + e^{-j3p\frac{\Phi}{\nu}} + \cdots\right] \\ &= -\frac{2\delta}{\pi\cos\frac{\Phi}{2}}\left(\sin\frac{\Phi}{2}\cos\frac{p\Phi}{4\nu} + j\sin\frac{p\Phi}{4\nu}\right)\,\zeta_N\!\left(\frac{p\Phi}{2\pi\nu}\right)e^{-j\frac{(2N-1)p\pi}{2N}}, \end{aligned}$$

where $\Phi$ is the phase advance per cell, $\beta_{\rm max}$ and $\beta_{\rm min}$ are values of the betatron amplitude function at the focusing and defocussing quadrupoles respectively, $f$ is the focal length of each quadrupole, and the diffracting function $\zeta_N(u)$ is given by Eq. (2.333). If $p\Phi/2\pi\nu = 0$ (Mod $N$), the diffracting function is equal to $N$. This means that each FODO cell contributes additively to the stopband integral. Fortunately, since $\Phi/2\pi$ is normally about 1/4 ($90^0$ phase advance) so that $p\Phi/2\pi\nu \approx p/4\nu \approx 1/2$, the chromatic stopband integral at $p \approx 2\nu$ due to $N$ FODO cells is small. In particular, if $N\Phi =$ integer $\times\pi$, the chromatic stopband of the arc adds up to zero at harmonics $p \approx 2\nu$, i.e. the stopband integrals at $p \approx [2\nu]$ resulting from $N$ FODO cells in the arcs is small if the total phase advance of these FODO cells is $N\Phi =$ integer $\times\,\pi$, where the transfer matrix of the arc becomes a unit matrix $I$ or a half-unit matrix $-I$.

# The chromatic stopband integral of insertions

Let $\Phi^{\text{ins}}$ and $J_p^{\text{ins}}$ be respectively the phase advance and the chromatic stopband integral of an insertion. The total contribution of two adjacent insertions becomes

$$J_p = J_p^{\text{ins}} \left[ 1 + \exp\left( j \frac{p\Phi^{\text{ins}}}{\nu} \right) \right]$$

At the harmonic $p \approx [2\nu]$, we obtain $J_p = 0$ if $\Phi^{\text{ins}} = (2n+1)\pi/2$. Thus, if the insertion is a quarter-wave module, the chromatic stopband integrals of two adjacent insertions cancel each other. This cancellation principle remains valid when two insertions are separated by a unit transfer matrix. Such a procedure was extensively used in the design of the RHIC lattice[92] and the SSC lattice.[93]

# Effect of the chromatic stopbands on chromaticity

$$\frac{\Delta\beta}{\beta} \approx -\frac{|J_p|\cos(p\phi+\chi)}{2(\nu-p/2)}$$

$$\Delta\nu_y = C_y^{(1)}\delta + C_y^{(2)}\delta^2 + \cdots$$

$$C_y^{(1)} = -\frac{1}{4\pi}\oint \beta_y(K_y - S_y D)ds,$$

$$C_y^{(2)} = -C_y^{(1)} - \frac{|J_{p,y}|^2/\delta^2}{4(\nu_y - p/2)}.$$

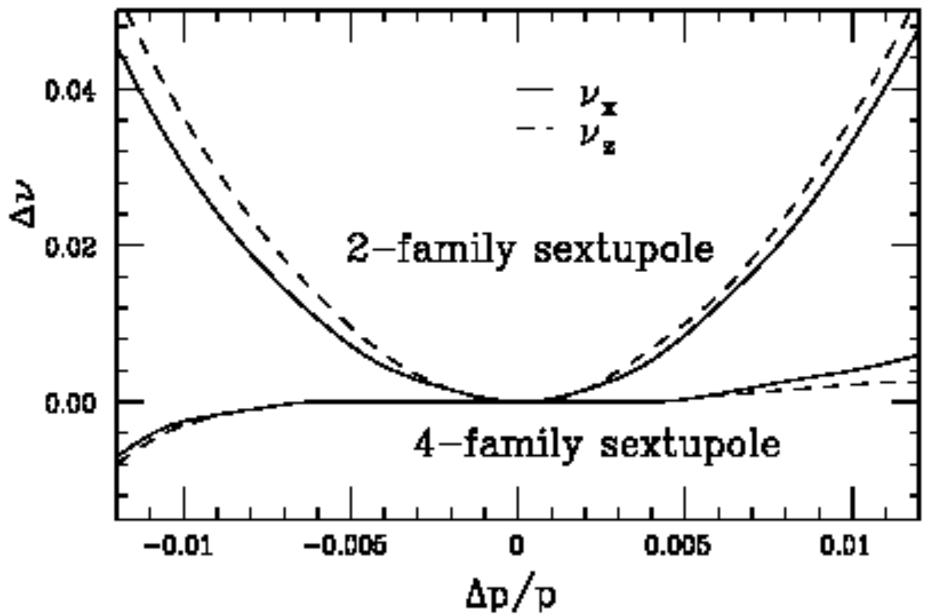

# Effect of sextupoles on the chromatic stopband integrals

First we evaluate the stopband integral due to the chromatic sextupoles. Let $S_{\rm F}$ and $S_{\rm D}$ be the integrated sextupole strength at QF and QD of FODO cells in the arc. The $p$-th harmonic stopband integral from these chromatic sextupoles is

$$J_{p,\rm sext} = \frac{\delta}{2\pi}\zeta_N\left(\frac{p\Phi}{2\pi\nu}\right)\left[\beta_{\rm F}S_{\rm F}D_{\rm F} + \beta_{\rm D}S_{\rm D}D_{\rm D}e^{-jp\Phi/2\nu}\right]e^{-j(N-1)p\Phi/2\nu},$$

The stopband integral is zero or small if $N\Phi/\pi$ = integer, i.e. the chromatic sextupole does not contribute significantly to the chromatic stopband integral if the transfer matrix of the arc is I or −I.

To obtain a nonzero chromatic stopband integral, sextupoles are organized in families. We consider an example of a four-family scheme with

$$\{S_{\rm F1} = S_{\rm F} + \Delta_{\rm F},\ S_{\rm D1} = S_{\rm D} + \Delta_{\rm D},\ S_{\rm F2} = S_{\rm F} - \Delta_{\rm F},\ D_{\rm D2} = S_{\rm D} - \Delta_{\rm D}\},$$

that is commonly used in FODO cells with 90° phase advance. Here the parameters $S_{\rm F}$ and $S_{\rm D}$ are determined from the first-order chromaticity correction, Since $\beta(s)$ and $D(s)$ are periodic functions of $s$ in the repetitive FODO cells, the parameters $\Delta_{\rm F}, \Delta_{\rm D}$ will not affect the first-order chromaticity, which is proportional to the zeroth harmonic of the stopband integral. However, the chromatic stopband integrals due to the parameters $\Delta_{\rm F}$ and $\Delta_{\rm D}$ are given by

$$\Delta J_{p,\rm sext} = \frac{\delta}{2\pi}\zeta_N\left(\frac{p\Phi}{2\nu\pi} - \frac{1}{2}\right)\left[\beta_{\rm F}\Delta_{\rm F}D_{\rm F} + \beta_{\rm D}\Delta_{\rm D}D_{\rm D}e^{-jp\Phi/4\nu}\right]e^{-j(N-1)[(p\Phi/2\nu\pi)-(1/2)]\pi}.$$

At $p \approx [2\nu]$ and $\Phi/2\pi \approx 1/4$ (90° phase advance), we have $\zeta_N \to N$, i.e. every FODO cell contributes additively to the chromatic stopband. The resulting stopband width is proportional to $\Delta_F$ and $\Delta_D$ parameters. By adjusting $\Delta_F$ and $\Delta_D$ parameters, the betabeat and the second-order chromaticity can be minimized. The scheme works best for a nearly 90° phase advance per cell with $N\Phi = \text{integer} \times \pi$, where the third-order resonance-driving term vanishes also for the four-family sextupole scheme. Fig. 2.42 shows an example of chromatic correction with four families of sextupoles in RHIC, where the second-order chromaticity and the betatron amplitude modulation can be simultaneously corrected.

Similarly, the six-family sextupole scheme works for 60° phase advance FODO cells, where the six-family scheme

$$\{S_{\rm F1}, S_{\rm D1}, S_{\rm F2}, D_{\rm D2}, S_{\rm F3}, S_{\rm D3}\} \tag{2.342}$$

has two additional parameters.

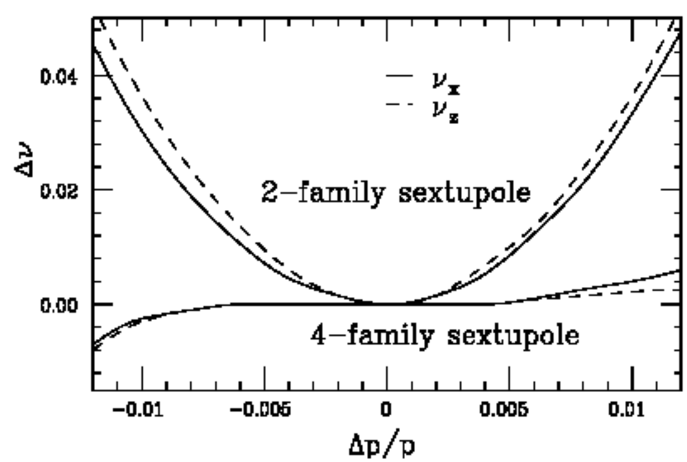

# Third order Resonances

$$H = \frac{1}{2}x'^2 + \frac{1}{2}K_x(s)x^2 + \frac{1}{2}z'^2 + \frac{1}{2}K_z(s)z^2 - eA_{s,NL}(x,z,s)$$

$$\widetilde{H} = \nu_x J_x + \nu_z J_z - eA_{s,NL}(J_x,\psi_x,J_x,\psi_x,\theta)$$

$$A_x = A_z = 0, \quad A_s = \frac{B_2}{6}(x^3 - 3xz^2), \qquad B_2 = \partial^2 B_z/\partial x^2\big|_{x=z=0}$$

$$H = \frac{1}{2}\left[x'^2 + K_x x^2 + z'^2 + K_z z^2\right] + V_3(x,z,s),$$

$$V_3(x,z,s) = \tfrac{1}{6}S(s)(x^3 - 3xz^2) \qquad S(s) = -\frac{B_2(s)}{B\rho}$$

$$x'' + K_x(s)x = -\frac{1}{2}S(s)(x^2 - z^2), \qquad z'' + K_z(s)z = +S(s)xz.$$

$$\Delta x' = -\frac{1}{2}\bar{S}(x^2 - z^2), \qquad \Delta z' = \bar{S}xz.$$

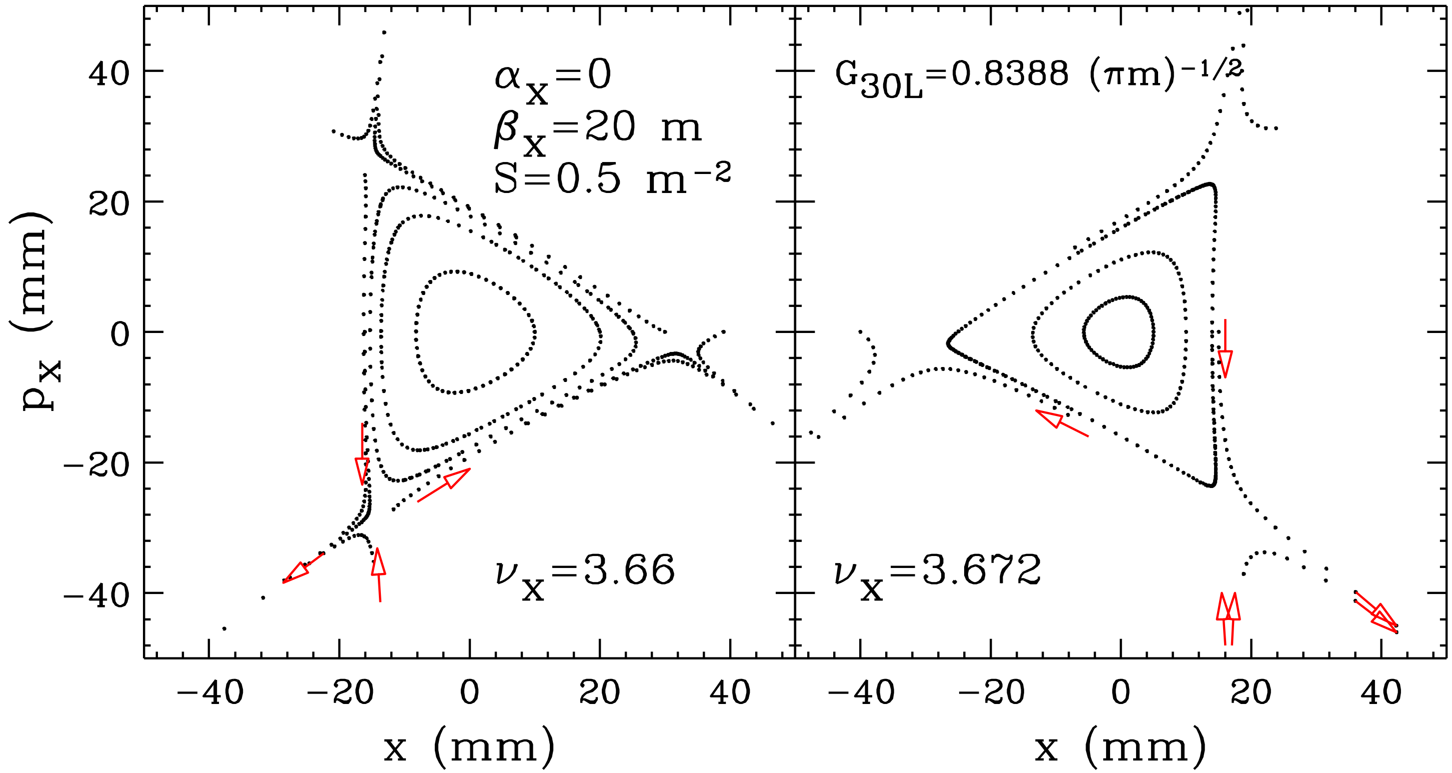


The Poincar´e maps for betatron motion perturbed by a single sextupole magnet at a tune below (left) and above (right) a third order resonance. The integrated sextupole strength is S=0.5m$^{-2}$ with lattice parameters $\beta_x$=20m, and $\alpha_x$=0. Arrows indicate directions of motion near a separatrix.

# The leading order resonances driven by sextupoles

$$y = \sqrt{2\beta\bar{J}}\cos\left(\bar{\psi} + \chi(s) - \nu\theta\right),$$
$$\mathcal{P}_y = \beta y' + \alpha y = -\sqrt{2\beta\bar{J}}\sin(\bar{\psi} + \chi(s) - \nu\theta),$$

$$\chi(s) = \int_0^s \frac{ds}{\beta}$$

$$x = \sqrt{2\beta_x J_x}\cos\Phi_x, \quad z = \sqrt{2\beta_z J_z}\cos\Phi_z$$

$$\Phi_x = \psi_x + \chi_x(s) - \nu_x\theta, \quad \Phi_z = \psi_z + \chi_z(s) - \nu_z\theta$$

$$H = \frac{1}{2}\left[x'^2 + K_x x^2 + z'^2 + K_z z^2\right] + V_3(x, z, s),$$

$$V_3(x, z, s) = \tfrac{1}{6}S(s)(x^3 - 3xz^2)$$

$$V_3 = \tfrac{1}{6}S(s)[2^{3/2}\beta_x^{3/2}J_x^{3/2}\cos^3\Phi_x - 3\cdot 2^{3/2}\beta_x^{1/2}J_x^{1/2}\beta_z J_z\cos\Phi_x\cos^2\Phi_z]$$
$$= \tfrac{\sqrt{2}}{12}S(s)\beta_x^{3/2}J_x^{3/2}\cos 3(\psi_x + \chi(s) - \nu_x\theta) + \ldots.$$

$$H = \nu_x J_x + \nu_z J_z + \sum_\ell G_{3,0,\ell}J_x^{3/2}\cos(3\psi_x - \ell\theta + \xi_{3,0,\ell}) + \ldots$$

$$G_{3,0,\ell}e^{j\xi_{3,0,\ell}} = \tfrac{\sqrt{2}}{24\pi}\oint S(s)\beta_x^{3/2}\exp(j[3\chi(s) - (3\nu_x - \ell)\theta])ds$$

$$
\begin{aligned}
H &= \nu_x J_x + \nu_z J_z + \sum_\ell G_{3,0,\ell} J_x^{3/2} \cos(3\phi_x - \ell\theta + \xi_{3,0,\ell}) \\
&\quad + \sum_\ell G_{1,2,\ell} J_x^{1/2} J_z \cos(\phi_x + 2\phi_z - \ell\theta + \xi_{1,2,\ell}) \\
&\quad + \sum_\ell G_{1,-2,\ell} J_x^{1/2} J_z \cos(\phi_x - 2\phi_z - \ell\theta + \xi_{1,-2,\ell}) + \cdots,
\end{aligned}
$$

where $\ell$ is an integer, $G_{3,0,\ell}$, $G_{1,2,\ell}$, $G_{1,-2,\ell}$ are Fourier amplitudes, $\xi_{3,0,\ell}$, $\xi_{1,2,\ell}$, $\xi_{1,-2,\ell}$ are the phase of the Fourier components, and $\cdots$ describes the remaining resonance driving terms at $\nu_x =$ integers. The Fourier amplitude $G_{3,0,\ell}$ drives the third order resonance at $3\nu_x = \ell$, and similarly, $G_{1,2,\ell}$ and $G_{1,-2,\ell}$ drive $\nu_x+2\nu_z = \ell$ and $\nu_x-2\nu_z = \ell$ resonances.

# The third order resonance at $3\nu_x = \ell$

The Hamiltonian near a third-order resonance at $3\nu_x = \ell$ is

$$H \approx \nu_x J_x + G_{3,0,\ell}\, J_x^{3/2} \cos\left(3\phi_x - \ell\theta + \xi\right)$$

where $G_{3,0,\ell}$ is the resonance strength, $J_x$, $\phi_x$ are conjugate phase-space coordinates, $\theta$ is the orbiting angle serving time coordinate, $\nu_x$ is the horizontal betatron tune.

$$G_{3,0,\ell}\, e^{j\xi_{3,0,\ell}} = \frac{\sqrt{2}}{24\pi} \oint \beta_x^{3/2}\, K_2(s)\, e^{j[3\chi_x(s)-(3\nu_x-\ell)\theta]} ds$$

Transform the phase space coordinate to a *resonance rotating frame* with a generating function to obtain new phase-space coordinates:

$$F_2 = (\phi_x - \frac{\ell}{3}\theta + \frac{\xi}{3})J, \quad \Longrightarrow \quad \phi = \phi_x - \frac{\ell}{3}\theta + \frac{\xi}{3}, \quad J = J_x.$$

The new Hamiltonian and Hamilton's equations of motion are

$$H = \delta J + G_{3,0,\ell} J^{3/2} \cos 3\phi,$$

$$\dot{\phi} \equiv \frac{d\phi}{d\theta} = \delta + \frac{3}{2} G_{3,0,\ell} J^{1/2} \cos 3\phi, \qquad \dot{J} \equiv \frac{dJ}{d\theta} = 3G_{3,0,\ell} J^{3/2} \sin 3\phi.$$

where $\delta = \nu_x - \ell/3$ is the resonance proximity parameter.

The fixed points (FPs) of the Hamiltonian are determined by $dJ/d\theta=0$ and $d\phi/d\theta=0$. Without nonlinear detuning, there is no stable fixed point for the third order resonance. The action and Hamiltonian value at the UFP, and small amplitude motion near the UFP are

$$J_{\rm UFP}^{1/2} = \left|\frac{2\delta}{3G_{3,0,\ell}}\right| \quad \text{with} \quad \begin{cases} \phi_{\rm FP} = 0,\ \pm 2\pi/3, & \text{if } \delta/G_{3,0,\ell} < 0, \\ \phi_{\rm FP} = \pm\pi/3,\ \pi, & \text{if } \delta/G_{3,0,\ell} > 0. \end{cases}$$

$$E_{\rm UFP} = \frac{\delta}{3}\left(\frac{2\delta}{3G_{3,0,\ell}}\right)^2,$$

$$\ddot{K} - 3\delta^2 K - 6\frac{\delta^2}{J_{\rm UFP}}K^2 = 0, \qquad K = J - J_{\rm UFP}$$

The motion near the fixed point is hyperbolic. Because of nonlinear term in the Equation above, the amplitude will grow faster than an exponential. The direction of particle motion near a separatrix is marked with arrows in the Figure.

Without a nonlinear detuning term, the third-order resonance appears at all values of δ. The stable motion is bounded by the curve of $J^{1/2}_{UFP}$. For a given aperture $J_{max}$ the width of the third-order betatron resonance is

$$|\delta|_{\rm width} = 3G_{3,0,\ell}\hat{J}^{1/2}/2.$$

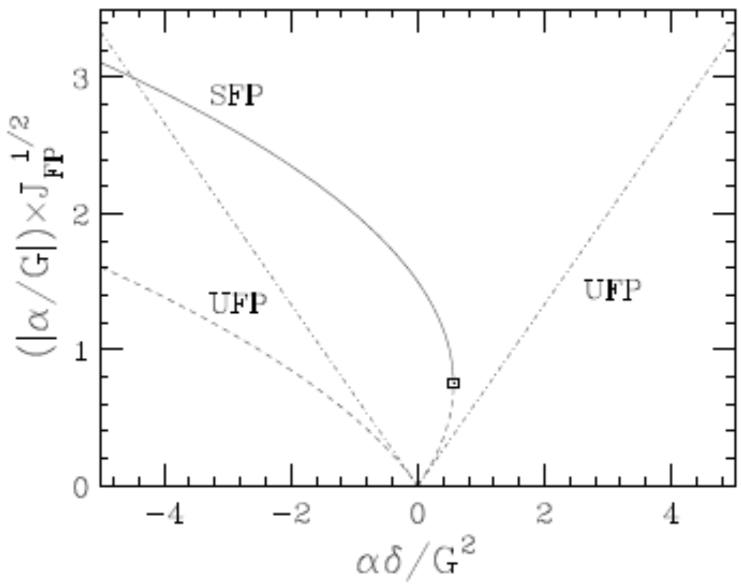


# Separatrix

The separatrix is the Hamiltonian torus that passes through the UFP, i.e. $H = E_{UFP}$. The separatrix orbit, for $\delta/G_{3,0,\ell} > 0$,

$$[2X-1]\left[P-\frac{1}{\sqrt{3}}(X+1)\right]\left[P+\frac{1}{\sqrt{3}}(X+1)\right]=0$$

$$X=\sqrt{J/J_{\rm UFP}}\cos\phi,\quad P=-\sqrt{J/J_{\rm UFP}}\sin\phi$$

$$X = 1/2$$
$$P = \tfrac{1}{\sqrt{3}}(X+1)$$
$$P = -\tfrac{1}{\sqrt{3}}(X+1)$$

$$(X,P)_{\rm UFP} = (-1,0),\quad (\frac{1}{2},\frac{\sqrt{3}}{2}),\quad (\frac{1}{2},-\frac{\sqrt{3}}{2})$$

Nonlinearity in accelerators has been employed to provide

- Beam manipulations such as slow extraction, beam dilution
- Landau damping for collective beam instabilities
- Overcoming spin depolarization resonances

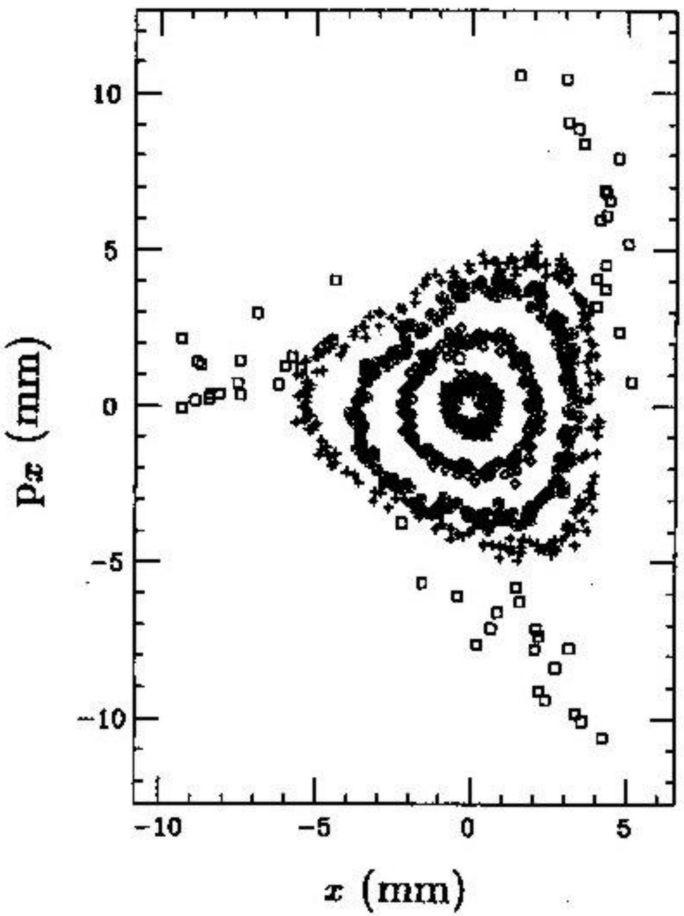


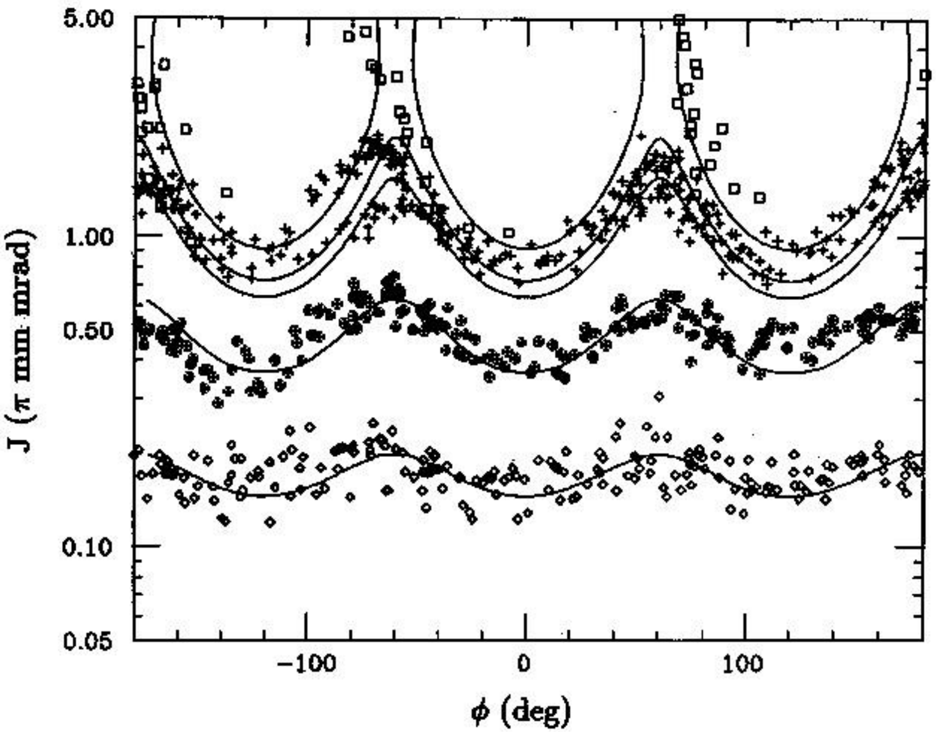

# Nonlinear detuning parameters:

Accelerator magnets may have many nonlinear magnetic multipoles. Some of them can introduce nonlinear perturbation to betatron motion, e.g.

$$V(s) = \frac{1}{6}K_2(s)(x^3 - 3xz^2) + \frac{1}{24}K_3(s)(x^4 - 6x^2z^2 + z^4) + \cdots$$

With Floquet transformation, the Hamiltonian becomes

$$H = \nu_x J_x + \nu_z J_z + \frac{1}{2}\alpha_{xx} {J_x}^2 + \alpha_{xz} J_x J_z + \frac{1}{2}\alpha_{zz} {J_z}^2 + \ldots\ldots$$

$$\alpha_{xx} = \frac{1}{16\pi}\oint \beta_x^2 K_3 ds, \quad \alpha_{xz} = \frac{-1}{8\pi}\oint \beta_x\beta_z K_3 ds, \quad \alpha_{zz} = \frac{1}{16\pi}\oint \beta_z^2 K_3 ds.$$

$$Q_x = \frac{d\psi_x}{d\theta} = \frac{\partial H}{\partial J_x} \approx \nu_x + \alpha_{xx} J_x + \alpha_{xz} J_z + \cdots$$

$$Q_z = \frac{d\psi_z}{d\theta} = \frac{\partial H}{\partial J_z} \approx \nu_z + \alpha_{xz} J_x + \alpha_{zz} J_z + \cdots$$

The coefficients α’s are called nonlinear detuning parameters

Betatron detuning: chromaticity $\Delta\nu_y = C_y^{(1)}\delta + C_y^{(2)}\delta^2 + \cdots$

octupole
$$Q_x = \nu_x + \alpha_{xx}J_x + \alpha_{xz}J_z$$
$$Q_z = \nu_z + \alpha_{xz}J_x + \alpha_{zz}J_z \qquad +\ldots..$$

$$\alpha_{xx} = \frac{1}{16\pi}\oint \beta_x^2 K_3 ds, \quad \alpha_{xz} = \frac{-1}{8\pi}\oint \beta_x\beta_z K_3 ds, \quad \alpha_{zz} = \frac{1}{16\pi}\oint \beta_z^2 K_3 ds.$$

sextupole

$$\alpha_{xx} = \frac{1}{64\pi}\sum_{i,j} S_i S_j \beta_{x,i}^{3/2}\beta_{x,j}^{3/2}\left[\frac{\cos 3(\pi\nu_x - |\psi_{x,ij}|)}{\sin 3\pi\nu_x} + 3\frac{\cos(\pi\nu_x - |\psi_{x,ij}|)}{\sin\pi\nu_x}\right],$$

$$\begin{aligned}\alpha_{xz} = \frac{1}{32\pi}\Bigg\{&\sum_{i,j} S_i S_j \beta_{x,i}^{1/2}\beta_{x,j}^{1/2}\beta_{z,i}\beta_{z,j}\left[\frac{\cos[2(\pi\nu_z - |\psi_{z,ij}|) + \pi\nu_x - |\psi_{x,ij}|]}{\sin\pi(2\nu_z + \nu_x)}\right.\\ &\left. + \frac{\cos[2(\pi\nu_z - |\psi_{z,ij}|) - (\pi\nu_x - |\psi_{x,ij}|)]}{\sin\pi(2\nu_z - \nu_x)}\right]\\ &-2\sum_{i,j} S_i S_j \beta_{x,i}^{3/2}\beta_{x,j}^{1/2}\beta_{z,j}\frac{\cos(\pi\nu_x - |\psi_{x,ij}|)}{\sin\pi\nu_x}\Bigg\},\end{aligned}$$

$$\begin{aligned}\alpha_{zz} = \frac{1}{64\pi}&\sum_{i,j} S_i S_j \beta_{x,i}^{1/2}\beta_{x,j}^{1/2}\beta_{z,i}\beta_{z,j}\left[\frac{\cos[2(\pi\nu_z - |\psi_{z,ij}|) + \pi\nu_x - |\psi_{x,ij}|]}{\sin\pi(2\nu_z + \nu_x)}\right.\\ &\left. + \frac{\cos[2(\pi\nu_z - |\psi_{z,ij}|) - (\pi\nu_x - |\psi_{x,ij}|)]}{\sin\pi(2\nu_z - \nu_x)} + 3\frac{\cos(\pi\nu_x - |\psi_{x,i} - \psi_{x,j}|)}{\sin\pi\nu_x}\right],\end{aligned}$$

# Effect of nonlinear detuning

Nonlinear magnetic multipoles also generate nonlinear betatron detuning, i.e. the betatron tunes depend on the betatron actions. Including the effect of nonlinear betatron detuning, the Hamiltonian near a third-order resonance is

$$H = \delta J + \frac{1}{2}\alpha J^2 + G J^{3/2} \cos 3\phi$$

With nonlinear detuning, stable fixed points appear. The fixed points of the Hamiltonian for á > 0 and G > 0 are

$$\frac{\alpha J_{\rm FP}^{1/2}}{G} = \begin{cases} -\frac{3}{4} + \frac{3}{4}\sqrt{1 - \frac{16\alpha\delta}{9G^2}}, & \phi = 0, \pm 2\pi/3 \quad \delta < 0 \qquad \text{(UFP)} \\ +\frac{3}{4} - \frac{3}{4}\sqrt{1 - \frac{16\alpha\delta}{9G^2}}, & \phi = \pi, \pm\pi/3 \quad 0 \le \delta \le \frac{9G^2_{3,0,\ell}}{16\alpha} \qquad \text{(UFP)} \\ +\frac{3}{4} + \frac{3}{4}\sqrt{1 - \frac{16\alpha\delta}{9G^2}}, & \phi = \pi, \pm\pi/3 \quad \delta \le \frac{9G^2}{16\alpha} \qquad \text{(SFP)} \end{cases}$$

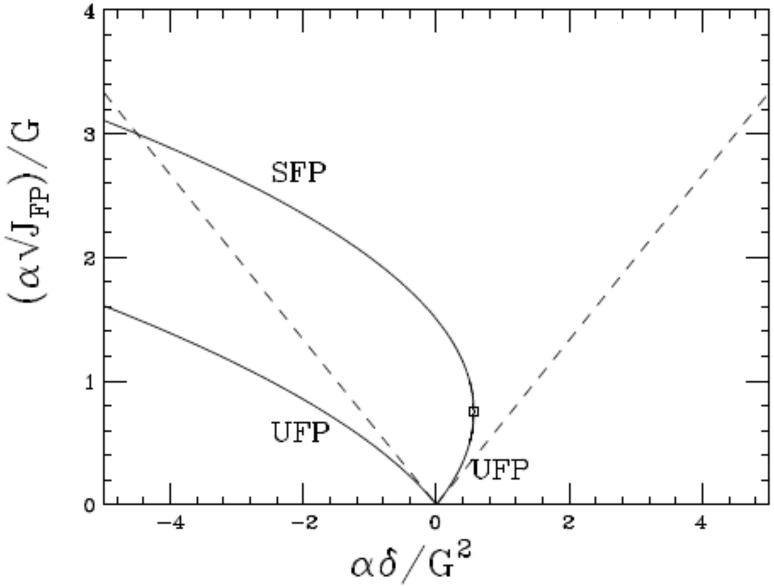


The bifurcation of third-order resonance islands occurs at $16\alpha\delta \le 9G_{3,0,\ell}^{\ 2}$. The Figure shows $\alpha J_{UFP}^{\ 1/2}/|G_{3,0,\ell}|$ vs $\alpha\delta/G_{3,0,\ell}^{\ 2}$ for the bifurcation of third-order resonance.

# Sextupole 3rd resonance

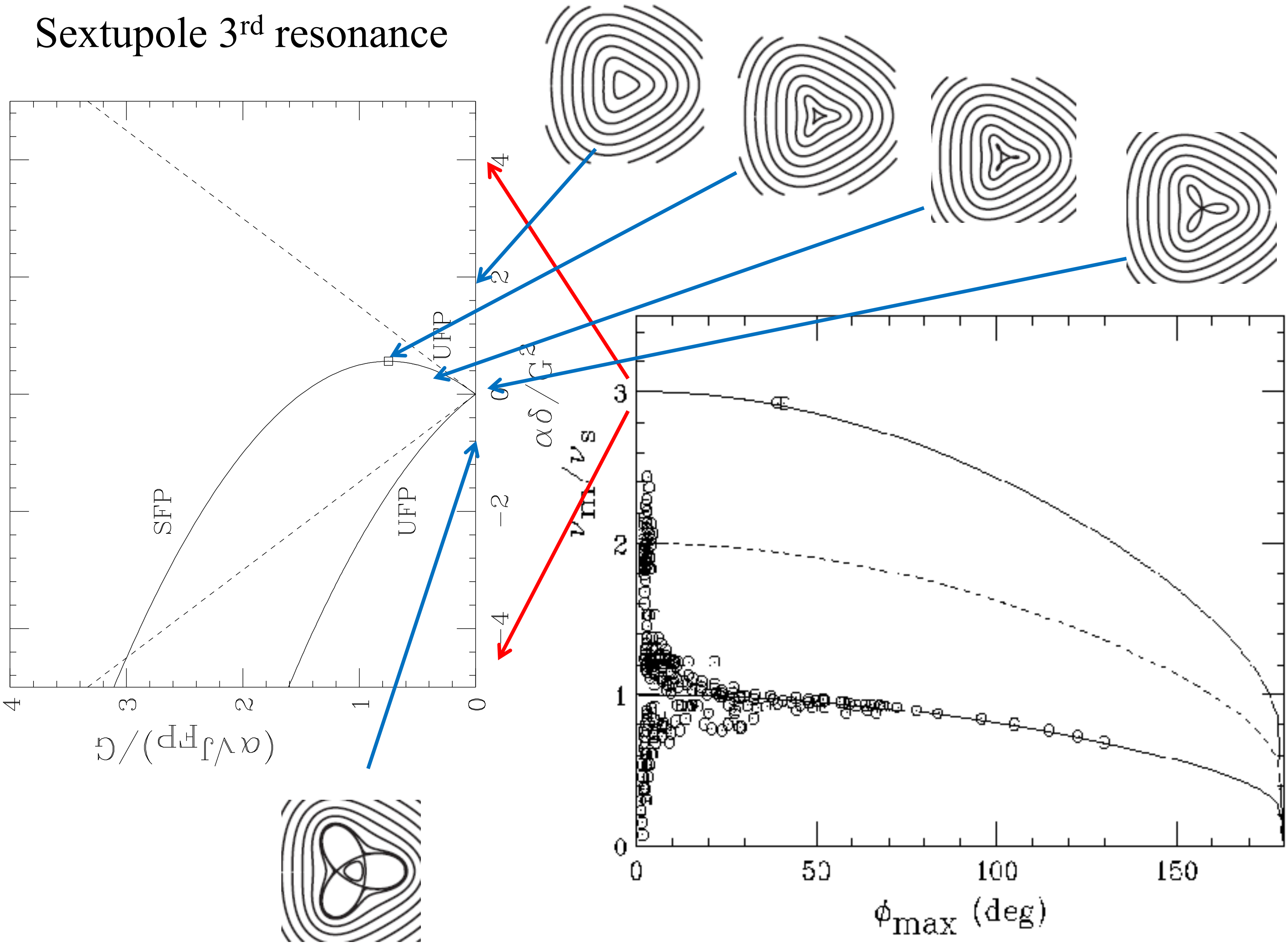

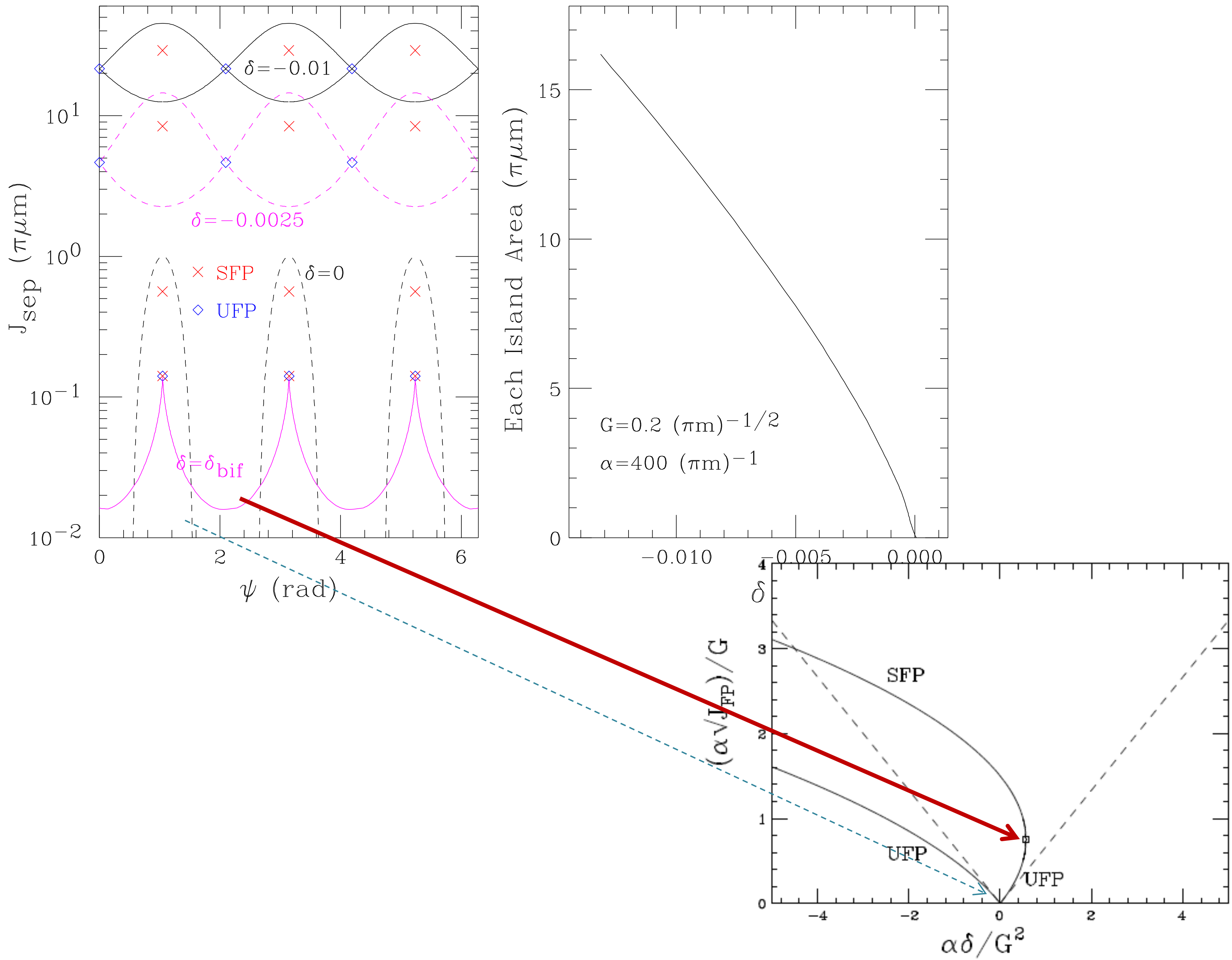

$\delta=-0.01$
$\delta=-0.0025$
SFP
UFP
$\delta=0$
$\delta=\delta_{bif}$
$J_{sep}$ $(\pi\mu m)$
$\psi$ (rad)
Each Island Area $(\pi\mu m)$
$G=0.2$ $(\pi m)^{-1/2}$
$\alpha=400$ $(\pi m)^{-1}$
SFP
UFP
UFP
$(\alpha\sqrt{J_{FP}})/G$
$\alpha\delta/G^2$
$\delta$

# Nonlinear beam dynamics on resonance crossing

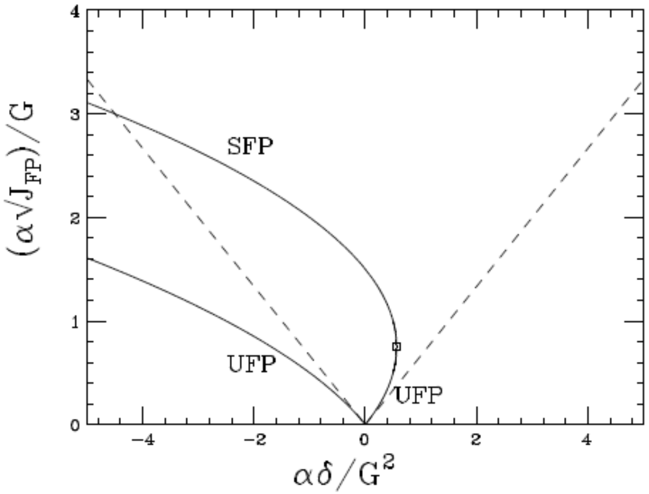


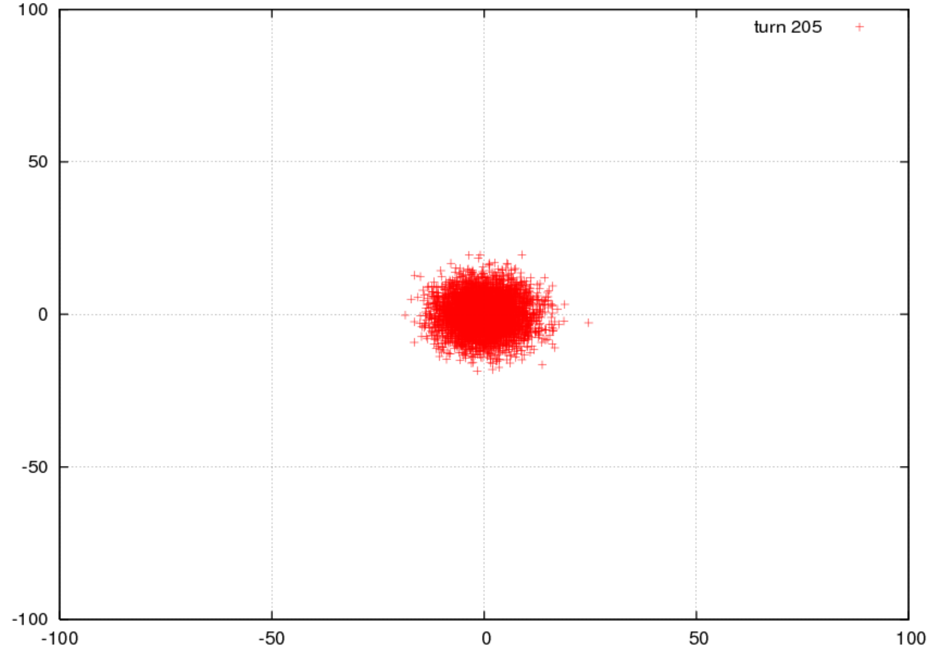


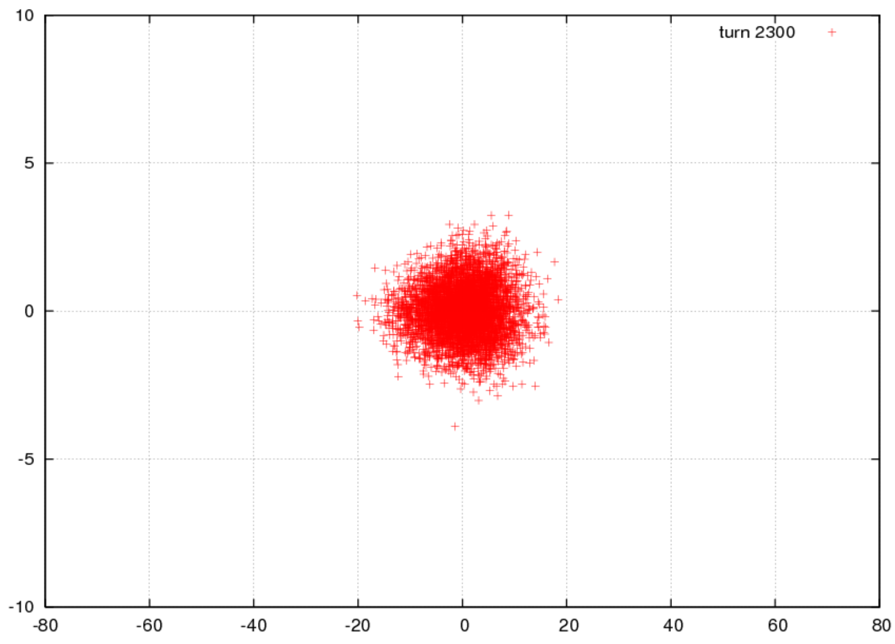


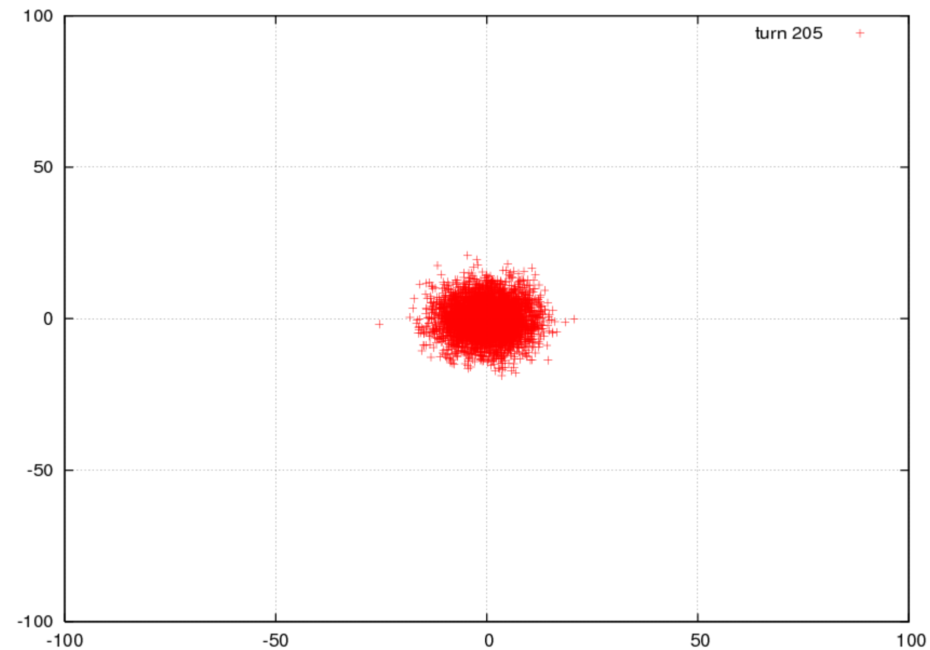

It appears that sextupoles will not produce resonances higher than the third order ones listed esarlier. However, strong sextupoles are usually needed to correct chromatic aberration. Concatenation of strong sextupoles can generate high-order resonances such as $4\nu_x$, $2\nu_x \pm 2\nu_z$, $4\nu_z$, $5\nu_x$, . . . , etc. The Figure below shows the Poincar´e maps of the single sextupole model at $\nu_x$=3.7496 and $\nu_x$=3.795, i.e. a single sextupole can also drive the fourth and higher order resonances. One can use a canonical perturbation method to explain the tracking result. Since resonance islands only exist with $\nu_x$<3.75 or $\nu_x$<3.8, the effective nonlinear detuning must be positive. The largest phase space map marks the boundary of stable motion.

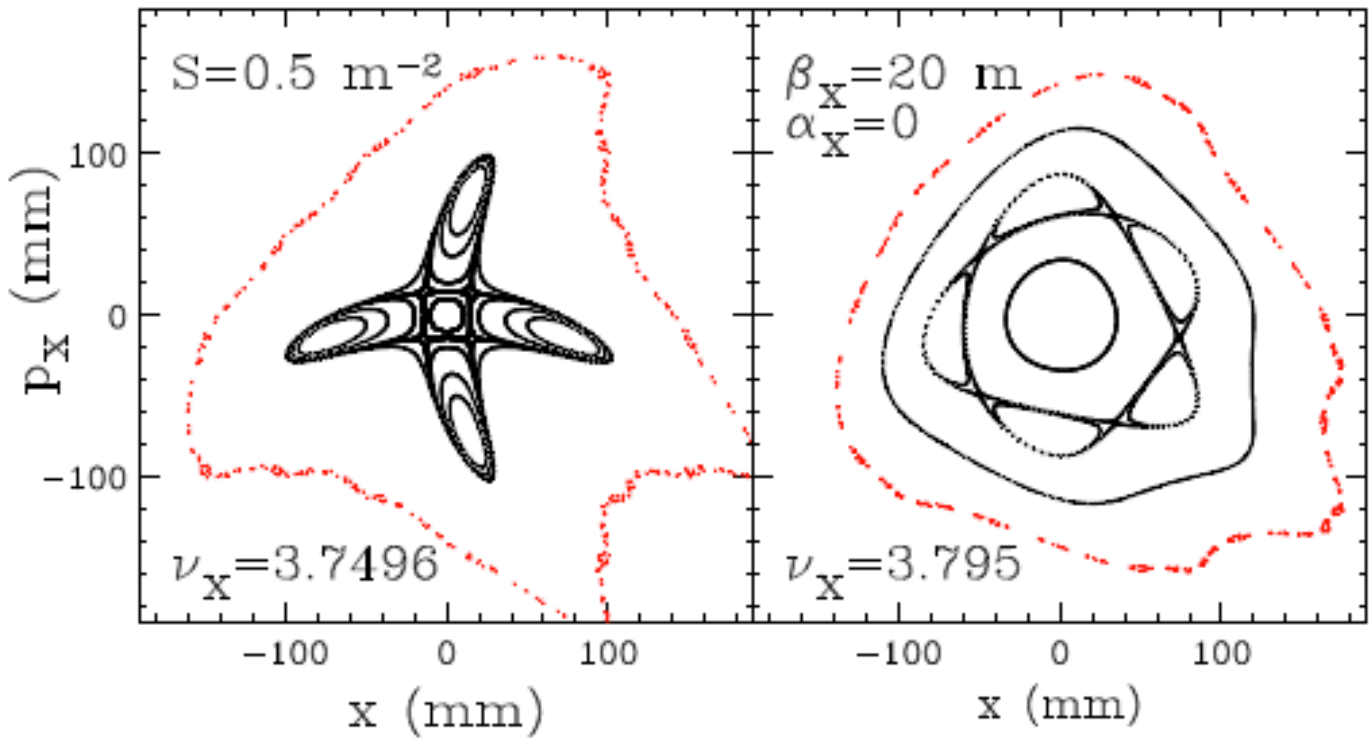

Near a *weak* fourth-order 1D resonance, the Hamiltonian can normally be approximated by

$$H = \nu_x J_x + \frac{1}{2}\alpha_{xx} J_x^2 + G_{4,0,\ell} J_x^2 \cos(4\psi_x - \ell\theta + \xi_{4,0,\ell}),$$

$$G_{4,0,\ell}\, e^{j\xi_{4,0,\ell}} = \frac{1}{96\pi} \oint \beta_x^2\, K_3(s)\, e^{j[4\chi_x(s)-(4\nu_x-\ell)\theta]} ds,$$

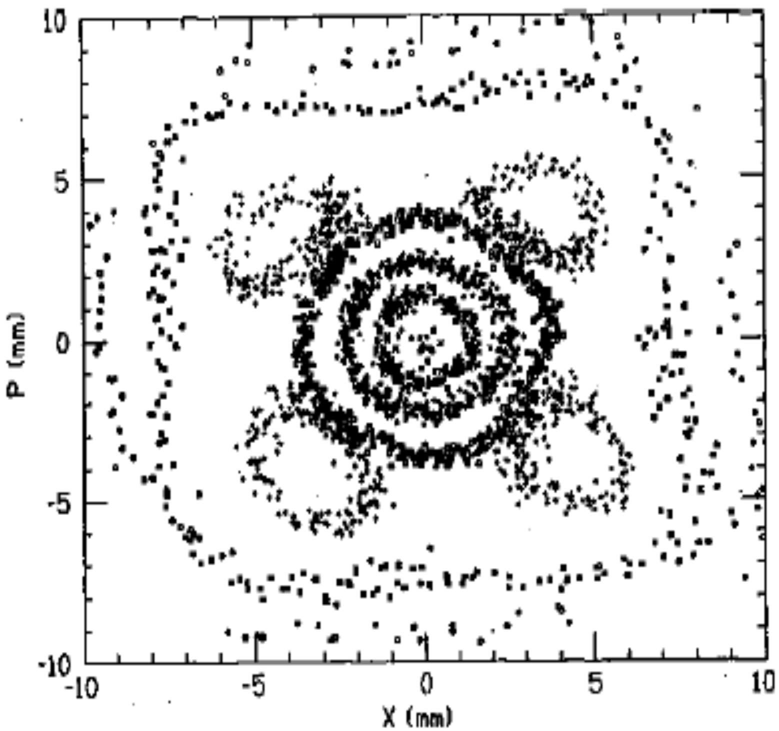


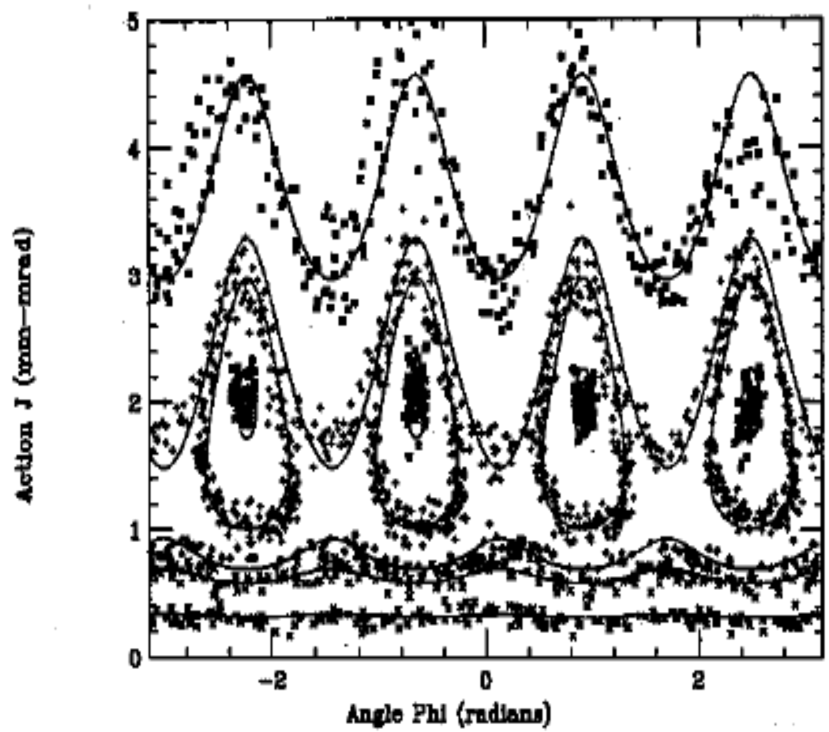


The solid lines are the Hamiltonian tori with parameters $\alpha_{xx}$=650$(\pi m)^{-1}$, $G_{4,0,15}$=80$(\pi m)^{-1}$, and $\nu_x-3.75=-7.8\times10^{-4}$.

$\nu_x - 2\,\nu_z = \ell$

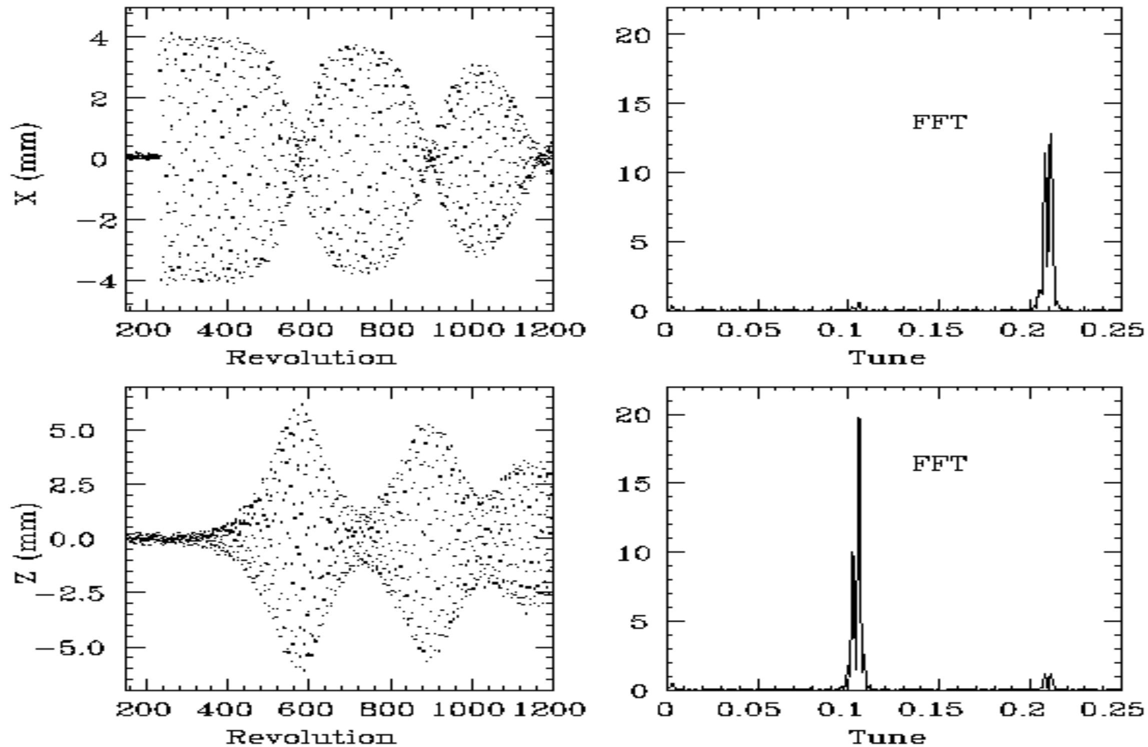


The betatron phase space can be visualized as a space filled by invariant tori, even near a nonlinear resonance.

For a difference resonance, the invariant is bounded!

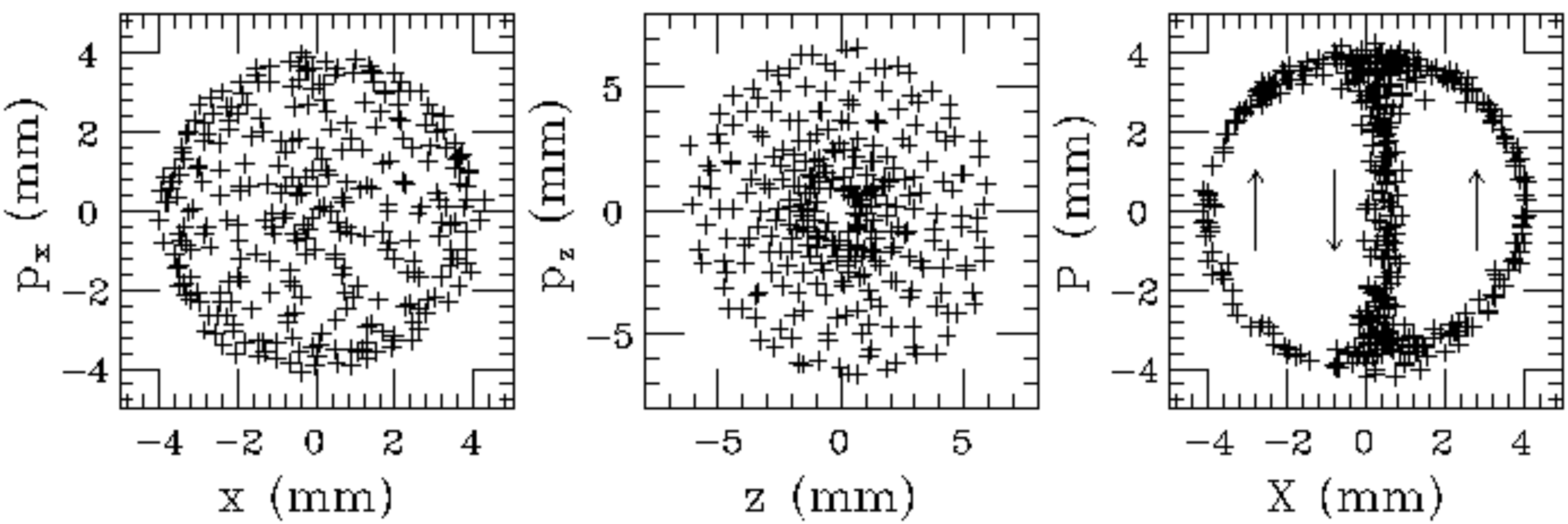

- The studies of sum resonances are not as successful. We have constructed a tune jump quadrupole to move betatron tunes onto a sum resonance $\nu_x+2\nu_z$ and observed betatron amplitude growth obeying the invariant at the resonance.
- Take $\mathbf{2\nu_x+2\nu_z}$ resonance as an example, we expect to see particle loss through tori as shown in the graph below. This means that the betatron phase space is filled with resonance lines, where particles that locked onto a resonance will leak out to a large amplitude betatron motion through these resonance tori. The invariant tori are unbounded for sum resonances!
- Experiments has yet to be carried out!

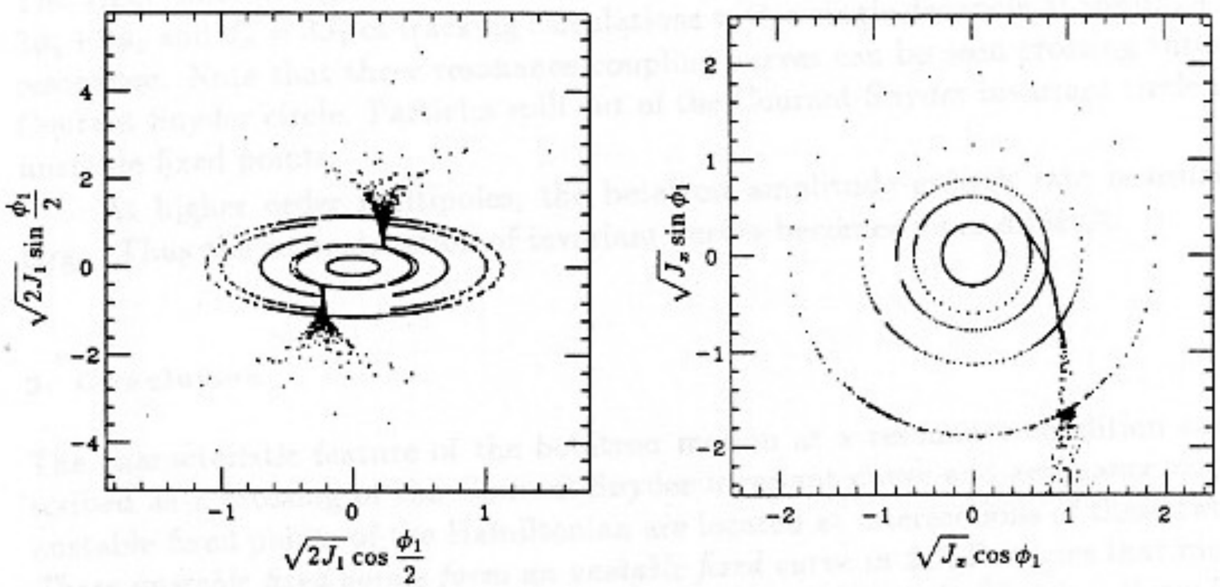


**Figure 3.** The Poincaré maps (see text for explanation) are shown for a Simple tracking calculation with a single octupole at a $2\nu_x+2\nu_z = \ell$ resonance.

Linear resonances

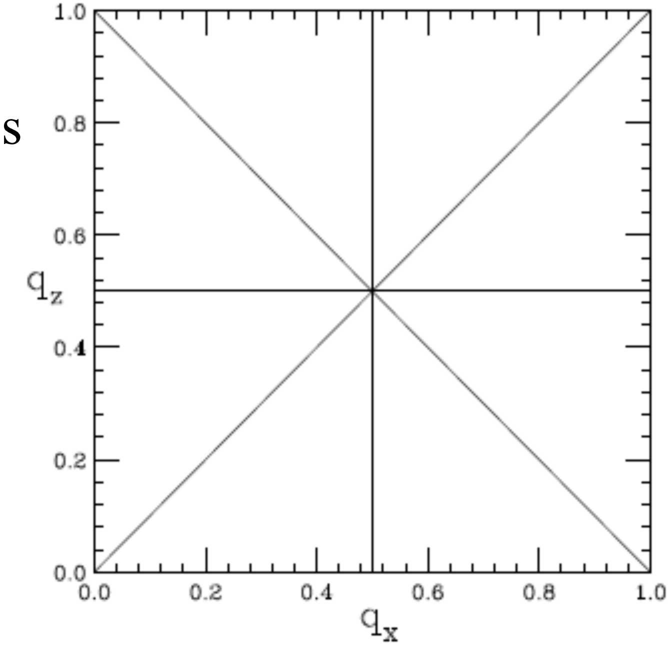


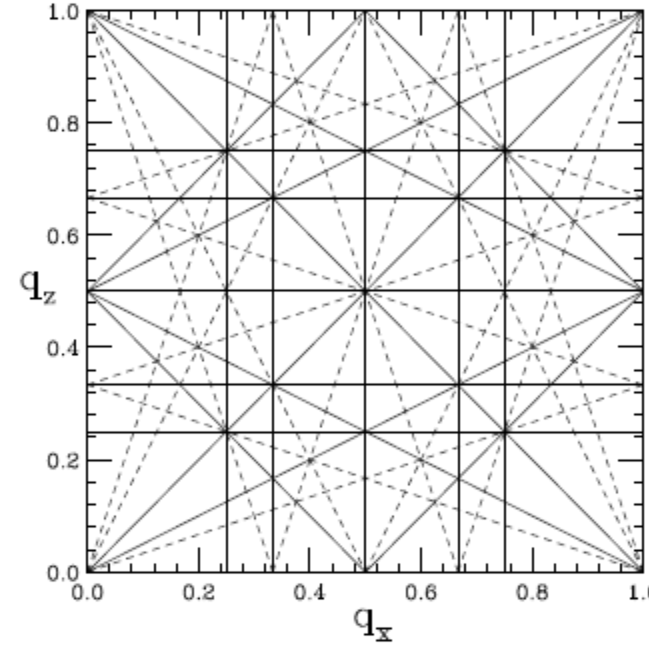


Resonances up to 4$^{th}$ order

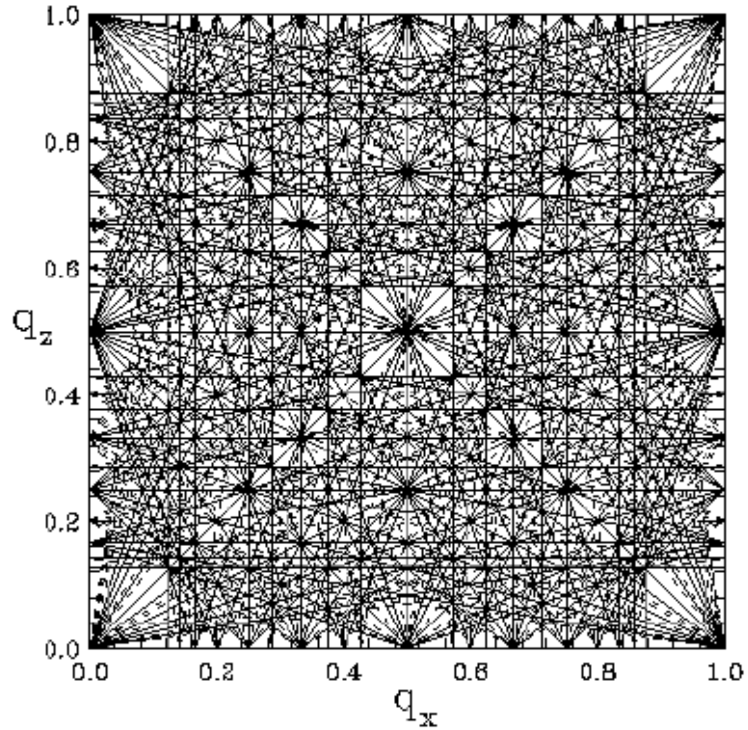


Up to 8$^{th}$ order resonances

# Space charge resonances in high power accelerators

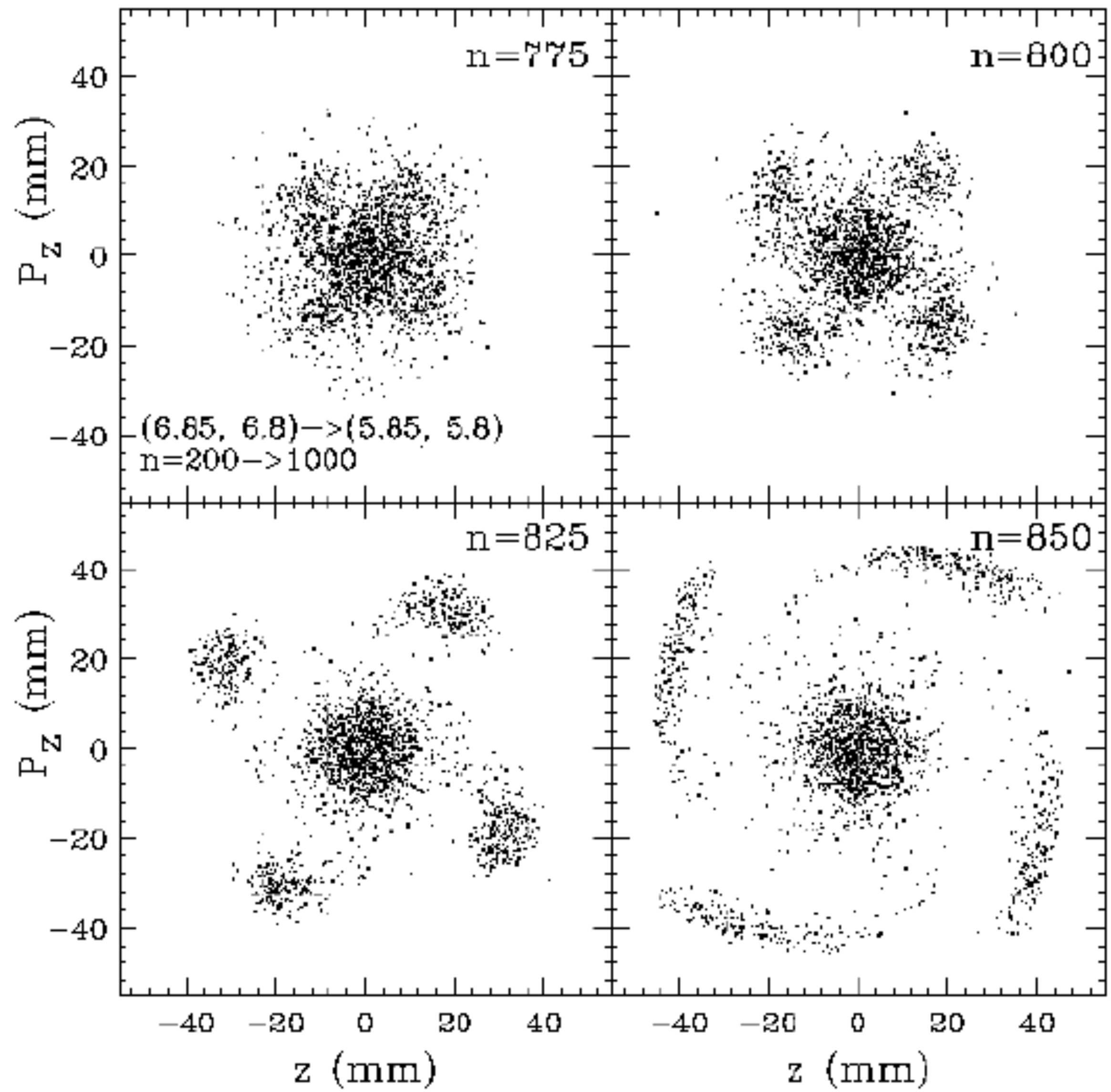

The next effect, which is important, is stochastic trajectories, which appear in the motion of the particles (turn by turn) – see Fig. 11. One of a simple criteria which was developed is called Chirikov criteria, stating that that stochastic layer in Poincare diagrams (the particles motion) appears when two non-linear resonances overlap. Careful look into fig 11 reveals that in addition to main resonance ($4^{th}$ and $3^{rd}$ order) there are additional high order resonance (islands) formed – some of them clearly identifiable, some destroyed and turned into a stochastic layer. Usually stochastic layer cause loss of particles at large amplitudes. It is also typical (with exception of beam-beam effects, when the nonlinearity of the beam is of the order of the beam size) that motion at large amplitudes becomes unstable and chaotic. Area of the dynamically (not physically) stable motion of particles is called "dynamic aperture" or DA.

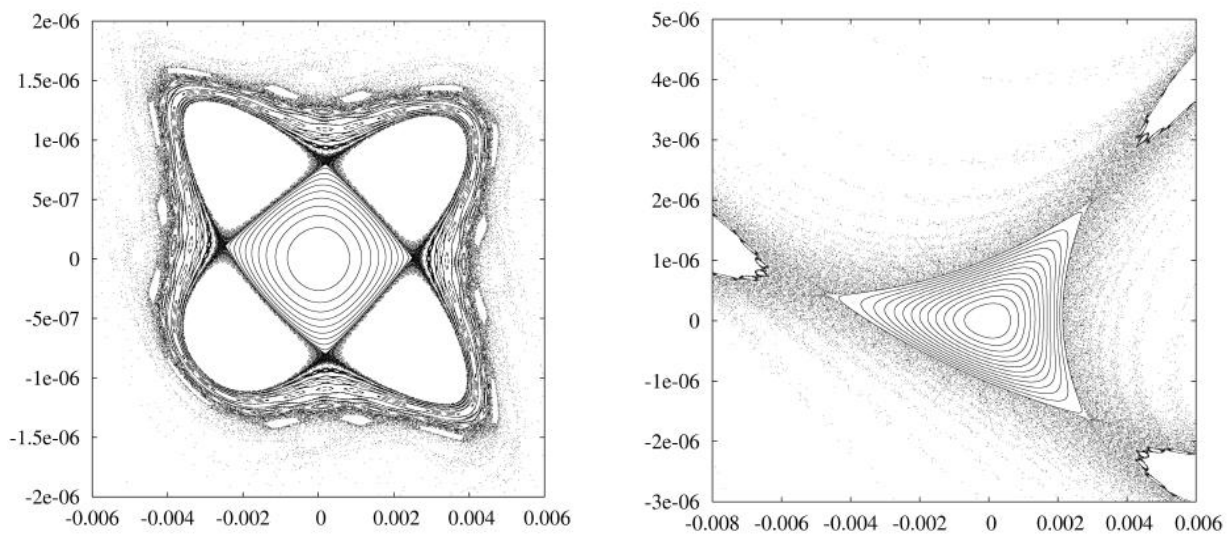


(a) (b)

Fig.11. Two tracking results: (a) with $4^{th}$ order and (b) $3^{rd}$ order resonance strictures.

# Nonlinear dynamics

Nonlinear effects in particle's motion in accelerators (or in Hamiltonian mechanics in general) some time can be treated in perturbative manner – the way we learned in this course. But while giving analytical expressions for the results, it is limited by – usually – second order perturbation and not necessarily converging when brought to higher orders. Needless to say it becoming very cumbersome even in the second order… Resonant approach, while giving a nice intuitive understanding of the resonances, is limited to (a) a single resonance, (b) ignores non-resonant terms which definitely distort or even – at large amplitude - ruin the simple picture we looked at. Fortunately there is a very systematic and rigorous method for non-linear dynamics developed by Prof. Alex J. Dragt (UM) and his follower (many of them his former students). This fundamental work started in late 1970s and brought to a well-formulated theory in early 1980s. Naturally, the work did not stopped there and there is a lot of new addition to this method (frequently oriented to computing and analyzing non-linear maps), which are extension of the method. Method itself is uses a number of mathematical concepts and power of Lie algebraic tools. It exploits symmetries of Hamiltonian systems and is – at present - the most comprehensive approach to the non-linear beam dynamics. We cannot follow each and every – some of them rather complex – derivations. Hence, we will deviate from tradition in our course to prove almost everything and will instead have a short introduction to this method. We may offer a dedicated course sometimes in near future.

Let's start from something we are well aware of: group (**G**) of 2n x 2n symplectic matrices (formally called **Sp(2n)**) satisfying simplicity conditions:

$$\mathbf{M^T S M = S}; \tag{26-1}$$

which satisfy group properties **G** :

1. It contains identity matrix **I**: since obvious $\mathbf{I^T S I = S}$

2. If $\mathbf{M} \in \mathbf{G} \to \mathbf{M}^{-1} \in \mathbf{G}$ (contains inverse matrix) :

$$\mathbf{M^T SM = S; ® M^{-1} = -SM^T S; ® M^T SM = S;}$$

$$\mathbf{M^{-1T} SM^{-1} = -SMSM^T S = S.}$$

3. $\mathbf{M,N} \in \mathbf{G} \to \mathbf{M \cdot N} \in \mathbf{G}$ : since $(\mathbf{MN})^T \mathbf{S \cdot MN} = \mathbf{N}^T \left(\mathbf{M}^T \mathbf{SM}\right)\mathbf{N} = \mathbf{N}^T \mathbf{SN} = \mathbf{S}$

4. $\mathbf{M(NL)} = (\mathbf{MN})\mathbf{L}$ , which is correct for any square matrices of the same order.

Thus, we proved that that symplectic matrices form symplectic group. Now we will focus on more formal definition of something we are familiar with, which is called lie algebraic properties. For any matrix **A** we defined exponential matrix function (heavily use in Lie algebras):

$$\exp(\mathbf{A}) = \sum_{n=0}^{\infty} \frac{\mathbf{A}^n}{n!}; \tag{26-2}$$

which converge for any **A** . A bit trickier is inverse, i.e. natural logarithm function:

$$\ln(\mathbf{A}) = \ln\left(\mathbf{I} - (\mathbf{I} - \mathbf{A})\right) = -\sum_{n=1}^{\infty} \frac{(\mathbf{I} - \mathbf{A})^n}{n}.; \tag{26-3}$$

uniqueness and convergence of which is much less trivial. It definitely converges when norm of $\mathbf{I} - \mathbf{A}$ is close to zero.

We know that for (real) matrix **A** with non-zero eigen values (e.g. non-zero determinant!) we can use Sylvester formula and find (a bit trickier to get it to be real) a solution of (26-3). We are all aware that *ln* of any number has branching at zero and is defined with accuracy of 2nπ. It means that $\mathbf{A}=\exp(\mathbf{B})$ has infinite number of solutions.

It is possible to show (a good exercise similar to proving exp(ln(x))=x) that if:

$$\mathbf{B}=\ln(\mathbf{A})\rightarrow\mathbf{A}=\exp(\mathbf{B}). \tag{26-4}$$

If **M** is real and symplectic, than

$$\mathbf{D}=\ln(\mathbf{M})\rightarrow\mathbf{D}^T\mathbf{S}+\mathbf{SD}=0;. \tag{26-5}$$

or **D** is anti-commute with **S**. It is easy to prove:

$$\begin{aligned}&\mathbf{D}=\ln(\mathbf{M});-\mathbf{D}=\ln\left(\mathbf{M}^{-1}\right)=\ln\left(\mathbf{S}^{-1}\mathbf{M}^T\mathbf{S}\right)=\mathbf{S}^{-1}\ln\left(\mathbf{M}^T\right)\mathbf{S}=-\mathbf{S}\ln\left(\mathbf{M}^T\right)\mathbf{S};\\&\mathbf{D}^T=\left(\mathbf{S}\ln\left(\mathbf{M}^T\right)\mathbf{S}\right)^T=\mathbf{S}\ln(\mathbf{M})\mathbf{S}=\mathbf{SDS};\rightarrow\mathbf{D}^T-\mathbf{SDS}=-(\mathbf{D}^T\mathbf{S}+\mathbf{SD})\mathbf{S}=0;\end{aligned}. \tag{26-6}$$

It means that (surprise-surprise) that **D=SH,** where **H** is symmetric matrix**:**

$$\mathbf{H}=-\mathbf{SD};\ \mathbf{D}^T=\mathbf{SDS}\rightarrow\mathbf{H}^T=\mathbf{D}^T\mathbf{S}=\mathbf{SDS}^2=-\mathbf{SD}=\mathbf{H}. \tag{26-7}$$

We already proved many times that for $\mathbf{H}^\mathbf{T}=\mathbf{H}$,

$$\mathbf{M}=\exp(\mathbf{SH})\rightarrow\mathbf{M}^T\mathbf{SM}=\mathbf{S}, \tag{26-8}$$

which is a two-liner:

$$\begin{aligned}&\mathbf{M}^T=\exp\left((\mathbf{SH})^T\right)=\exp(-\mathbf{HS})=\exp\left(-\mathbf{S}^{-1}\mathbf{SHS}\right)=\mathbf{S}^{-1}\exp(-\mathbf{SH})\mathbf{S}=\mathbf{S}\exp(-\mathbf{SH})\mathbf{S}\\&\mathbf{S}^{-1}=-\mathbf{S};\ \mathbf{M}^T\mathbf{SM}=-\mathbf{S}\exp(-\mathbf{SH})\mathbf{S}^2\exp(\mathbf{SH})=\mathbf{S}\exp(\mathbf{SH}-\mathbf{SH})=\mathbf{S}.\end{aligned}$$

What we shown is that symplectic matrix can be written on form

$$\mathbf{M}^T\mathbf{S}\mathbf{M} = \mathbf{S} \rightarrow \mathbf{M} = \exp\left(\mathbf{S}\mathbf{H}\right), \mathbf{H}^T = \mathbf{H}. \tag{26-9}$$

Now we are ready to define Lie algebra for matrices: A set of matrices forms **Lie algebra** if:

1. If matrix **A** is in the Lie algebra, than so any product with a scalar **a**, **aA** ;
2. If matrices **A** and **B** is in the Lie algebra, then so their sum **A+B**.
3. If matrices **A** and **B** is in the Lie algebra, then so their commutator **[A,B]**, defined as

$$\left[\mathbf{A},\mathbf{B}\right] = \mathbf{AB} - \mathbf{BA}, \tag{26-10}$$

which is something new we did not touched yet in our course, but something having a very fundamental relation with Poisson brackets in Hamiltonian mechanics. The next is to show that our **D=SH**, $\mathbf{H}^\mathbf{T}$**=H** set of matrices **D** form an Lie algebra. From observing that **H=-SD**, two first conditions are trivial adding symmetric matrices and multiplying them by a scalar keeps them symmetric. Third condition is a new and can be easily proved:

$$\begin{gathered}
\mathbf{A} = \mathbf{S}\mathbf{H}_1, \mathbf{B} = \mathbf{S}\mathbf{H}_2; \left[\mathbf{A},\mathbf{B}\right] = \mathbf{S}\mathbf{H} \\
\mathbf{H} = -\mathbf{S}\left[\mathbf{A},\mathbf{B}\right] = \mathbf{SBA} - \mathbf{SAB} = \mathbf{H}_1\mathbf{S}\mathbf{H}_2 - \mathbf{H}_2\mathbf{S}\mathbf{H}_1; \\
\mathbf{H}^T = \left(\mathbf{H}_1\mathbf{S}\mathbf{H}_2 - \mathbf{H}_2\mathbf{S}\mathbf{H}_1\right) = \left(\mathbf{H}_2{}^T\mathbf{S}^T\mathbf{H}_1{}^T - \mathbf{H}_1{}^T\mathbf{S}^T\mathbf{H}_2{}^T\right) = \mathbf{H}_1\mathbf{S}\mathbf{H}_2 - \mathbf{H}_2\mathbf{S}\mathbf{H}_1 = \mathbf{H};
\end{gathered} \tag{26-11}$$

which proves that $\left[\mathbf{A},\mathbf{B}\right] = \mathbf{S}\mathbf{H}$ with $\mathbf{H}^T = \mathbf{H}$.

Further, is possible to prove that symplectic matrix can be presented in form of the product of exponents

$$\mathbf{M} = \exp(\mathbf{SH}_a)\exp(\mathbf{SH}_s), \mathbf{SH}_a = -\mathbf{H}_a\mathbf{S}; \mathbf{SH}_c = \mathbf{H}_c\mathbf{S}; \tag{26-12}$$

with commuting and anti-commuting generating matrices $\mathbf{H}_a, \mathbf{H}_c$. This can be proven using the fact that an arbitrary real non-singular matrix can be decomposed as product of real positive definite symmetric matrix $\mathbf{P}$ and orthogonal matrix $\mathbf{O}$ (we use it without prove!):

$$\mathbf{M} = \mathbf{PO}; \ \mathbf{P}^T = \mathbf{P}; \ \ \mathbf{O}^T = \mathbf{O}^{-1}; \tag{26-13}$$

For symplectic matrix we have

$$\mathbf{M} = \mathbf{S}^{-1}\left(\mathbf{M}^{-1}\right)^{\mathbf{T}}\mathbf{S} \rightarrow \mathbf{PO} = \left(\mathbf{S}^{-1}\mathbf{P}^{-1}\mathbf{S}\right)\left(\mathbf{S}^{-1}\mathbf{OS}\right)$$

where we used $\mathbf{P}^T = \mathbf{P}; \ \mathbf{O}^T = \mathbf{O}^{-1}$ and with $\mathbf{S}^{-1}\mathbf{P}^{-1}\mathbf{S}$ being real, symmetric and positive definite and $\mathbf{S}^{-1}\mathbf{O}^{-1}\mathbf{S}$ real and orthogonal. Since polar decomposition is unique (we use it without prove!) than

$$\mathbf{P} = \mathbf{S}^{-1}\mathbf{P}^{-1}\mathbf{S}; \mathbf{O} = \mathbf{S}^{-1}\mathbf{OS}; \rightarrow \mathbf{P} = -\mathbf{S}\left(\mathbf{P}^{-1}\right)^T\mathbf{S}; \mathbf{O} = -\mathbf{S}\left(\mathbf{O}^{-1}\right)^T\mathbf{S}.;$$

$$\mathbf{P}^T\mathbf{SP} = \mathbf{P}^T\left(\mathbf{P}^{-1}\right)^T\mathbf{S} = \mathbf{S}; \qquad \mathbf{O}^T\mathbf{SO} = \mathbf{O}^T\left(\mathbf{O}^{-1}\right)^T\mathbf{S} = \mathbf{S}\,\#$$

e.g. both of these matrices are symplectic. A bit more of exercises are needed to prove that $\mathbf{A} = \ln\mathbf{O}$ is asymmetric matrix $\mathbf{A}^T = -\mathbf{A}$ and $\mathbf{B} = \ln\mathbf{P}$ is symmetric matrix $\mathbf{B}^T = \mathbf{B}$: $-\mathbf{A} = \ln\mathbf{O}^{-1} = \ln\mathbf{O}^T = \mathbf{A}^T; \mathbf{B}^T = \ln\mathbf{P}^T = \ln\mathbf{P} = \mathbf{B}$. As we found that for any logarithm of symplectic matrix condition (26-5) applies $\mathbf{D} = \ln(\mathbf{M}) \rightarrow \mathbf{D}^T\mathbf{S} + \mathbf{SD} = 0;$ requiring:

$$\begin{aligned} &\mathbf{A}^T\mathbf{S} + \mathbf{SA} = 0 \rightarrow \mathbf{AS} = \mathbf{SA}; \mathbf{A} = \mathbf{SH}_c \rightarrow \mathbf{H}_c\mathbf{S} = \mathbf{SH}_c \\ &\mathbf{B}^T\mathbf{S} + \mathbf{SB} = 0 \rightarrow \mathbf{BS} = -\mathbf{SB}; \mathbf{B} = \mathbf{SH}_a \rightarrow \mathbf{H}_a\mathbf{S} = -\mathbf{SH}_a\,\# \end{aligned} \tag{26-14}$$

This proves (relying on a couple of theorem from linear algebra we took for granted) that (26-12) is correct. Since, $\mathbf{S}^2 = -\mathbf{I} = (i\mathbf{I})^2$ and generating matrices either commute or anti-commute with $\mathbf{S}$, one can find real $\mathbf{H}_a, \mathbf{H}_c \ldots$ again without proof.

Now we are ready to connect our – so far an abstract exercise – to Poisson brackets, which are defined for two functions of coordinates and momenta as

$$X = \{x_i, i = 1,2n\} = \{\{q_k, P^k\} k = 1,n\};$$

$$f = f(X,s) \equiv f(q_k, P^k, s); g = g(X,s) \equiv g(q_k, P^k, s);$$

$$[f,g]_{def} = \sum_{k=1}^{n} \left( \frac{\partial f}{\partial q_k} \frac{\partial g}{\partial P^k} - \frac{\partial g}{\partial q_k} \frac{\partial f}{\partial P^k} \right) = \sum_{i,j=1}^{2n} \left( \frac{\partial f}{\partial x_i} S_{ij} \frac{\partial g}{\partial x_j} \right) = \tag{26-15}$$

$$(\partial_X f, \mathbf{S} \cdot \partial_X g) = (\partial_X f)^T \mathbf{S} \cdot (\partial_X g).$$

From Hamiltonian mechanics we know that

$$\frac{df}{dt} = \frac{\partial f}{\partial t} + [f,H] = \frac{\partial f}{\partial t} + \frac{\partial f}{\partial X} S \frac{\partial H}{\partial X} = \frac{\partial f}{\partial t} + \frac{\partial f}{\partial q_k} \frac{\partial H}{\partial P^k} - \frac{\partial f}{\partial P^k} \frac{\partial H}{\partial q_k};$$

and time-independent function “commuting” with Hamiltonian are invariants of motion.

Let's now introduce one more object, **Lie operator** *:f:* defined as :

$$:f:g=[f,g];$$
$$:f:^0=g;:f:^2 g=\left[f[f,g]\right];\ :f:^{n+1} g=\left[f,:f:^n g\right]. \tag{26-16}$$

together with its powers. Obviously the Lie operator and its power are linear operators

$$:f:^n(a\cdot g+b\cdot h)=\left(a\cdot:f:^n g+b\cdot:f:^n h\right) \tag{26-17}$$

since functions the operator acts upon appearing linearly. Similarly, since $:f:$ is a differential operator, the following rule

$$:f:(g\cdot h)=(:f:g)\cdot h+g\cdot(:f:h) \tag{26-18}$$

is trivial to prove. Furthermore, similarly to the ordinary differentiation $:f:^n$ obeys Leibnitz rule

$$:f:^n(g\cdot h)=\sum_{m=0}^{n} C_m^n\left(:f:^m g\right)\left(:f:^{n-m} h\right);\ C_m^n=\frac{n!}{m!(n-m)!}. \tag{26-19}$$

Finally, the Jacoby identity

$$\left[f,[g,h]\right]=\left[[f,g],h\right]+\left[g,[f,h]\right] \tag{26-20}$$

which I recommend you to prove as an exercise (not a home work!) is equivalent to identity for Lie operators

$$:f:[g,h]=[:f:g,h]+[g,:f:h] \tag{26-21}$$

Now we will convert linear Lie operators into a linear algebra by defining their product (algebraic, not simple multiplication) of Lie operators:

$$\{:f:,:g:\}=:f::g:-:g::f: \tag{26-22}$$

or using Jacoby identity

$$\{:f:,:g:\}h=(:f::g:-:g::f:)h=[:f:,:g:]h=:[f,g]:h \tag{26-23}$$

with $:[f,g]:$ being a compact form of the product of two operators.

Hence we established homomorphism between the Lie algebra of function (Poisson brackets) and Lie operators. Naturally (26-22) turns the set Lie operators into Lie algebra.

We are not done yet with definitions: we define Lie transform as an exponent of the Lie operators:

$$\exp(:f:) = \sum_{n=0}^{\infty} \frac{:f:^n}{n!} \tag{26-24}$$

which have unbelievably beautiful properties:

$$\exp(:f:)(gh) = \left(\exp(:f:)g\right)\left(\exp(:f:)h\right) \tag{26-25}$$

which can be prove using Leibnitz rule in manner similar to prove of $\exp(x+y) = \exp(x)\exp(y)$ in mathematical analysis.

Applying it to

$$\exp(:f:)x^n = \left(\exp(:f:)x\right)^n;$$
$$g(X) = \sum_{n=0}^{\infty} g_n X^n \rightarrow \exp(:f:)g(X) = \sum_{n=0}^{\infty} g_n \left(\exp(:f:)X\right)^n = g\left(\exp(:f:)X\right). \tag{26-26}$$

with the later being the most remarkable quality: Lie transformation of a function is a function of Lie transformation of its argument! (We cheated a bit here – we really needed to expand function of multiple variables as $\sum_{k=0}^{\infty} g_{k_1 \ldots k_{2n}} x_1^{k_1} \cdot\cdot x_{2n}^{k_{2n}}$ with the same final result). Lastly, the important (and elegant) property we will use later:

$$\exp(:f:)[g,h] = \left[\exp(:f:)g, \exp(:f:)h\right] \tag{26-27}$$

It worth noting that all relations mentioned above without checking are relatively straight forward to prove, but proves are not necessarily compact.

Let's now switch to symplectic maps denoted as:

$$\mathtt{M} : x \to \bar{x}(x,s); \mathtt{M} : X \to \bar{X}(x,s); \tag{26-26}$$

which generate local symplectic matrices

$$\mathbf{M}(s,X) = \left[ \frac{\partial \bar{x}_i}{\partial x_j} \right] = \frac{\partial \bar{X}}{\partial X}; \quad \mathbf{M}^T \mathbf{S} \mathbf{M} = \mathbf{S}. \tag{26-29}$$

We discussed the invariants and result of these important features of symplectic maps such as Poincare invariants and will not repeat it. Instead we will focus on connection between Lie algebras and symplectic maps. First, let's show that Lie transformation is symplectic, lets consider

$$\bar{x} = \mathtt{M}x; \mathtt{M} = \exp(:f:); \tag{26-30}$$

than we have

$$\left[\bar{x}_i, \bar{x}_j\right] = \left[\left(\exp(:f:)x\right)_i, \left(\exp(:f:)x\right)_j\right] = \exp(:f:)\left[x_i, x_j\right] = S_{ij} \tag{26-31}$$

which proves the symplecticity of local transformation and the map as a whole.

As we discussed in our class, accelerator physics is interested in particles motion around the reference orbit, e.g. in maps which map origin X=0 into itself. It easy very easy to show that

$$\mathtt{M} = \exp(:f:);\ f = \sum_{k=1}^{2n} a_i x_i; \tag{26-32}$$

generate a displacement of the origin. For example $f = ax$ generates

$$f = ax, a[x,p] = \frac{\partial x}{\partial x}\frac{\partial p}{\partial p} = a;\ \bar{p} = a;\ \ :x:^n [x,p] = 0, n > 0 \tag{26-33}$$

First, we are not interest in such trivial shifts. Second, in general case, we always eliminate shift of the origin by choosing appropriately coefficients in (26-32).

Let's, for a moment, consider a Lie transformation with quadratic terms

$$f_2 = -\frac{1}{2} X^T \mathbf{H} X = -\frac{1}{2}\sum_{i,j=1}^{2n} h_{ij} x_i x_j; \mathbf{H}^T = \mathbf{H}. \tag{26-34}$$

Let's calculate action of $:f_2:$ on $x_k$:

$$\begin{gathered} :f_2: x_k = -\frac{1}{2}\sum_{i,j=1}^{2n} h_{ij}\left[x_i x_j, x_k\right]; \\ \left[x_i x_j, x_k\right] = \left[x_i, x_k\right] x_j + x_i\left[x_j, x_k\right] = S_{ik} x_j + S_{jk} x_i \\ -\frac{1}{2}\sum_{i,j=1}^{2n} h_{ij}\left(S_{ik} x_j + S_{jk} x_i\right) = \sum_i^{2n} (\mathbf{SH})_{ki} x_i \\ :f_2: x_k = (\mathbf{SH})_{ki}\, x_i \rightarrow :f_2: X = \mathbf{SH} X \end{gathered} \tag{26-35}$$

to see that it generates a linear matrix transformation.

Then we prove that Lie transformation with second order Hamiltonian polynomial as a generation function

$$:f_2:X=(\mathbf{SH})X;\ :f_2:^n X=(\mathbf{SH})^n X;$$
$$\exp(:f_2:)=\exp(\mathbf{SH}). \tag{26-36}$$

generates linear transformation. Which is equivalent to that generated by s-independent Hamiltonian of linear motion. As we discussed, linear motion is a trivial (when stable!) and is reduced to **n** independent oscillators with their amplifies (actions) and phases.

So far we had shown that Lie transforms are symplectic maps, that linear Lie map generated by second order Hamiltonian generate linear symplectic matrix and, vice versa, we can find such Lie transform for any symplectic matrix (for example using Sylvester formula for ln**M**). The remaining and very potent question remains: if a any analytical symplectic map can be presented in exponential form of a Lie operator? The answer is given by the **factorization theorem**: the keystone for application of the Lie transformation to non-linear Hamiltonian maps.

**Factorization theorem**: For an analytical symplectic map $\mathtt{M}$ (which transfers the origin in itself) and relation are assumed to be expandable into as power series:

$$\bar{X}=\mathtt{M}X;\ \bar{x}_i=M_{ik}x_k+\sum_{\sum_{i=1}^{2n}p_i=2}^{\infty} a_{1\ldots 2n}x_1^{p_1}\cdots x_{2n}^{p_{2n}}; \tag{26-37}$$

the map can be written in from of

$$\mathtt{M}=\exp(:f_2:)\exp(:f_3:)\exp(:f_4:)\exp(:f_5:)\ldots \tag{26-38}$$

where $f_m$ are homogeneous polynomials of power m of $\{x_i\}, i=1,2n$ .

Sketch of a proof – which is long- in based on the observation that if $f_m$ and $g_k$ are homogenies polynomials of order m and k, than their Poisson bracket

$$\left[f_m, g_k\right] = p_{m+k-2}$$

is also a homogeneous polynomial of order m+k-2. This is why $f_2$ generates linear map with linear polynomial X. Hence, $f_3$ will generate second order term and its exponential will generate all higher orders as well.

Let's apply using the linear map at the origin (X=0) the inverse transformation:

$$\exp\left(-:f_2:\right) = \exp\left(-\mathbf{SH}\right) \tag{26-39}$$

to both sides of (26-37)

$$\exp\left(-:f_2:\right)\bar{X} = \exp\left(-:f_2:\right)\mathtt{M}X =$$

$$X + \exp\left(-:f_2:\right)\left(\sum_{2+}^{\infty} a_{1...2n} x_1^{p_1} \cdots x_{2n}^{p_{2n}}, \text{higher orders}\right) \tag{26-40}$$

$$\exp\left(-:f_2:\right)\bar{x}_i = x_k + \exp\left(-:f_2:\right)\sum_{2+}^{\infty} a_{1...2n} x_1^{p_1} \cdots x_{2n}^{p_{2n}};$$

Suppose that $f_3$ is some cubic polynomial

$$\exp\left(-:f_3:\right)\exp\left(-:f_2:\right)\bar{X} = X - :f_3:X + (\text{higher orders}); \tag{26-41}$$

Than (hopefully) we can select coefficients of $f_3$ to leave only cubic and higher order terms. Than we repeat the procedure for $f_4, f_5$.....

$$.....\exp\left(-:f_5:\right)\exp\left(-:f_5:\right)\exp\left(-:f_3:\right)\exp\left(-:f_2:\right)\bar{X} \to X \tag{26-42}$$

with natural conclusion that multiplying (26-42) by (26-38) we get:

$$\bar{X} = \mathtt{M}X. \tag{26-43}$$

While logically straightforward, the process (especially for 3D case) becomes cumbersome right away and in real situation (with few exceptions which prove the rule) computers do it much better.

Thus, we concluded that any analytical symplectic map can be presented as a product of linear (Gaussian optics) Lie transformation and product of Lie transformations comprising homogeneous polynomials of increasing power:

$$\mathrm{M} = \overbrace{\exp(:f_2:)}^{Gaussian\,optics} \bullet \overbrace{\exp(:f_3:)\exp(:f_4:)\exp(:f_5:)...}^{Abberations,\ Nonlinear\ effects} \tag{26-44}$$

While looking as a final result, the remaining question is – how we can use it?

While there are hundreds of very important Lie algebraic relations and many-many tricks, one is important for interpretation (normalization) of the non-linear symplectic maps. In linear case we have set the action and angle canonical pairs describing each oscillator:

$$\{\varphi_k, I_k\} \Leftrightarrow \tilde{x}_k = \sqrt{2I_k}\cos(\psi + \varphi_k); \tilde{p}_k = -\sqrt{2I_k}\sin(\psi + \varphi_k); I_k = \frac{\tilde{x}_k^{\ 2} + \tilde{p}_k^{\ 2}}{2}; \tag{26-45}$$

where $\{\tilde{x}_k, \tilde{p}_k\}$ are also canonical pairs. We could bring our linear map (matrix) to an oscillator turn using

$$U = [...,\mathrm{Re}\,Y_k; \mathrm{Im}\,Y_k...]; MY_k = e^{i\mu_k}Y_k \to M \cdot U = UR; k = 1,..,n$$

$$R = \begin{bmatrix} ... & 0 & 0 \\ 0 & R_k & 0 \\ 0 & 0 & ... \end{bmatrix}; R_k = \begin{bmatrix} \cos\mu_k & -\sin\mu_k \\ \sin\mu_k & \cos\mu_k \end{bmatrix}; \ U^{-1} \cdot M \cdot U = R = \exp(:\vec{\mu} \cdot \vec{I}:).$$

(26-46)

In linear approximation trajectories in $\{\tilde{x}_k, \tilde{p}_k\}$ planes are boring circles with radius $\sqrt{2I_k}$ . This representation is called normal form of representation for linear symplectic map.

# Normal form treatment

Instead of describing the dynamics in a beam line using an s-dependent Hamiltonian, we can construct a map, for example, in the form of a Lie transformation. Such a map may be constructed by concatenating the maps for individual elements. The beam dynamics (for example, the strengths of different resonances) may then be extracted from the transformation.

To better understand the concept of map (transformation), we take a look at the well-known linear transport matrix for a periodic accelerator (say, a storage ring)

$$\mathrm{M} = \begin{pmatrix} \cos\Phi + \alpha\sin\Phi & \beta\sin\Phi \\ -\gamma\sin\Phi & \cos\Phi - \alpha\sin\Phi \end{pmatrix}, \ \beta\gamma = 1 + \alpha^2$$

the matrix is symplectic.

Normal form analysis of a linear system involves finding a transformation to variables in which the map appears as a pure rotation.

Consider matrix

$$N = \begin{pmatrix} \frac{1}{\sqrt{\beta}} & 0 \\ \frac{\alpha}{\sqrt{\beta}} & \sqrt{\beta} \end{pmatrix}$$

We find that

$$NMN^{-1}$$

$$= \begin{pmatrix} \frac{1}{\sqrt{\beta}} & 0 \\ \frac{\alpha}{\sqrt{\beta}} & \sqrt{\beta} \end{pmatrix} \begin{pmatrix} \cos\Phi + \alpha\sin\Phi & \beta\sin\Phi \\ -\gamma\sin\Phi & \cos\Phi - \alpha\sin\Phi \end{pmatrix} \begin{pmatrix} \sqrt{\beta} & 0 \\ \frac{\alpha}{\sqrt{\beta}} & \frac{1}{\sqrt{\beta}} \end{pmatrix}$$

$$= \begin{pmatrix} \cos\mu & \sin\mu \\ -\sin\mu & \cos\mu \end{pmatrix} = R$$

Becomes a pure rotation in phase space.

The coordinates are "normalized" $\vec{x}_N = N\vec{x}$

And the normalized coordinates transform in one revolution as

$$\vec{x}_N \longrightarrow NM\vec{x} = NMN^{-1}N\vec{x} = RN\vec{x} = R\vec{x}_N$$

Is simply a rotation in phase space.

Note that since the transformation N is symplectic, the normalized variables are canonical variables.

The treatment of nonlinear dynamics follows the same procedure however more complicated.

We can assume the map can be represented by a Lie transformation and factorized as

$$\mathrm{M} = Re^{:f_3:}e^{:f_4:}\cdots$$

Where f3 is a homogeneous polynomial of order 3 of the phase space coordinates and f4 is a homogeneous polynomial of order 4. The detailed order depends on the truncation.

The linear part of the map can be written in action angle variables as

$$R = e^{:-\mu J:}$$

To simplify this map, i.e., separate the contribution from different orders, we can construct a map M3

$$U = e^{:F_3:} M e^{:-F_3:}$$

Where F3 is a generator that removes resonance driving terms from $e^{:f_3:}$

So we have

$$U = e^{:F_3:} R e^{:f_3:} e^{:f_4:} e^{:-F_3:} = R R^{-1} e^{:F_3:} R e^{:f_3:} e^{:-F_3:} e^{:F_3:} e^{:f_4:} e^{:-F_3:}$$

Using relation $$e^{:h:} e^{:g:} e^{:-h:} = e^{:e^{:h:} g:}$$

$$U = R e^{:R^{-1} F_3:} e^{:f_3:} e^{:-F_3:} e^{:e^{:F_3:} f_4:}$$

Using Baker-Campbell-Hausdorff formula

$$e^{:A:}e^{:B:} = e^{:C:}, \quad where \quad C = A + B + \frac{1}{2}[A, B] + \cdots$$

The map now becomes

$$U = Re^{:R^{-1}F_3 + f_3 - F_3 + O(4):} e^{:e^{:F_3:} f_4:}$$

We can further reduce it to (non-trivial)

$$U = Re^{:f_3^{(1)}:} e^{:f_4^{(1)}:} = Re^{:R^{-1}F_3 + f_3 - F_3:} e^{:f_4^{(1)}:}$$

Where $f_3^{(1)} = R^{-1}F_3 + f_3 - F_3$ contains all the 3rd order contribution.

Thus the solution is

$$F_3 = \frac{f_3 - f_3^{(1)}}{I - R^{-1}}$$

Since f3 is periodic in the angle variable Φ, we can write

$$f_3 = \sum_m \bar{f}_{3,m}(J) e^{im\phi}$$

We can construct a f3(1) that does not have phase dependence, i.e., we can write it as

$$f_3^{(1)} = \bar{f}_{3,0}(J)$$

Thus now the generation function F3 reads

$$F_3 = \sum_{m \neq 0} \frac{\bar{f}_{3,m}(J) e^{im\phi}}{1 - e^{-im\mu}}$$

Taking Octupole as an example (assume it is the only nonlinear element in the beam line), we can write the map as

$$\mathbf{M} = Re^{:f_4:}$$

where f4 is

$$f_4 = -\frac{1}{24}k_3 l x^4$$

Rewrite it in action-angle variables

$$x = \sqrt{2\beta J}\cos\Phi$$

$$f_4 = -\frac{1}{6}k_3 l\beta^2 J^2\cos^4\Phi = -\frac{1}{48}k_3 l\beta^2 J^2(3+4\cos 2\Phi+\cos 4\Phi)$$

Thus the generation function for normalized map $f_{4,0}$ reads

$$f_{4,0} = -\frac{1}{16}k_3 l\beta^2 J^2$$

And the normalized map becomes (with BCH theorem)

$$\mathbf{M}_4 = Re^{:f_{4,0}:} = e^{:-\mu J-\frac{1}{16}k_3 l\beta^2 J^2:}$$

Thus the mapping of action-angle variables becomes

$$J \to J$$
$$\Phi \to \Phi + \mu + \frac{1}{8} k_3 l \beta^2 J$$

In other words, we see the tune shift with amplitude right away.

Similar to previous case for sextupole, we have

$$\mathrm{M}_4 = Re^{:f_{4,0}:} = e^{:-\mu J - \frac{1}{16} k_3 l \beta^2 J^2:} \doteq e^{:F_4:} M e^{:-F_4:}$$

Last equation is valid if we keep the normalization up to 4th order.

We can obtain the normalization generator $F_4$ easily

$$F_4 = \sum_{m \neq 0} \frac{f_{4,m}(J) e^{im\phi}}{1 - e^{-im\mu}}$$

$$F_4 = -\frac{1}{96} k_3 l \beta^2 J^2 \left( \frac{4[\cos 2\Phi - \cos 2(\Phi + \mu)]}{1 - \cos 2\mu} + \frac{\cos 4\Phi - \cos 4(\Phi + \mu)}{1 - \cos 4\mu} \right)$$

The normalized map now contains only action variable (easy to integrate) while all the phase information has been pushed to higher order.

From the generator $F_4$, we see the octupole drives half integer and quarter integer resonances. We can track the Poincare map using exact map and the normalized map respectively (assum $k_3 l = 4800\ m^{-3}$ and $\beta = 1$ m). Assuming the tune $\mu$ is $0.33 \times 2\pi$ far from resonances

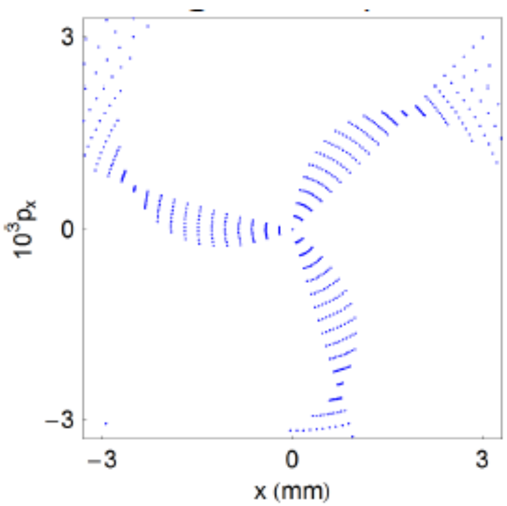


exact map

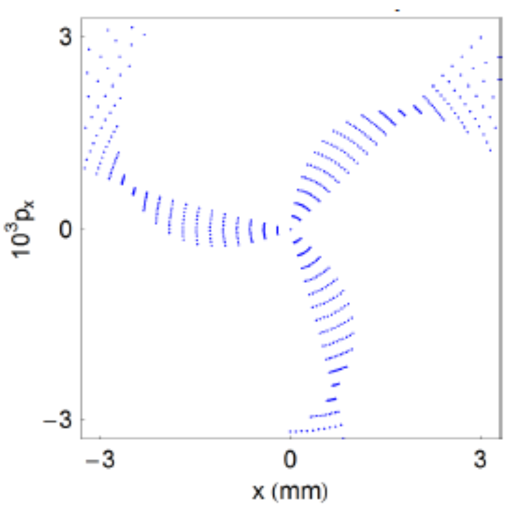


normalized map

30 turns

Tune shift with amplitude!!

Tracking for longer turns results in different feature where we pay the price of the simplified (normalized) map. Some of the phase information (3rd order resonance island) is lost during this process.

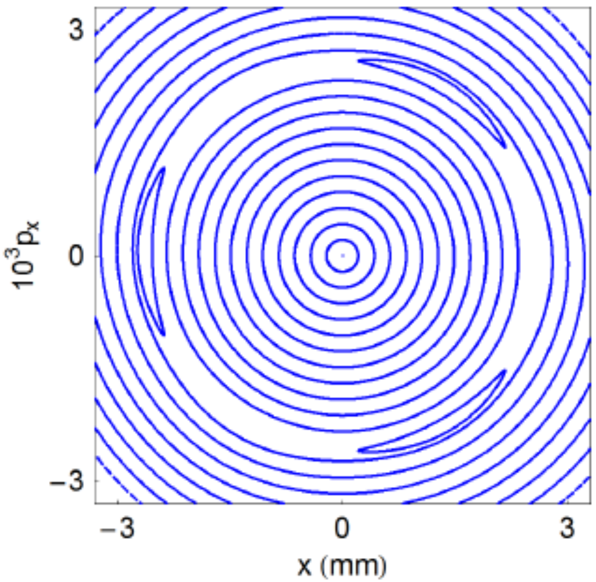


exact map

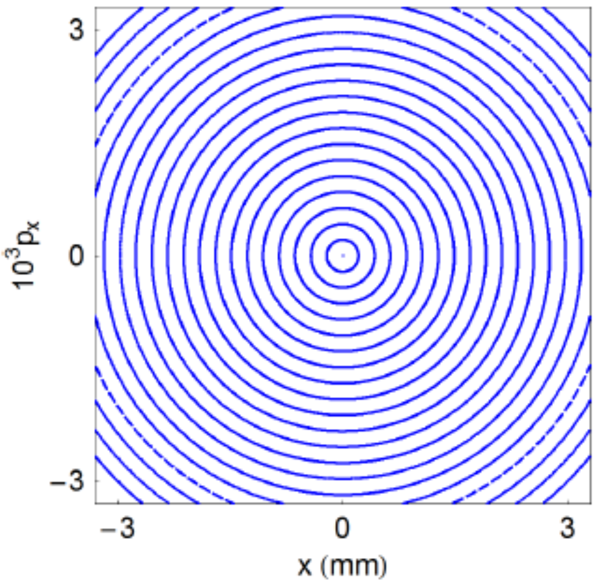


normalized map

2500 turns

Tracking for tunes near 4th order resonance is a bit tricky. Since the $k_3l$ is positive, the tune shift with amplitude drives the tune up. Thus if the tune $\mu$ is $0.252\times2\pi$, we barely see resonances. The two tracking results resemble

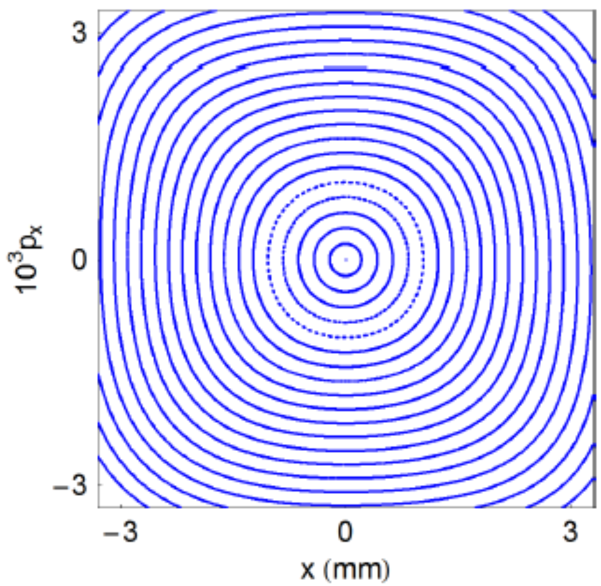


exact map

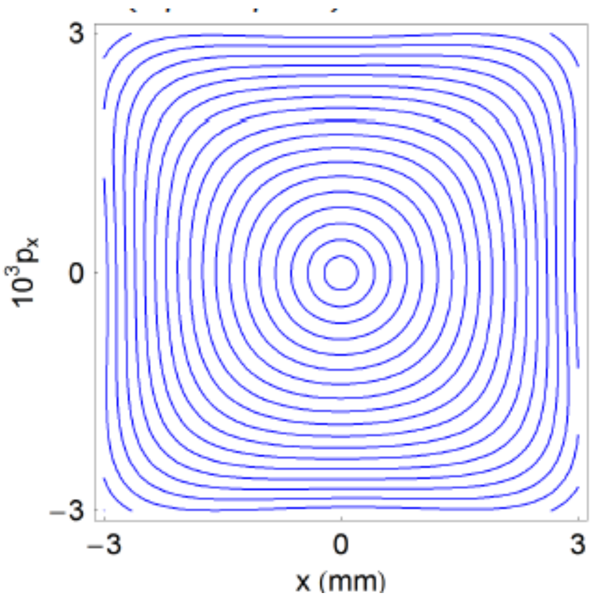


normalized map

2500 turns

For a tune less than quarter integer, i.e.,μ is 0.248×2π, we see strong resonances from exact tracking while for the normalized map, we only see a rotation in phase space.

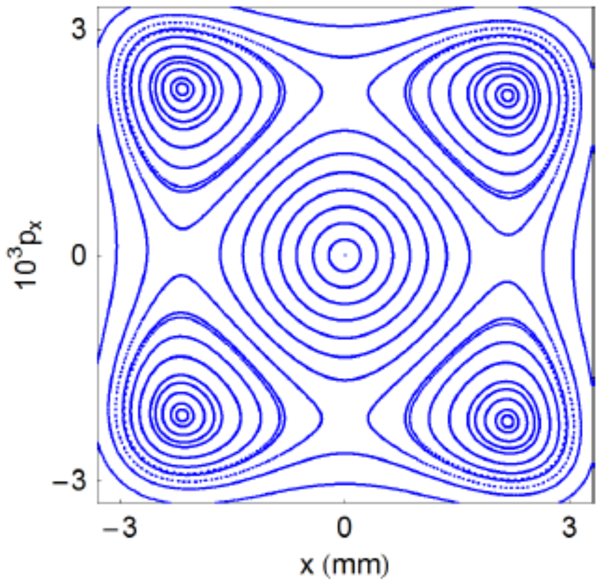


exact map

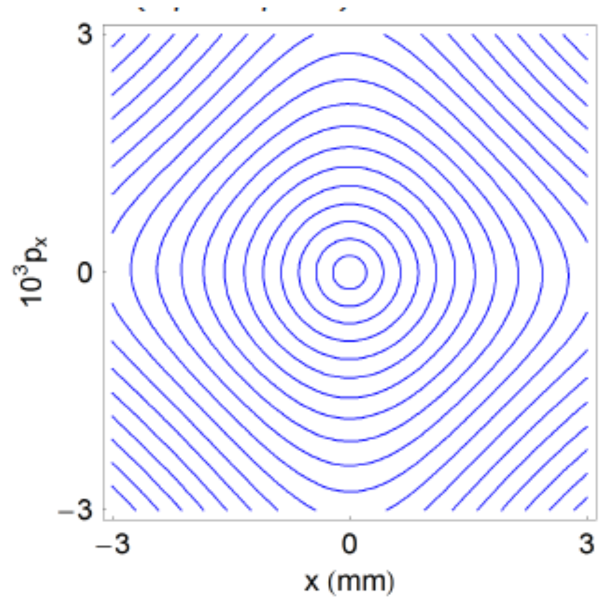


normalized map

2500 turns

Normal form of a one turn map preserves the information on tune amplitude dependence while loses the key phase information (when close to resonances). Need to retain higher order terms!

# Resonance driving terms(RDTs)

We can interpret the Fourier coefficients $\overline{f}_{3,m}(J)$ as resonance strengths. And the generating function diverges when resonance condition mμ=2π is satisfied, meaning such driving term has large effect. Put it into polynomial expression, the generating function can be written as

$$F = \sum_{jklm} f_{jklm} \varsigma_x^{+} \varsigma_x^{-} \varsigma_y^{+} \varsigma_y^{-} = F_3 + F_4 + \cdots$$

where

$$f_{jklm} = \frac{h_{jklm}}{1 - e^{i2\pi[(j-k)\nu_x + (l-m)\nu_y]}}$$

hjklm are called resonance driving terms in many accelerator tracking codes. The entire process of the normal form the one turn map can be visualized as

$$\begin{tikzcd}
\overline{x(n)} \arrow[r, "M(J,\phi)"] \arrow[d, "\Phi"'] & \overline{x(n+1)} \arrow[d, "\Phi = e^{:F:}"] \\
\overline{\varsigma(n)} \arrow[r, "U(J) = e^{:H:}"] & \overline{\varsigma(n+1)}
\end{tikzcd}$$

# Resonance driving terms(RDTs)

Incorporating the optics of a lattice, the resonance driving term (RDT) coefficients $h_{jklm}$ ($1^{st}$ order RDT) are usually calculated as

$$h_{jklm} = c\sum_{i=1}^{N} S_2 \beta_{xi}^{(j+k)/2} \beta_{yi}^{(l+m)/2} e^{i[(j-k)\mu_{xi}+(l-m)\mu_{yi}]}$$

It is very sensitive to linear lattice thus a carefully designed linear lattice with proper phase advance per periodic structure benefits greatly in reducing the RDTs (we will talk about a few tactics later).

# Dynamic aperture (DA)

1. Dynamic aperture determines the stable region in 2d real space (x-y) while particles travel along the accelerator. It is very important for particle dynamic study especially in effects that requires tracking over many revolutions (decided by system's damping time, could range from 1000 (light sources) to 1,000,000 (proton/heavy ion storage rings).
2. Dynamic aperture is a clear indication of nonlinear resonances that reside in an accelerator. Its size is limited by the utilize of nonlinear magnets to correct chromatic aberration. Thus designing the lattice with the nonlinear magnets' strengths reduced is crucial in improving DA.
3. Careful tuning of multipole nonlinear elements can also result in reducing the resonance driving terms thus improving the DA.
4. There are many ways of determining the DA of a specific lattice. Mostly commonly used techniques include line search mode (single-line, n-line,etc…) and frequency map analysis.

# Line search analysis

Line search mode requires tracking particles with different initial positions (or gradually increasing the particle offset till it is lost) to determine the boundary of the stable region. Itself is machine expensive however can be easily parallelized.

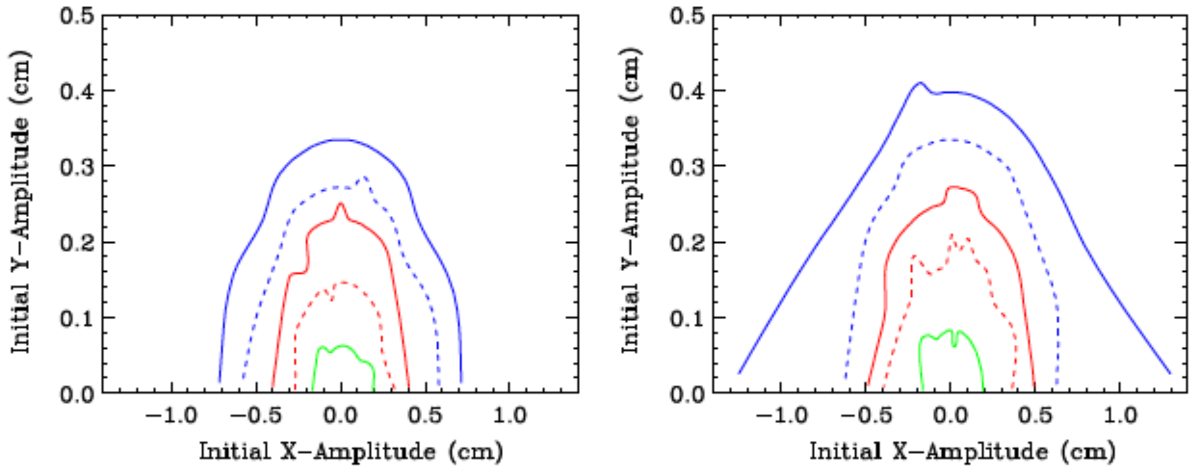


Figure 10: *Momentum dependent dynamic aperture without errors for OPA (left) and 4th-order geometric achromat (right) solutions with chromaticity set to zero, where:* $\delta = 0$ *(blue solid), 0.5% (blue dash), 1% (red solid), 1.5% (red dash), 2% (green).*

# Frequency map analysis(FMA)

If we perform a discrete Fourier transform on the tracking data with initial position. We can obtain the betatron tunes (for N turn tracking, the precision is merely 1/N). If we repeat this process with different initial positions, we can obtain a tune map. To indicate the variation of the tunes over different turns of the ring, we can define a diffusion or regularity which describes the difference between the tunes over various periods (usually the first half of the tracking ($Q_{x1}$, $Q_{y1}$) and the second half($Q_{x2}$, $Q_{y2}$)). In other words, we define a diffusion constant D

$$D = \log_{10} \sqrt{(Q_{y2} - Q_{y1})^2 + (Q_{x2} - Q_{x1})^2}$$

The rule of thumb is when D is small, the variation is low (or regular) and particle motion is stable. On the other hand, when D is large, the variation is high (or irregular) and particle motion is unstable (chaotic). The points in tune space with large variation (chaotic) usually lies on the crossing of different resonance lines.

# Frequency map analysis(FMA)

The obtained resonance feature in frequency space (tune space) can then be easily related into 2 dimension x-y real space and used as an indicator of the size of stable region. It may discover some resonance islands that line search is not capable of finding as well as the important tune shifts and strong resonances that we need to avoid. FMA is often used in accelerator design to identify the dynamical behavior.

Experimental construction of FM requires very high precision measurements and some data mining techniques to further improve the precision, e.g., Hanning filter, data interpolation, NAFF, etc…

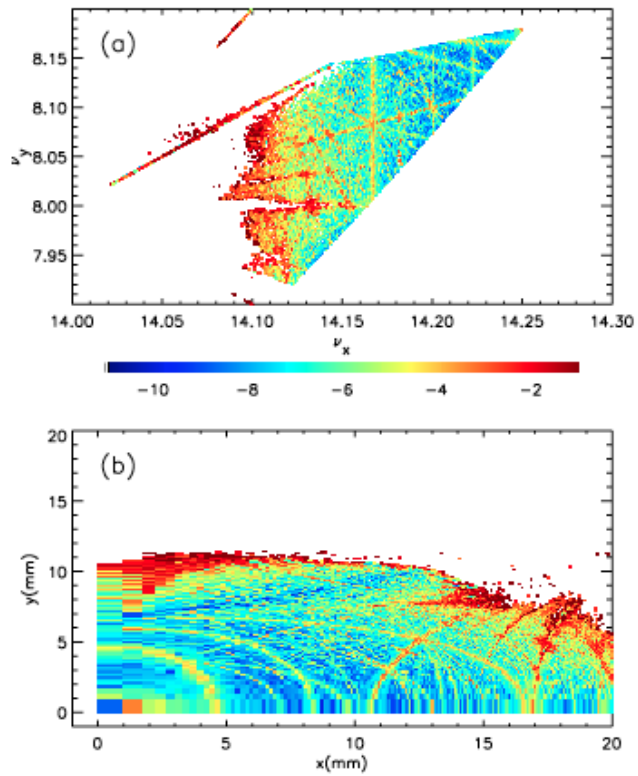


D

A plot showing the FM for an ideal lattice for ALS in tune space (a) and real space (b).

# DA optimization strategy(s)

## We are opening a Pandora's box here!

In short, there is no unique guideline of how DA can be optimized. It is largely performed on case by case scenario, i.e., what works for you may not work for me!

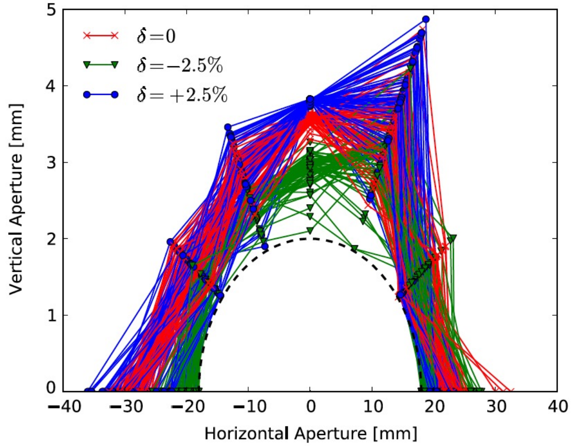


In general, people call a DA is optimized so that the stable region in 2D real space (for on and off momentum, this is another topics which has not been touched yet) is large enough so that off axis injection/extraction can be tolerated. Another criteria is that particle loss (believe it or not, there is always particle loss every single turn) is low enough that top-off injection etc techniques can be used to have constantly stable beam current in SR.

# DA size and RDT

Good news!

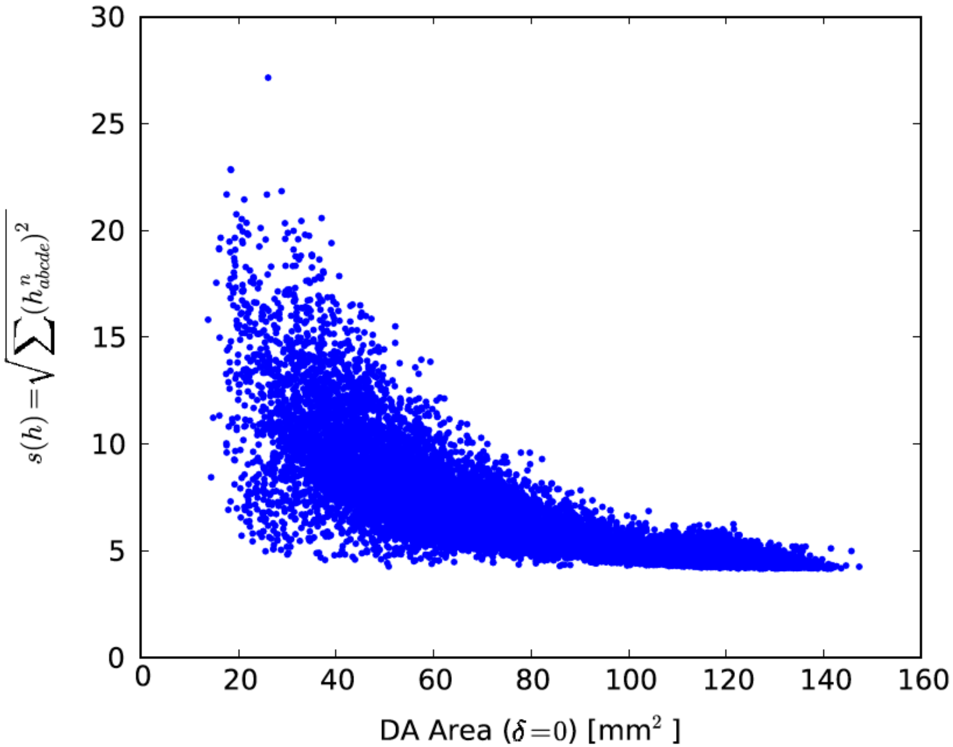


The majority of the materials we covered in this lecture prove to be of less help in determining a good design of DA as it is only a necessary requirement to control all RDTs for a large DA solution. In other words, low RDTs are not a sufficient condition in achieving large DA : (.

# Brute force optimization

Recent years, people are normally referring to means of searching the optimal magnet layouts in parametric space using model-free, large number of parallelized particle tracking with powerful computers. The common objective functions, in these long and expensive searches, usually include the DA size, target emittances, sometimes betatron tunes, bunch lengths, etc.

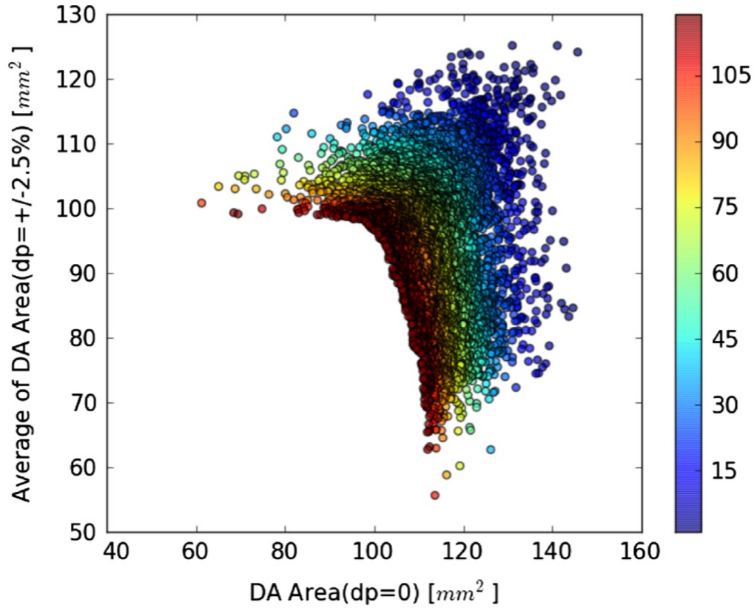


An example of well-known multi-objective genetic optimization involves large amount of individual separate simulations in single generation.

# Convergence and optimal selections

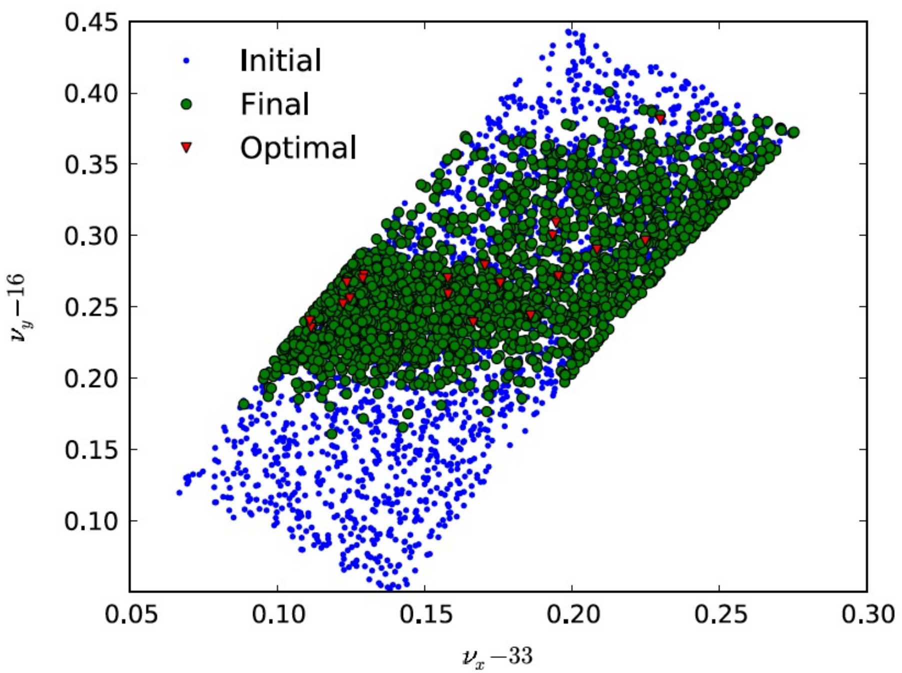


Convergence speed for such algorithms usually highly depends on underlying model: a pure numerical tracking (becomes a statistical problem -- purely Math problem) would take a much longer time while incorporating analytical estimation of RDTs into tracking would significantly improve convergence speed.